

MICROBIAL CONVERSION OF SYNGAS TO
ETHANOL

By

SRINIVASAN RAJAGOPALAN

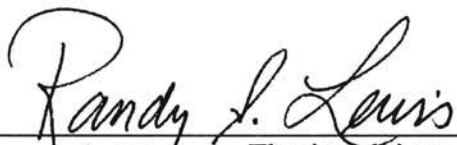
Bachelor of Technology
Anna University
Madras, India
1994

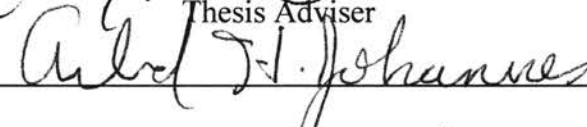
Master of Technology
Indian Institute of Technology
Madras, India
1997


Submitted to the Faculty of the
Graduate College of the
Oklahoma State University
in partial fulfillment of
the requirements for
the Degree of
DOCTOR OF PHILOSOPHY
May, 2001


MICROBIAL CONVERSION OF SYNGAS TO
ETHANOL


Thesis Approved:




Thesis Adviser










Dean of the Graduate College

ACKNOWLEDGEMENTS

My loving parents, V. Rajagopalan and V. Kamalaveni, have been my inspiration all along my life. I thank them for all the sacrifices they have made in my making. I fondly remember my sister, Kala, for her effort in keeping my spirits high all these years. My loving brother, Ashok, has made my life meaningful with a deep sense of responsibility. My niece, Pooja, who has showered me with so much joy and my brother-in-law, Raju will be fondly remembered. I dedicate my dissertation to my family.

I would like to thank my advisers, Dr. Randy Lewis and Dr. AJ for their sincere efforts. A perfect adviser in my opinion is one who directs his students with a firm, but gentle manner. He is a person who knows when to let the student find his own directions and when to personally take the lead. He is a person who knows when to be severe and when to be loving. Dr. Lewis fits this description.

Dr.AJ! I do not know if this Ph.D. would have been possible without this wonderful person. I do not know if my personal debt to this loving person will be ever settled. Thank you Dr. AJ, just for being what you are.

I am grateful to Dr. Russ Rhinehart, Dr. Khaled Gasem and Dr. John Veenstra for their caring guidance and interests in my research. I thank my friends at the “chemee” department, Charles Baker, Pat Swart, Sarah Sloan, Carol Brown, and Amber Grim, who have made my official errands less official but a lot more funnier than I deserved.

I thank my friend and colleague, Rohit Datar, for all his love and support. I thank my friends, Johnnetta Nesbitt, Xunbao Duan, Heather Gappa, Probir Shah, Kiran Rao, and Jason Beene for their support.

I thank the departments of chemical engineering and biosystems and agricultural engineering for their support. Dr. Ray Huhnke, Dr. Bill Barfield, and Dr. Jerry Lalman will deserve a special mention. I thank Dr. Ralph Tanner, Rossukon Laopaiboon and Jack Liou at the University of Oklahoma for providing the “great smelling” inocula for my experiments.

Specially, I thank those men whose backstage efforts are rarely visible to the naked eye, yet so essential for a Ph.D. of this sort. Wayne Kiner and Rob Harshman at the biosystems workshop will always be remembered for their efforts. Karla Rider and Pam Tauer will be remembered for the encouragement they gave me.

Finally, I thank all the sponsors of this research project and the Biomass Group at Oklahoma State University.

TABLE OF CONTENTS

Chapter	Page
1. INTRODUCTION TO BIOMASS CONVERSION TO ETHANOL	1
1.1 Introduction	1
1.2 Advantages of ethanol-blended fuels	2
1.2.1 Renewable source of supply	4
1.2.2 Cleaner environment	4
1.2.3 Less dependence on imported light crude oil	6
1.2.4 Pollution concerns over MTBE	7
1.3 Economics of ethanol as a fuel	7
1.4 Ethanol manufacturing processes	8
1.4.1 Ethanol from corn	8
1.4.2 Ethanol from cellulosic feedstocks	11
1.5 Gasification and fermentation process- A holistic approach	14
1.6 Purpose of the Study	17
2. SYNGAS FERMENTATION - LITERATURE REVIEW	20
2.1 Introduction	20
2.2 Microbiology of syngas fermentations	22
2.3 Syngas fermentations	24
2.3.1 Microbial catalysts used in syngas fermentations	24
2.3.2 Bioreactor designs used for syngas fermentations	25
2.3.3 Process parameters and modeling of syngas fermentations	28
2.3.4 Engineering issues in syngas fermentations	31
2.4 Optimization of process conditions	31
2.5 Objectives of the research	33
3. STABILIZATION OF CELL CONCENTRATION	34
3.1 Introduction	34
3.2 Objective of the study	35
3.3 Materials and methods	36
3.3.1 Microorganism	36
3.3.2 Media	36
3.3.3 Bioreactor design and operation	37

Chapter	Page
3.3.4 Analytical Procedure	42
3.4 Results	45
3.4.1 Cell instability with cell recycle	45
3.4.2 Cell instability without recycle	46
3.4.3 Cell stability with sodium sulfide	54
3.5 Discussion	61
3.6 Conclusion	64
4. CELL GROWTH, SUBSTRATE UTILIZATION AND PRODUCT FORMATION	 65
4.1 Introduction	65
4.2 Objectives of the study	67
4.3 Materials and methods	67
4.3.1 Microorganism	67
4.3.2 Bioreactor media	68
4.3.3 Bioreactor operation	68
4.3.4 Methodology	69
4.3.4.1 Rate limiting mechanism	69
4.3.4.2 Kinetic parameters	70
4.4 Results	76
4.4.1 Rate controlling step	76
4.4.1.1 Cell growth	76
4.4.1.2 CO utilization	79
4.4.2 Kinetic parameters	81
4.5 Conclusions	92
5. EFFECTS OF PROCESS PERTURBATIONS	 94
5.1 Introduction	94
5.2 Objectives of the study	95
5.3 Materials and methods	96
5.3.1 Microorganism	96
5.3.2 Bioreactor media	96
5.3.3 Bioreactor design and operation	96
5.3.4 Process perturbations	97
5.4 Results	97
5.4.1 Effect of dilution rate on bioreactor performance	97
5.4.1.1 Cell growth	98
5.4.1.2 CO utilization	102
5.4.1.3 Product formation	102
5.4.1.4 Discussion on dilution rate	106

Chapter	Page
5.4.2 Effects of trace metal composition	109
5.4.2.1 Cell growth	110
5.4.2.2 CO utilization	112
5.4.2.3 Product formation	112
5.4.2.4 Discussion on trace metal composition	115
5.4.3 Cell Recovery from temperature shock	117
5.4.4 Response to CO ₂ cut- off	117
5.4.4.1 Discussions on CO ₂ cut-off	121
5.4.5 Response to pH shock	124
5.5 Conclusions	125
6. PROCESS IMPROVEMENT TECHNIQUES	126
6.1 Introduction	126
6.1.1 Hydrogen utilization	127
6.1.2 Cell recycle system	128
6.1.3 Media optimization	129
6.2 Objectives of the study	130
6.3 Materials and Methods	130
6.3.1 Microorganism	130
6.3.2 Media	130
6.3.3 Experimental set-up	131
6.3.3.1 Hydrogen utilization and cell recycle in a bubble column bioreactor	131
6.3.3.2 Hydrogen utilization (one liter flask)	132
6.3.3.3 Screening experiments	132
6.4 Results and Discussions	135
6.4.1 Hydrogen utilization	135
6.4.1.1 Hydrogen utilization (bubble column bioreactor)	135
6.4.1.2 Hydrogen utilization (one liter flask)	140
6.4.1.3 Discussions on H ₂ utilization	142
6.4.2 Cell recycle system (bubble column bioreactor)	143
6.4.3 Discussions on cell recycle	148
6.4.4 Nutrient screening	151
6.4.4.1 Design of experiment	151
6.4.4.2 Results	154
6.4.4.3 Discussions on screening	156
6.5 Conclusions	162
7. CONCLUSIONS	164
REFERENCES	171

Chapter	Page
APPENDIX I. THE “Acetyl CoA” PATHWAY OF AUTOTROPHIC GROWTH	179
APPENDIX II. ERROR ANALYSIS FOR THE ESTIMATION OF THE SPECIFIC CELL GROWTH RATE	187

LIST OF TABLES

Table	Page
1.1. Comparison of ethanol and gasoline prices	9
2.1. Experimental kinetic parameters estimated for syngas fermentations	29
3.1. Cost of nutrients for P7 growth	38
3.2. Bubble column specifications	39
4.1. Growth rate and doubling times for P7	83
4.2. CO utilization, specific CO uptake rate, cell yield from CO and CO ₂ yield from CO for P7	85
4.3. Product yields from CO and the specific ethanol production rate for P7	87
6.1. Plackett-Burman design for screening nutrients	152
6.2. Factors and ranges selected for the Plackett-Burman design	153
6.3. Regression analysis for cell concentration	155
6.4. Residuals from the regression analysis for cell concentration	157
6.5. Results of regression analysis for ethanol yield	159
6.6. Residuals from the regression analysis for ethanol yield	160

LIST OF FIGURES

Figure	Page
1.1. Ethanol production in the 1000 barrels/day (b/d) in the United States for the year 2000	3
1.2. Biomass energy strategy - A holistic approach	15
3.1. Bubble column bioreactor - Experimental layout	40
3.2. Optical density (O.D) versus cell concentration	44
3.3. Cell instability with total cell recycle	47
3.4. pH profile without automatic pH controller	48
3.5. Cell instability with partial cell recycle	49
3.6. pH profile with an automatic controller	51
3.7. CO utilization with partial cell recycle	52
3.8. CO ₂ generation with partial cell recycle	53
3.9. Ethanol concentration (wt.%) with partial cell recycle	55
3.10. Cell concentration (O.D) profile	56
3.11. CO utilization	58
3.12. Product concentrations	59
3.13. Cell concentration profile with partial cell recycle	60
3.14. CO utilization with partial cell recycle	62
3.15. Product concentrations (wt. %) with partial cell recycle	63

Figure	Page
4.1. Effect of trace metal concentrations on cell growth	77
4.2. Temperature profile versus time	78
4.3. CO utilization and specific CO uptake rate by P7	80
4.4. Batch growth curve of P7	82
5.1. Perturbations in the flow rate of nutrients	99
5.2. Cell concentrations in the bioreactor for different dilution rates	100
5.3. pH profile in the bioreactor	101
5.4. Percentage CO utilization and specific CO utilization for different values of dilution rates	103
5.5. Concentrations of ethanol and butanol for different dilution rates	104
5.6. Production rates of ethanol, butanol and cells for different dilution rates	105
5.7. Yields of ethanol, butanol and CO ₂ from CO	107
5.8. Carbon balance for the bioreactor	108
5.9. Effect of trace metal composition on cell growth	111
5.10. CO utilization and specific uptake rate by P7 for changes in trace metal compositions	113
5.11. Product concentration for changes in trace metal concentration	114
5.12. Yields of products from CO for changes in trace metal composition	116
5.13. Effects of CO ₂ cut-off in the feed stream	119
5.14. pH profile showing sudden spike	120
5.15. CO utilization (%) as a function of CO ₂ in the feed stream	122
5.16. Ethanol concentration as a function of CO ₂ in the feed gas stream	123

Figure	Page
6.1 Experimental set-up for the screening design	134
6.2. Cell concentration (O.D units) during the hydrogen utilization experiment	136
6.3 CO utilization, CO ₂ yield and H ₂ feed composition	138
6.4. Ethanol concentration during the hydrogen utilization experiment	139
6.5. Cell concentration and pH profiles for hydrogen utilization experiment	141
6.6. Effects of total cell recycle on cell concentration in the bubble column	144
6.7. CO utilization and CO yield in the experiment with total cell recycle	146
6.8. Product concentrations with for the experiment with total cell recycle	147
6.9. Cell concentration profile with total cell recycle	149
6.10. Product concentrations with total cell recycle	150
6.11. Experimental cell O.D and absolute residuals from regression	158
6.12. Experimental ethanol yield and absolute residuals from regression	161

NOMENCLATURE

BuOH	Butanol
D	Dilution rate (hr^{-1})
EtOH	Ethanol
F_G	Gas flow rate (ml/min.)
F_L	Liquid flow rate (ml/min.)
H	Henry's law constant ($\text{atm. m}^3/\text{mol.}$)
HAc	Acetic acid/acetate
K_{La}	Average liquid phase mass transfer coefficient (hr^{-1})
k_d	Specific cell death rate (hr^{-1})
N	Number of trials
O.D.	Optical density
P_G	Gas phase partial pressure (atm.)
P_L	Liquid phase partial pressure (atm.)
q_{CO}	Specific CO uptake rate (mole CO/min. g cells)
q_{EtOH}	Specific ethanol production rate (mole C in EtOH/min. g cells)
R	Gas constant ($\text{atm. m}^3/(\text{mole. K})$)
R_x	Rate of cell production (gcells/hr)

S	Limiting substrate concentration in the media
S_0	Initial concentration of limiting substrate in the media
t	time (min.)
t_D	Doubling time (hr)
t_G	Gas residence time (s)
t_L	Liquid residence time (hr)
T	Temperature (K)
X	Cell concentration (gcells/ml or O.D.)
X_0	Cell concentration at time = 0 (gcells/ml or O.D.)
y	Gas phase mole fraction
Y	Yield
μ	Specific cell growth rate (hr^{-1})

MICROBIAL CONVERSION OF SYNGAS TO ETHANOL

ABSTRACT

A newly discovered bacterium, P7, converts components of syngas into liquid products such as ethanol, butanol and acetic acid. Isolated from an agricultural lagoon, the bacterium was studied in a four and one-half liter bubble column using artificial blends of syngas. In view of the limited knowledge available in syngas fermentations, the research was targeted on investigating some of the critical engineering issues. Maintaining sodium sulfide concentration (0.1 – 1 ppm) was found to be essential for cell stability of P7. The controlling step for the overall process was found to be the availability of liquid nutrients to the bacterial cells. Intrinsic kinetic parameters for the bacterium were determined. The effects of various process conditions, such as, dilution rate of liquid nutrients, concentrations of trace metal solution, pH and temperature, gas phase compositions of CO₂ on P7 were determined. Process enhancement techniques, such as, introduction of H₂ in the feed gas, cell recycle, and screening of nutrients were performed to improve the cell and ethanol productions in the bioreactor. Future works required to improve the process performance were identified.

The bioconversion of syngas to ethanol is a key component in an overall “biomass to energy” strategy currently investigated at Oklahoma State University to produce fuel ethanol from inexpensive agricultural crops and residues.

KEYWORDS: Syngas, clostridium, fermentation, ethanol, bubble column, biofuel

CHAPTER 1

INTRODUCTION TO BIOMASS CONVERSION TO ETHANOL

1.1 Introduction

The conversion of renewable biomass to fuel ethanol is an important process being investigated as a possible alternative to the fast depleting resources of petroleum. Industries and automobiles are consuming more energy and hence, more fuels, than in the past resulting in a rapid decline in the available reserves of fossil fuels (Yacobucci and Womach, 2000). Fuel ethanol (or 'Gasohol') is a water-free ethanol with a high octane rating. Fuel ethanol contains up to 35% oxygen by weight.

During the past decade, the production of ethanol from renewable biomass such as inexpensive agricultural crops and residues has received considerable attention. Biomass is abundant in the United States and is a potential candidate to produce fuel-ethanol for industrial consumption. Unlike fossil fuels, ethanol from renewable biomass is environmentally benign in maintaining global CO₂ balance and reducing toxic emissions (Hohenstein and Wright, 1994). Ethanol is traditionally used as a blending ingredient at 5% to 10% concentrations (termed E5 or E10, respectively) in gasoline or as a raw material to produce high-octane rated fuel additives (Yacobucci and Womach, 2000). Evidently, the scope for research towards large-scale production of ethanol from indigenously available biomass is enormous due to its potential as an environmentally friendly alternative to fossil fuels.

The concept of ethanol as a fuel began as early as the first Model T car designed by Henry Ford. American usage of ethanol-blended gasoline began in the late 1970s (CRFA Report, 2000). The initial stimulus for ethanol production in the mid-1970s was the drive to develop alternative, indigenous renewable supplies of energy within the United States to meet the challenges of the oil embargo against the United States. Ethanol production has also been encouraged by a partial exemption from the motor fuels excise tax. Environmentally, the use of ethanol blends has been encouraged by the United States Clean Air Act of 1990, which requires oxygenated or reformulated gasoline to reduce emissions of carbon monoxide and volatile organic compounds (Yacobucci and Womach, 2000). Ethanol contains about 22,400 (high heating value) BTUs per liter. Due to the higher combustion efficiency of ethanol compared to gasoline and the octane credit of ethanol at the refinery, internal combustion engines are more efficient on ethanol than gasoline (CRFA Report, 2000). The daily production of ethanol in the United States is shown in Figure 1.1 (EIA Monthly Oxygenate Report, 2000).

1.2 Advantages of ethanol-blended fuels

Approximately 1.4 billion gallons of fuel ethanol were consumed in the United States in 1998, representing 1.2% of the 120 billion gallons of gasoline consumption during the same year. Despite its low utilization as an additive to gasoline, ethanol-based fuels have been projected as a primary candidate to supplement and even replace gasoline

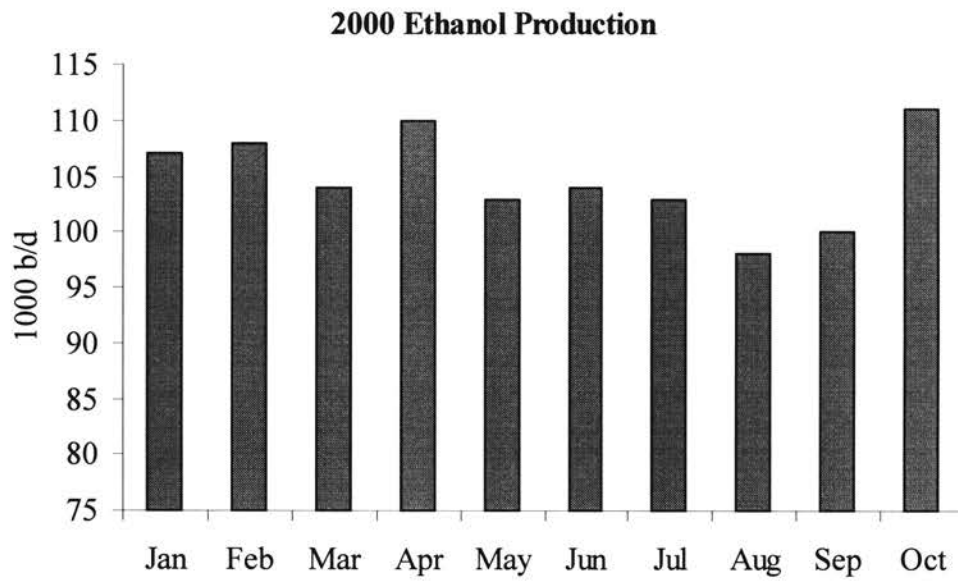


Figure 1.1. Ethanol Production in 1000 barrels/day (b/d) in the United States for the year 2000.

in the future (Yacobucci and Womach, 2000). The role of ethanol as a potential alternative to gasoline is an ongoing debate. Arguments favoring ethanol over gasoline and *vice versa* are not yet fully resolved. The advantages of biomass-based fuel ethanol provided below are excerpts from the arguments favoring ethanol over gasoline:

1.2.1 Renewable source of supply

Agricultural crops and residues that supply biomass for the production of fuel ethanol are renewable sources of raw materials. On the other hand, fossil fuels like petroleum are derived from non-renewable sources.

1.2.2 Cleaner environment

One of the main motivations for using ethanol is improved air quality. Ethanol is primarily used in gasoline to meet minimum oxygenate requirements of the Clean Air Act Amendments of 1990. The proposed environmental benefits of fuel ethanol are:

Net reduction in ground level ozone-forming emissions. Ground-level ozone causes human respiratory problems and damages many plants, but does nothing to increase ozone concentration in the stratosphere that protects the earth from the sun's ultraviolet radiation. The emissions produced by burning ethanol are less reactive with sunlight than those produced by burning gasoline. This results in a lower potential for forming the damaging ozone (DOE Report, 1999).

The "Greenhouse Effect" and the fate of CO₂. The 'Greenhouse Effect' refers to the Earth's atmosphere trapping the sun's radiation. The term is often used synonymously with 'Global Warming', which refers to the increasing average global

temperature, arising from an increase in greenhouse gases from industrial activity and population growth. Greenhouse gases contributing to the Greenhouse Effect include carbon dioxide, methane, and nitrogen oxides. The term 'Climate Change' refers to a wide range of changes in weather patterns that result from global warming. A substantial increase in the earth's average temperature could result in a change in agricultural patterns and melting of polar ice caps, raising sea levels and causing flooding of low-lying coastal areas. Under current conditions, use of ethanol-blended fuels, such as E85 (85% ethanol and 15% gasoline), can reduce the net emissions of greenhouse gases from automobile-fuel by as much as 37%. Notably, automobiles account for 25% of the overall CO₂ emissions to the atmosphere (Wyman et al., 1994). Ethanol-blended fuels, such as E10 (10% ethanol and 90% gasoline), reduce greenhouse gases by up to 3.9% (DOE Report, 1999).

Carbon dioxide is released into the atmosphere when ethanol (like other fuels) is burned in an automobile engine. However, this carbon dioxide is recycled into organic tissue during plant growth. Only about 40 percent or less of the organic matter is actually removed from farm fields for ethanol production (CRFA Report, 2000). The rest is returned to the soil as organic matter, increasing fertility and reducing soil erosion. The vast areas of agricultural cropland in the United States could benefit from increasing soil organic matter (DOE Report, 1999). Ethanol use in gasoline has tremendous potential for a net reduction in atmospheric carbon dioxide levels.

Reduction in carbon monoxide (CO) emissions. Carbon monoxide, formed by the incomplete combustion of fuels, is produced most readily from petroleum fuels, which contain no oxygen in their molecular structure. Because ethanol and other “oxygenated” compounds contain oxygen, their combustion in automobile engines is more complete. The result is a substantial reduction in carbon monoxide emissions. Research shows that reductions range up to 30%, depending on type and age of the automobile, the automobile emission system used, and the atmospheric conditions in which the automobile operates. Because of health concerns over carbon monoxide, the 1990 amendments to the United States Clean Air Act mandate the use of oxygenated gasoline in many major urban centers during the winter (when atmospheric carbon monoxide levels are highest) to reduce this pollution. (DOE Report, 1999).

1.2.3 Less dependence on imported light crude oil

Ethanol reduces the United States reliance on imported oils (Yacobucci and Womach, 2000) making the United States less vulnerable to a fuel embargo similar to the one in the 1970s. The United States imports more than half of its petroleum requirements from the Middle East and the imports are likely to grow to about 75% by 2020 if steps are not taken to reduce the nation’s dependence on imported petroleum (DOE Report, 1999). With the current automobile technology, the use of E10 can lead to a 3% reduction in the fossil energy use per vehicle mile, while the use of E95 (95% ethanol in gasohol) could lead to a 44% reduction in fossil energy use (Kovski, A., 1998). Contrarily, based on 1997 and 1998 estimates, fuel ethanol only displaces 1.2% of the gasoline consumption

in the United States (US-GAO, 1997, Yacobucci and Womach, 2000) contributing to a small fragment of the overall fuel consumption in the United States to substantially affect the imports of petroleum. In summary, increased ethanol production within the United States can alleviate the country's reliance on imported fuel.

1.2.4 Pollution concerns over MTBE

The two commonly used oxygenates for gasoline are ethanol and MTBE (methyl tertiary butyl ether). MTBE is less expensive than ethanol and is available in greater supply. However, studies conducted in California have determined the presence of MTBE, a possible human carcinogen, in subterranean water. Despite the cost differential, ethanol is advantageous because of its higher oxygen content (twice that of MTBE), sustainable production from agricultural feedstocks and most importantly, easy biodegradability (Yacobucci and Womach, 2000). With a ban on MTBE, ethanol would be the likely candidate to replace MTBE leading to an increase in the production capacity of ethanol in the United States (CRS Report, 1998).

1.3 Economics of ethanol as a fuel

A major constraint for the use of fuel ethanol as an additive, or possibly as a future replacement to gasoline, is the high price of ethanol. Wholesale ethanol prices, prior to incentives from the federal and state governments, are approximately twice that of gasoline. The primary federal incentive to favor ethanol production is 5.4 cents per gallon that the gasohol-blenders receive from the 18.4 cents federal excise tax on fuels ((US-DOE Report, 1998). With ethanol (as E10) comprising only 10% in the blend, the

exemption amounts to an effective subsidy of 54 cents per gallon of pure ethanol, as shown in Table 1.1 (Yacobucci and Womach, 2000).

Arguments in favor of the tax incentives include improved air quality and increased economic opportunities to the agrarian communities across the country (Olson, 1997). Arguably, ethanol as a fuel could not survive without the tax exemption, emphasizing on less expensive routes for its production. The tax exemption was projected to cause the Highway Trust Fund a loss in revenue up to \$ 10.4 billion (US GAO, 1997). Thus, less expensive production methods for ethanol production are required to economically compete with gasoline.

1.4 Ethanol manufacturing processes

The current ethanol processes use carbohydrates from sugar or starch based crops as the starting material. Research is also progressing to utilize other inexpensive agricultural crops and residues for ethanol production.

1.4.1 Ethanol from corn

In the United States, corn constitutes 90% of the feedstock for ethanol production, the rest being catered by other crops such as sorghum, barley, wheat, cheese-whey, and potatoes. An estimated 570 million bushels of corn were used to produce fuel ethanol in 1999/2000. With an increasing ethanol demand, the demand and market price for corn is likely to increase (Yacobucci and Womach, 2000).

Ethanol Wholesale Price	103 cents/gallon
Alcohol Fuel Tax Incentive	54 cents/gallon
Effective Price of Ethanol	49 cents/gallon
Gasoline Wholesale Price	46 cents/gallon

Table 1.1. Comparison of Ethanol and Gasoline Prices (Yacobucci and Womach, 2000).

Approximately 60% of the corn used for ethanol is processed in “wet” milling plants using chemical extraction and the rest is processed by “dry” mills. The basic steps in both processes include:

- Enzymatic treatment to separate the fermentable sugars
- Fermentation by yeast to produce ethanol
- Distillation of the product to high purity of ethanol
- Denaturation of the product (gasoline acts as denaturant)

Since it is profitable (with the tax incentive) to produce ethanol in the proximity of the feedstocks, the major corn producing states (Illinois, Nebraska, Minnesota, Iowa and Indiana) are the major ethanol producers. The geographic concentration of ethanol production is a major obstacle for the use of ethanol in the non-producing states of the country (NREL Report, 1999). The potential for expanding ethanol production to such regions has motivated research on the production of ethanol from alternate raw materials, such as inexpensive cellulosic feedstocks.

In addition to ethanol, the corn processes generate gluten feed, gluten meal, corn oil and distillers’ grains. Revenue from the byproducts helps offset the cost of ethanol production. The net cost of corn relative to the price of ethanol and the difference between ethanol and wholesale gasoline prices are the major determinants of the level of ethanol production. The production cost of fuel ethanol should be comparable to that of gasoline to justify its role as an alternative fuel. Since feedstocks contribute to a major share in the total costs, reducing feedstock costs would lead to lower overall production costs (NREL Report, 1999).

1.4.2 Ethanol from cellulosic feedstocks

Lignocellulosic materials, such as grasses, wood chips or paper wastes, are inexpensive carbohydrate sources available for the production of ethanol. The advantages of lignocellulosic substrates for ethanol production are:

- Abundant supply from forests, paper mills and agricultural sources
- Considerably inexpensive than sugar or starch based substrates
- Marginal lands can be utilized to cultivate wild grass varieties as feedstocks for ethanol
- Wide varieties of raw materials ranging from prairie grass, wood chips, paper wastes, agricultural residues, etc. can be utilized

The composition and structure of lignocellulosic materials depends on the source, but some generalizations can be made. Cellulose fibers, the main components of these materials, are usually surrounded by a hemicellulosic sheath, which in turn are embedded in a lignin matrix. Cellulose is a polymer of glucose (a six-carbon sugar) units. Hemicellulose is a polymer of five-carbon sugars, primarily xylan. Lignin is a very complex polymeric material made up of both aliphatic and aromatic subunits. The average composition of lignocellulosic materials is approximately 40 - 60% cellulose, 20 - 30% hemicellulose and 10 - 25% lignin (Slaff, 1984).

Several processes are currently popular for the production of ethanol from lignocellulosic materials, the chief among them being:

- Acid-hydrolysis followed by fermentation
- Enzymatic hydrolysis followed fermentation
- Gasification followed by fermentation process

Current research thrusts on bio-ethanol production from lignocellulosic materials are towards developing different technologies for large-scale production of fuel-grade ethanol. The estimated yield of ethanol from lignocellulosic biomass, such as switchgrass and other energy crops, is projected to approximately 100 billion gallons per year in the United States. Softwood wastes, sugarcane wastes, hardwood sawdust wastes and herbaceous crops are some of the potential feedstock for the process.

Acid-hydrolysis followed by fermentation. The conversion of lignocellulosic material to alcohol is a four-step process. First, pretreatment is required to remove the lignin from the lignocellulose. Second, the cellulose and hemicellulose are treated with dilute sulfuric acid (0.2 – 2 %) at 120° C to 200° C to produce a hemicellulosic syrup containing fermentable sugars. Third, genetically engineered bacteria and yeasts ferment the reduced sugars to ethanol. Fourth, the product is distilled to separate ethanol from the fermentation broth. Genetically engineered *E.coli* (Ingram et al., 1997) and *Saccharomyces* yeast (Krishnan et al., 1997) are some of the strains tested successfully for ethanol-production.

A challenging issue in the process is the efficient hydrolysis of cellulose and hemicellulose. A major disadvantage of the acid treatment process is the formation of unwanted decomposition products such as hydroxymethyl furfural. Normally, a significant portion of the hydrolyzed cellulose is converted to unwanted by-products (Slaff, 1984). Lignin, which amounts up to 25% of the total biomass feedstock, is not converted/utilized by the acid treatment process. Disposal of lignin is another major problem in the process, its limited use in plastic and synthetic wood industries,

notwithstanding. Considerable effort is being invested in this area to develop a cost-effective technology for converting lignocellulose to bio-ethanol.

Enzymatic hydrolysis followed by fermentation. The enzymatic process is similar to the acid-hydrolysis where in the lignocellulose is broken down by enzymes. Special classes of enzymes produced by certain bacteria, fungi, and protozoa called cellulases and xylanases are capable of breaking down the cellulose and hemicellulose of the biomass to soluble sugars. The sugars are subsequently fermented to ethanol by yeast or bacteria. The advantages of the enzymatic route over the acid hydrolysis method are that no decomposition by-products are formed and the sugar solution can be directly fermented. The disadvantages are the high cost of the enzymes and a long process time for the hydrolysis (Slaff, 1984). Also, similar to the acid hydrolysis, the enzyme hydrolysis process can only utilize the cellulose and hemicellulose, leaving lignin as the residue to be disposed. New technologies are required that can utilize all the available carbon in the feedstock to improve the yield of ethanol from the biomass.

Gasification followed by fermentation. Gasification technologies can convert almost all of the carbon contained in lignocellulosic materials to gaseous products that can be fermented by bacteria (Reed, 1988). It is also possible to derive useful energy when the gasification process is exothermic. In this approach, the crops are incinerated under controlled conditions and the by-product gas mixture, primarily composed of CO, CO₂, and H₂ (syngas) is converted to ethanol by bacteria. Biomass, such as switchgrass, on pyrolysis with oxygen yield significant quantities of syngas. Progressive research in this area includes developing strategies such as fluidized-bed

gasification, to achieve high heat and mass transfer rates between the particulate and gas streams. The product gases are converted biochemically to ethanol by special strains of bacteria such as *Clostridium ljungdahlii* and *Clostridium acetoethanogenum* under anaerobic (oxygen-free) conditions. These biochemical processes are heterogeneous in nature involving complex, reaction kinetics and mass transfer mechanisms.

During the last decade, significant work has been in progress to develop cost-efficient processes and high-yielding strains to commercially produce bio-ethanol from syngas. The advantages of biological synthesis over chemical processes for syngas include higher specificity of the biocatalysts over chemical catalysts, higher yields of products, and lower energy costs than chemical processes at ambient conditions of temperature and pressure (Vega et al., 1990, Phillips et al., 1994).

1.5 Gasification and fermentation process- A holistic approach

The overall process of producing ethanol from lignocellulosic material via gasification and fermentation is illustrated in Figure 1.2. The raw materials, such as switchgrass, are first dried and chopped. The chopped grass is fed to a gasifier to be converted to syngas in a controlled supply of air. The syngas is purified and fed to a bioreactor where anaerobic bacteria convert the components of syngas to products such as ethanol and acetic acid. The products are separated from the fermentation broth and purified.

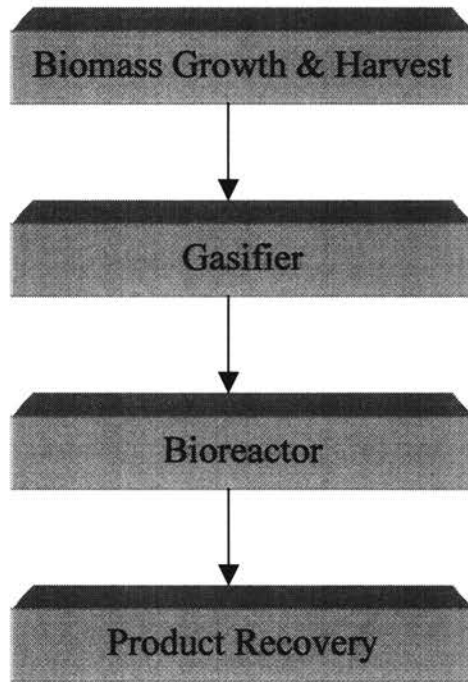


Figure 1.2. Biomass energy strategy- A holistic approach.

Syngas can be produced using several variations in the gasification process. Steam reforming is used when the hydrogen and CO are predominantly desired in the final product. However, steam reforming is an endothermic process requiring external addition of heat to the gasifier. On the other hand, dry gasification involves pyrolysis and/or partial oxidation of biomass under a reduced supply of air or oxygen. The process is exothermic and the energy released from the process can be utilized for heating requirements. However, a significant amount of CO₂ is produced by the process compared to steam reforming (Reed, 1988).

A fluidized bed gasifier is set up to produce syngas via the dry process at Oklahoma State University, Stillwater. The gasifier is capable of utilizing biomass, such as switchgrass, Bermuda grass, saw dust, wood waste, and corn residues to generate syngas. The product gas currently contains tar, ashes and other impurities that are expected to be removed prior to the bioconversion process. Current efforts on the gasifier are invested towards optimizing the process conditions to generate syngas with maximum CO and H₂ and provide a stable composition of the syngas over long operational periods.

The next important process in the biomass energy strategy is the bioconversion of syngas to ethanol using anaerobic bacteria in a bioreactor. Currently, a five liter bubble column bioreactor is in operation at Oklahoma State University. The bacteria catalyze the conversion of the components of syngas to ethanol and by-products such as acetic acid via an acetogenic pathway (Wood, 1984). The heterogeneous conversion of syngas is facilitated by special clostridial bacteria under anaerobic conditions. Successful technology transfer of the syngas conversion from test tube to commercial scale systems

requires that interphase mass, heat and momentum transfer be optimized (Moo-Young, 1987).

The most common problem associated with syngas conversion is reported to be the low productivity of ethanol and limitations on mass transfer of the gaseous reactants to the active sites of the microbial catalysts (Worden, 1997). Methods to enhance the productivity of the process include increasing mass transfer rates, increasing cell densities, optimizing nutrient requirements of the bacteria and reducing the production of unwanted by-products.

The choice of the bioreactor plays an important role in the mass transfer phenomena. Stirred tanks are commonly used in the fermentation industries. However, the high power input requirements associated with stirring, especially at higher scales, is a major disadvantage of stirred tank bioreactors. In view of simplicity of construction and operation, low capital costs and easy maintenance, bubble columns are leading rivals to stirred tanks (Bailey, 1986). Additionally, the plug flow nature of the bubbles in the column reduces back-mixing problems encountered in stirred tanks. Advanced bubble forming techniques, such as microbubble generation, can greatly enhance the energy efficiency of bubble columns on scale-up as compared to stirred tanks (Worden, 1997). Evidently, bubble columns are well suited for gas-liquid reactions requiring high efficiency and low energy costs.

1.6 Purpose of the Study

The gasification and fermentation process for the production of ethanol from agricultural crops and other lignocellulosic feedstocks is an emerging technology.

Syngas fermentations using anaerobic bacteria along with data on intrinsic kinetics and yield parameters are rarely reported in literature.

The individual steps involved in the overall process of synthesizing ethanol from agricultural crops (using switchgrass as the model feedstock) are currently being handled by a team of agricultural engineers, economists and chemical engineers at Oklahoma State University. In view of the limited knowledge available in syngas fermentations, the objective of this research is to investigate some of the critical engineering issues involved with the bioreactor process. Characteristics of the process, such as cell stability, productivities, inhibitory effects of substrates/products, pH and temperature effects, and optimization of the media for maximum ethanol productivities need to be investigated. Experimentation is required with synthetic blends of syngas to determine the feasibility of the syngas fermentation at a higher scale than test-tube level runs. The test-tube level experiments performed at the University of Oklahoma ranged from 10 ml to 100 ml cultures. Scale-up ratios of 10 to 500 are commonly used with bioreactors (Bailey, 1986). A five-liter bubble column bioreactor has been selected for this purpose. The isolated microorganism is a new species of clostridial bacteria that must be experimentally investigated in the five liter bioreactor in an attempt to scale-up the process. In closing, the four main areas of focus of this research are:

- Establish cell stability of P7 in a bubble column bioreactor.
- Obtain kinetic parameters for cell growth, substrate utilization and product formation for P7.

- Determine the effects of process perturbations such as changes in nutrient and feed gas compositions, dilution rates, and pH and temperature shocks on the performance of P7.
- Enhance the performance of P7 by increasing the cell concentrations in the bioreactor using a cell recycle system, increasing ethanol yields by using H₂ in the feed gas, and increasing cell growth and ethanol yields by optimizing the growth media of P7.

The ultimate aim of this research is to investigate some of the critical engineering issues involved with the bioreactor process that are critical components of the holistic approach to produce ethanol from inexpensive agricultural crops.

CHAPTER 2

SYNGAS FERMENTATION - LITERATURE REVIEW

2.1 Introduction

The potential of biomass as a viable alternative to fossil fuels in the United States has been discussed by Hohenstein and Wright (1994). Biomass supplied 2.76 exajoules (10^{18} J) of primary energy in 1990 and accounted for nearly 3.3% of the total energy supply in the United States. Agricultural residues like corn stover, wheat straw, and saw dust that could be used as biomass feedstocks for the production of ethanol amounted to 306 million metric dry weight tons in the United States in 1999 (Rooney et al., 1999). The projected estimates for biomass energy increase in the United States by 2010 are 58-188% (Hohenstein and Wright, 1994). Ethanol is one of the energy components that can be generated from biomass. Large scale production of ethanol from biomass would require dedicated energy crops as part of the supply system (Glassner, 1999).

Considerable effort has been invested to develop dedicated crops as feedstocks including short rotation woody crops grown on forest regions and herbaceous crops for marginal lands (Hohenstein and Wright, 1994). Oak Ridge National Laboratory (ORNL-BFDP) estimates indicate 225 and 324 million acres of land available in the US for energy crops. Switchgrass has been selected as the model crop for ethanol production because switchgrass is a perennial crop cultivable on marginal lands (McLaughlin, 1993).

Comparative studies on corn and switchgrass indicate energy gains of 34% and 343% respectively, from producing ethanol (McLaughlin and Walsh, 1998).

Specific to Oklahoma, the current supply of lignocellulosic biomass amounts from 3 to 6 dry tons/acre/year with an available 27 million acres of native rangeland, 8.5 million acres of cropland and 1 million acres of USDA Conservation Reserve Program (Ball et al., 1991, Taliaferro et al., 1975). Specific fertility, harvest management and cultivation requirements of the dedicated crops are currently being investigated by Oklahoma State University. Machinery costs involved with biomass production, harvesting, transporting and storage were estimated to be 50% of the annual cost of producing energy crops (Huhnke and Bowers, 1994).

Gasification of lignocellulosic biomass is a well known process for the generation of syngas, a mixture of CO, CO₂, and H₂. Gasification technology can be classified based upon the reactor type, operating pressure, and gasifying agent used. Steam, air and oxygen are the common gasifying agents. Several gasification procedures are described in literature (Gomez et al., 1998, Gil et al., 1997, Reed, 1981). Biomass gasification with air has been demonstrated at commercial scales for the production of syngas (Gil et al., 1997). Biomass gasification with steam has also been demonstrated. Several reactor designs were discussed in literature for biomass gasification. Fluidized, moving and fixed bed reactors have been demonstrated using feedstocks, such as, sawdust, woodchips, sugarcane bagasse and solid wastes (Narvaez et al., 1996, Natarajan et al., 1998, Reed, 1981). Fluidized bed reactors are commonly used to enhance uniform heat distribution and control the gas-solid interphase reactions (Reed, 1981).

2.2 Microbiology of syngas fermentations

Several anaerobic bacteria have been found to grow autotrophically, synthesizing cell materials from simple inorganic substrates such as CO, H₂, CO₂, minerals and water. Wood et al. (1986) have described an autotrophic organism as one that uses CO or CO₂ as the source of carbon for cell growth. These bacteria follow a metabolic pathway that was proposed by Ljungdahl and Wood, called the acetyl-CoA pathway or the Wood-Ljungdahl pathway for autotrophic growth (Phillips et al., 1994). The key characteristics of the pathway are the formation of the methyl moiety from the components of syngas, transfer of the methyl moiety to CO dehydrogenase (CODH) via a corrinoid enzyme and a CODH-catalyzed condensation of the methyl group with a CO-derived carbonyl and coenzyme A to form a acetyl-CoA intermediate, which is hydrolyzed to acetic acid and subsequently to ethanol, butyrate or butanol.

The mechanism of the acetyl- CoA pathway has been described for *C. thermoaceticum* (Wood et al., 1986). The distinctive feature of any autotrophic pathway is the mechanism by which CO₂ is utilized for the total synthesis of an organic compound from which succeeding anabolic reactions proceed. The pathway illustrates that H₂ is required as a source of energy and electrons when the bacteria grow on CO₂. The enzyme hydrogenase produces these electrons from H₂. With CO as the carbon source, the CO also can serve as an electron donor, catalyzed by CODH to form CO₂ in the process. The ability of the bacteria to utilize both H₂ and CO is beneficial for syngas fermentations.

The overall reactions occurring in syngas fermentation for the formation of ethanol and acetate and are given as follows (Phillips et al., 1994, Klasson et al., 1992):

(i) *Acetate Synthesis*



(ii) *Ethanol Synthesis*



Evidently, a combination of the above reactions is possible with the availability of all syngas components. When butanol and butyrate are the by-products, as exhibited by certain bacteria from lignocellulosic sources, four enzymes namely, thiolase, beta-hydroxybutyryl-CoA dehydrogenase, crotonase and butyryl-CoA dehydrogenase are considered to catalyze the metabolic steps (Jones and Wood, 1986). The bioconversion of CO to butanol, BuOH, and butyrate, Bu, follows the following stoichiometry (Worden et al., 1991),



The enzymatic studies on the acetyl-CoA acetogenic pathway were reported by Ljungdahl (1986) and Wood et al. (1986). The characteristics of individual enzymes involved in the metabolic pathway for syngas fermentations, such as formate dehydrogenase, CODH, hydrogenase, and corrinoid enzyme, were described. The type of reactions catalyzed, the physiological nature and composition of the active sites of the enzymes were examined. The significance of cofactors, such as iron, nickel, and cobalt, and coenzymes such as vitamin B₁₂ was illustrated (Ljungdahl, 1986).

Methods to measure enzymatic activities that control the metabolic pathways have been discussed (Menon and Ragsdale, 1996, Lamed and Zeikus, 1980, Adams et al.,

1981). Analytic techniques for measuring the activities of hydrogenase and CODH, such as spectrophotometry, have been described by Kim et al. (1984). Analysis of enzymes such as coenzyme A transferase, butyraldehyde dehydrogenase and hydrogenase, involved in the fermentation for acetate and butanol formation by *C. acetobutylicum* are discussed by Andersch et al. (1983).

2.3 Syngas fermentations

2.3.1 Microbial catalysts used in syngas fermentations

Several species of bacteria have been reported to produce ethanol, acetate, and other by-products from syngas. *C. ljungdahlii* has been used for the biological conversion of coal-based syngas to ethanol and acetate (DOE Report, 1994, Gaddy et al., 1992, Klasson et al., 1992 and 1993, Vega et al., 1989). The organism was studied on a system of two continuous stirred tanks in series, one for maximizing cell growth and the other for maximizing ethanol production (DOE Report, 1994). The product concentration after 1100 hours of continuous operation showed 20 g/L ethanol and 4 g/L acetic acid, for a product ratio of 5 g/g. Cultured in aqueous nutrient medium under anaerobic conditions, the organism was shown to facilitate acetate production during the growth phase and ethanol during the non-growth phase. Reducing agents and nutrients affected ethanol production and the molar products ratios when the organism was studied under batch conditions (Klasson et al., 1992). *C. ljungdahlii* was shown to utilize CO, H₂ and CO₂ with conversions up to 90% based on CO and H₂ (Vega et al., 1989).

C. autoethanogenum has been isolated and utilized to produce ethanol and acetate from syngas (Abrini et al., 1994). The bacterium also utilized a wide range of

carbohydrates such as pyruvate, xylose and fructose as carbon sources. The maximum product concentrations were 0.4 g/L ethanol and 0.5 g/L acetate under batch growth conditions.

P. productus has been used to produce ethanol, acetate and methane from syngas (Klasson et al., 1991, Vega et al., 1990 and 1989). Under batch cultures, the organism produced acetate predominantly with a yield of 0.25 mol / mol CO (Vega et al., 1989). The growth rate and CO conversions by the bacterium were found to be affected by gas phase concentrations of CO. The mass transfer rate of CO from the bulk of the gas phase to the bacterial cells in solution was the limiting step for the overall process (Vega et al., 1990).

In this research, a newly discovered bacterium termed P7 is being investigated. Cell growth, substrate utilization and product formation characteristics of the bacterium must be determined to establish the viability of the process.

2.3.2 Bioreactor designs used for syngas fermentations

Several bioreactor designs have been used for the microbial conversion of bottled syngas to ethanol. Batch reactors have been commonly used to produce ethanol and by-products from syngas (Gaddy et al., 1992, Klasson et al., 1993, Vega et al., 1989, Madhukar et al., 1996). A series of reactors were used to maximize ethanol production and minimize the production of by-products (DOE Report, 1994). The design included two CSTRs in series with an ethanol recovery system using membrane extraction. The cell concentration was enhanced using a tangential filter. The conversion levels achieved for CO was 90% in the first reactor and 70% in the second. Corresponding H₂

conversions were 75% and 10% and ethanol concentrations were 8 g/L and 27 g/L in the two reactors.

Cell recycle systems were used to increase the concentration of the cells fermenting syngas in a CSTR (Klasson et al., 1993). The cell concentration increased from 0.8 g/L without cell recycle to 4 g/L with recycle. The conversion of CO was around 90% after 150 hours and that of H₂ was around 70% after 500 hours. The total product concentration increased proportional to the cell concentration. The ethanol concentration reached a maximum value of 48 g/L with 560 hours of operation.

A comparative study on bioreactor performance was performed for bottled syngas fermentations using batch, continuously stirred tank and bubble column bioreactors (Vega et al., 1990). The effects of mass transfer rates and headspace pressures in the bioreactors were reported. The bubble column provided considerably higher conversions than the CSTR at the same retention and mass transfer rates. Higher CO pressure provided increased cell concentrations in both batch and continuous cultures. Values of the mass transfer coefficient, $K_L a$, for syngas fermentations carried out in a CSTR, a packed-bubble column and a trickle-bed reactor were reported (Klasson et al., 1992). The trickle-bed reactor provided the highest mass transfer rates as compared to the CSTR and bubble column.

The power requirement for bioreactors is a critical parameter for scale-up and commercialization. For bubble columns, power is used to overcome the resistance for gas flow in the spargers and the hydrostatic head of the fluid. Bubble columns are suitable for low viscosity Newtonian fluids and provide higher energy efficiency (gas transferred/energy input) than stirred tanks (Schuler and Kargi, 1992). The absence of

moving parts in bubble columns also facilitates easy maintenance and low capital costs. The low shear environments in bubble columns are also ideal for shear-sensitive microorganisms. Foaming and bubble coalescence are the major drawbacks for bubble columns.

Spargers of various types are currently used for dispersing the gases into tiny bubbles in bubble columns (Worden et al., 1997). The disadvantages of spargers are high-pressure drops across the spargers making them unsuitable for scaled-up reactors. A method to produce micro-bubbles has been investigated and applied to syngas fermentation (Sebba, 1984, Worden et al. 1998). This method generates microbubbles by dispersing the gas in a surfactant solution at a high speed of mixing. Surfactant-stabilized microbubbles (aphrons) on the order of 25 μm have been produced using this method.

In this research work, the performance of the newly isolated bacterium, P7, will be experimentally studied in a five liter bubble column bioreactor. The design of the bubble column is expected to provide a high mass transfer area for the CO uptake by the cells. Under such circumstances, the limiting step for the overall process will be determined. Cell stability must be established at the higher scale of operation. Process performance is expected to be enhanced by cell recycle and optimization of the growth conditions for P7. Process parameters related to cell growth, substrate utilization rates and ethanol yields will be determined experimentally and optimized to enhance the commercial viability of the process. The process parameters estimated from the bubble column bioreactor will be utilized in future work on an integrated gasifier-bioreactor system for a detailed economic analysis of the entire process, scale-up to a 50 L bioreactor and finally, commercialization of the process.

2.3.3 Process parameters and modeling of syngas fermentations

Mass transfer and biochemical kinetic parameters required for the modeling and analysis of syngas fermentations include mass transfer coefficients, percentage utilization of reactants, yields of products, selectivities or molar product ratios, specific rates of cell growth, substrate uptake and product formation. Bubble columns using aphrons have shown the greatest potential for high mass transfer rates (Worden et al., 1997).

Intrinsic kinetics of the biocatalysts used in syngas fermentation to form ethanol and other products are summarized in Table 2.1. The maximum specific cell growth rate, μ_{\max} , the yield of ethanol from CO, $Y_{\text{EtOH/CO}}$, and yield of cells from CO, $Y_{X/\text{CO}}$ and the molar acetate to ethanol ratio, HAc/EtOH are the commonly reported kinetic parameters.

Cell growth kinetics for *C. butyricum* and *K. pneumoniae* under multiple product limitations, including ethanol, butanol and acetic acid were described by Zeng et al., 1994. A general growth model was proposed to describe the non-competitive nature of the inhibition kinetics. Similarly, the inhibitory effects of the products on the growth of *C. acetobutylicum* were determined by Yang et al., 1994.

A mathematical model was developed to evaluate the conversion of CO under mass transfer controlled conditions (Vega et al., 1990). The model included material balances for CO, and CO₂ in the gas phase and for CO₂ and bicarbonate equilibrium system in the liquid medium. The model assumed that the CO generated by the metabolic activity in the liquid phase, is in equilibrium with the gas-phase CO₂ and the bicarbonate in the liquid. The model was used to describe the utilization rates of CO in several bioreactor types including batch reactors, bubble columns and CSTRs (Vega et al., 1990).

Reference	μ_{max} (hr ⁻¹)	$Y_{EtOH/CO}$ (mole C/moleC)	$Y_{X/CO}$ (g/mol)	$HAc/EtOH$ (mol/mol)
Vega et al., 1989	-	-	-	0.8 to 5
Klasson et al., 1993	0.04	42.7	0.79	-
Gaddy et al., 1994	-	-	-	3 to 8
Phillips et al., 1994	0.06	0.062	1.378	1.5

Table 2.1 Experimental kinetic parameters estimated for syngas fermentations.

μ_{max} is the maximum specific cell growth rate, $Y_{EtOH/CO}$ is the ethanol yield from CO, $Y_{X/CO}$ is the cell yield from CO and $HAc/EtOH$ is the selectivity of acetate over ethanol. Microbes may differ with each reference.

As part of the modeling efforts, monod-model parameters for *Petostreptococcus productus* in batch culture with CO as the sole source of carbon and energy were reported (Vega et al., 1990, Klasson et al., 1993). Also, monod-model parameters for *Petostreptococcus productus* in batch culture with CO as the sole source of carbon and energy were reported (Vega et al., 1990).

2.3.4 Engineering issues in syngas fermentations

Methods to improve mass transfer rates of gaseous substrate to the biocatalysts were discussed in several articles [Sebba et al., 1985, Worden et al., 1997 and 1998]. Microbubbles, formed by dispersing the gases in liquid using high-speed agitated-vessels, were reported to increase mass transfer rates of gases significantly Worden et al. (1998). The role of microbubbles in enhancing oxygen transfer rates in a yeast fermentation was investigated by Jeffrey et al. (1990).

Methods to increase ethanol productivity in bioreactors includes media optimization, cell recycle systems and improved bioreactor designs (Klasson et al., 1992 and 1993). Reducing agents and amino acids influenced the cell and concentrations, and the selectivity of ethanol over acetate in *C. ljungdahlii* (Klasson et al., 1992). Cell concentrations were enhanced using a tangential flow recycle filter. The ethanol concentrations increased proportional to the cell concentrations (Klasson et al., 1993). Similarly, improving bioreactor designs, such as bioreactors in series, continuous fermentation and stripping of ethanol, were used to increase ethanol productivities (Taylor et al., 1998, DOE Report, 1994).

2.4 Optimization of process conditions

Optimization of the process conditions, such as media composition, pH, and temperature, to maximize cell and ethanol yields from bioconversion of syngas have been reported (Rani et al., 1997, Lovitt et al., 1988). The influence of reducing agents and hydrogen on ethanol yields and selectivity were discussed by Rani et al. (1997) on strains of *C. thermocellum* growing on cellulosic substrates. Metabolic regulation studies on the effects of head-space gases and sodium azide on ethanol production were also reported. Lovitt et al. (1988) found that H₂ inhibition on *C. thermohydrosulfuricum* 39E was due to the increased NADH/NAD ratio and required an electron acceptor to overcome the inhibition. Optimum temperature and pH for growth and ethanol production from cellulosic biomass were reported by Rani et al. (1998). Enhancement of ethanol production with significant suppression of acetic acid was observed in the presence of sodium azide and polyethylene glycol in *C. thermocellum* (Rani et al., 1994).

Specific to syngas fermentations, Klasson et al. (1992) reported the influence of reducing agents such as methyl viologen, benzyl viologen, ascorbic acid, etc. on ethanol production and selectivities from *C. ljungdahlii*. Reducing equivalents were reportedly directed to the formation of NADH, which in turn, resulted in increased ethanol levels in the product. The influence of nutrients such as cellobiose or rhamnose was found to favor cell and ethanol levels as compared to yeast extract.

Statistical design of experiments is popularly employed in fermentation processes where several factors that may influence the process are involved. Optimization of the factors, such as nutritional requirement, process conditions for biological reactions, has been widely studied. Central composite designs were used for the optimization of media

and process conditions for various biological processes (Gomes et al., 2000, Bowman and Geiger, 1984). Optimization of process conditions for maximal ethanol yield and productivity in a fermentation system of four CSTRs in series were reported by Kalil et al. (2000). The methodology involved an initial screening step using Plackett-Burman designs to evaluate the main effects of the factors on the response. Once the significant factors were identified, a complete factorial design was performed to assess interactions between the factors. This assessment was followed by a response surface analysis to locate the optimal operating points of the process. Similar studies on process optimization using complete or fractional factorial designs were reported in several studies (Medeiros et al., 2000, Grado and Chandra, 1998, Hwang and Hansen, 1997).

2.5 Objectives of the research

As explained in Chapter 1, the undertaken research on syngas fermentation is a critical portion of the holistic approach to produce ethanol from agricultural crops. The specific objectives for the research are:

- Establish cell stability of P7 in a bubble column bioreactor.
- Obtain kinetic parameters for cell growth, substrate utilization and product formation for P7.
- Determine the effects of process perturbations such as changes in nutrient and feed gas compositions, dilution rates, and pH and temperature shocks on the performance of P7.
- Enhance the performance of P7 by increasing the cell concentrations in the bioreactor using a cell recycle system, increasing ethanol yields by using H₂ in the

feed gas, and increasing cell growth and ethanol yields by optimizing the growth media of P7.

CHAPTER 3

STABILIZATION OF CELL CONCENTRATION

3.1 Introduction

P7 is a newly discovered bacterial species that converts syngas constituents to ethanol. To successfully grow P7 and produce ethanol on a continuous mode for long operational periods, data on critical process conditions for stable cell concentration and ethanol production, such as, the optimum pH and temperature ranges, gas and liquid flow rates, nutrient and feed gas compositions, and mass transfer and kinetic rate limitations are required.

P7 grows on a defined media first developed by Hungate (1950) for anaerobic cultures. P7 is a strict anaerobe that has been found to have low (approximately, 7000 ppm) tolerance to oxygen during the inoculum preparation stage at the University of Oklahoma. Maintaining an oxygen free (anoxic) condition in the bioreactor is very critical for cell growth and optimal enzyme activities. Enzymes, such as the reversible hydrogenase, responsible for H₂ uptake, are extremely sensitive to oxygen (Adams et al., 1981) and are instantaneously deactivated on exposure to oxygen. Evidently, a challenging task in the bioreactor design is the maintenance of anoxic conditions for the entire duration of the experiment.

Following isolation, P7 was grown under high headspace gas pressures (2 to 4 atm.) in batch cultures at the University of Oklahoma. However, cell viability of P7 over

long experimental periods under continuous operation in larger bioreactors needs to be determined, especially, since mass transfer limitations and mixing environments change with scale-up.

3.2 Objective of the Study

The specific objective was to establish process conditions such that stable concentrations of P7 are achieved over long periods of time in a bubble column bioreactor. Two bioreactor configurations were assessed:

- Chemostat with partial recycle: The stability of the cell concentration of P7 was assessed in a bubble column bioreactor under a chemostat mode of operation. The fermenter broth was continuously recirculated. A part of the recirculated liquid was withdrawn as the product and the rest was returned to the bioreactor. Fresh nutrients were added continuously at the same rate as the product removal. The gaseous reactants were continuously bubbled into the bioreactor.
- Chemostat with total recycle: The cell concentration stability of P7 was assessed when a total cell recycle system was incorporated in the bioreactor. A tangential flow membrane filter was used to separate and recycle cells from the product stream back to the bioreactor. Both the cell-free filtrate (permeate) and fresh feed were withdrawn/added continuously.

3.3 Materials and Methods

3.3.1 Microorganism

The bacterium P7 was kindly provided by Ralph Tanner, University of Oklahoma. The bacteria was isolated from an agricultural lagoon and grown in a nutrient media using strict anoxic techniques, previously described (Hungate, 1950). The media contained (per liter) 1.0 g NH₄Cl, 0.8 g NaCl, 0.1 g KCl, 0.1 g KH₂PO₄, 0.2 g MgSO₄ · 7H₂O, 0.02 g CaCl₂ · 2H₂O, 1.0 g NaHCO₃, 1.0 g yeast extract, 0.2 g cysteine hydrochloride, 0.2 g Na₂S · 9H₂O, 10 ml of trace metal solution and 10 ml of vitamin solution (see below for solution content). Enrichments were established in a mineral medium under a 100% CO atmosphere and incubated at 37°C. Bromoethanesulfonic acid (20 mM) was included to inhibit the growth of methanogenic bacteria (Tanner et al., 1998). P7 is a novel clostridial species, based on 16S rDNA sequence analysis. The organism grows autotrophically on CO and CO₂. P7 is a gram-positive, motile, rod-shaped bacterium that occasionally sporulates. In addition to syngas, the organism can also utilize sugars as carbon sources. P7 grows in the pH range of 5 to 6.

3.3.2 Media

A defined medium containing Pfenning's minerals and trace metals, vitamins, and reducing agents was used to prepare the inocula and cultivate cells in the bioreactor. The mineral stock solution contained (per liter) 40 g NaCl, 50 g NH₄Cl, 5 g KCl, 5 g KH₂PO₄, 10 g MgSO₄, and 2 g CaCl₂. The vitamin stock solution contained (per liter) 10 mg pyridoxine, 5 mg thiamine, 5 mg riboflavin, 5 mg calcium pantothenate, 5 mg thioctic

acid, 5 mg para-amino benzoic acid, 5 mg nicotinic acid, 5 mg vitamin B₁₂, 2 mg D-biotin, 2 mg folic acid, and 1 mg MESNA (2-Mercaptoethanesulfonic acid). The trace metal stock solution contained (per liter) 2 g nitrilotriacetic acid, 1 g manganese sulfate, 0.8 g ferrous ammonium sulfate, 0.2 g cobalt chloride, 0.2 g zinc sulfate, 0.02 g cupric chloride, 0.02 g nickel chloride, 0.02 g sodium molybdate, 0.02 g sodium selenate, and 0.02 g sodium tungstate. The media contained (per liter) 30 ml mineral stock solution, 10 ml vitamin stock solution, 10 ml metal stock solution, 5 g MES (N-Morpholinoethane sulfonic acid), 0.5 g yeast extract, and 5 ml of 4% cysteine-sulfide solution. 1 ml/L of 0.1% resazurin solution was added as an oxygen indicator. The chemicals were purchased from Sigma Chemical Company (St. Louis, Mo). The media costs are provided in Table 3.1.

3.3.3 Bioreactor Design and Operation

Experiments were performed in a bubble column bioreactor made of plexiglass with a height of 24 inches and inside diameter of 4.5 inches (Figure 3.1 and Table 3.2). The liquid volume was 4 to 5 liters with a one-liter, gas headspace. A fritted glass fiber disc (Ace Glass Inc., Vineland, NJ.) with a pore size between 4 and 6 microns, assembled to the base of the column, dispersed the feed gas as small bubbles. Liquid in the bubble column was recirculated at 200-300 ml/min to enhance mixing.

Saturated steam was used to sterilize the bioreactor and feed tanks. A steam generator supplied steam at 1 atm. and 100⁰C continuously to the bioreactor and accessories for at least 30 minutes. Additionally, the gases were filtered through a microporous membrane filter (0.2 μm) for sterilization. The liquid feed was sterilized by

Chemical	Cost
Mineral salts	\$ 0.026/L
Vitamins	\$ 0.009/L
Trace metals	\$ 0.002/L
MES buffer	\$ 1.365/L
Yeast extract	\$ 0.060/L
Resazurin	\$ 0.047/L
Cysteine - sodium sulfide	\$ 0.002/L
Total	\$ 1.510/L

Table 3.1. Cost of nutrients for P7 growth.

Bioreactor	Specifications
Liquid Volume	4-5 liters
Gas head space	1-2 liters
Height	75 cm
Inside Diameter	15 cm
Wall Thickness	0.6 cm
Material of Construction	Plexiglas (poly methyl methacrylate)
Liquid Flow rate	0.22 liter/hr
Total gas flow rate	18 liter/hr. at 1 atm
Product Filter	Specifications
Surface area	50 cm ²
Diameter	1.9 cm
Length of fibers	12.5 cm
Pore size	0.2 microns
Sintered Glass Filter Disc	Specifications
Diameter	15 cm
Thickness	1 cm
Pore size	0.4 microns

Table 3.2. Bubble column specifications

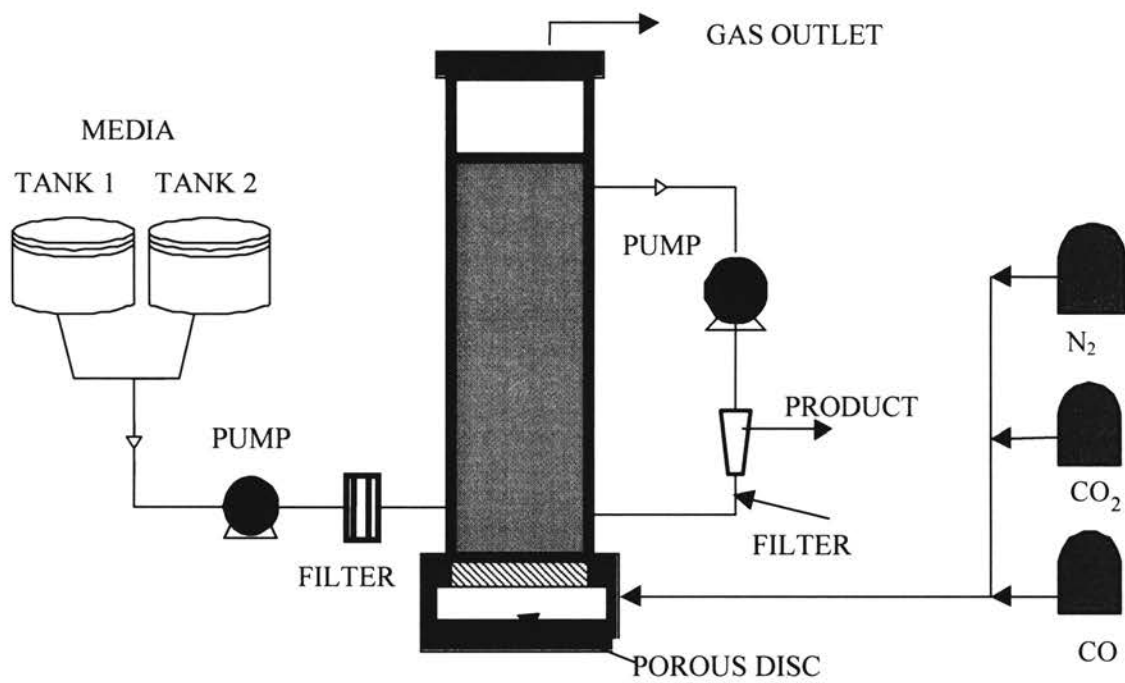


Figure 3.1. Bubble column bioreactor- Experimental layout

microporous (0.2 μm) tangential flow filter (Cole Parmer, Vernon Hills, IL) at the feed inlet of the bioreactor.

The liquid feed was prepared in two 20-liter glass tanks and kept under a N_2 atmosphere. Following the bioreactor sterilization, the media was fed to the bioreactor through a sterilization filter at 2 ml/min using a peristaltic pump to fill the bioreactor to 4.5 L. The nutrient solution was initially bubbled under N_2 for 30 minutes without sodium sulfide, cooled down to room temperature and totally deoxygenated with sterile sodium sulfide solution. Each tank was alternatively used to provide a continuous supply of fresh liquid media to the bioreactor. In the chemostat mode, the product containing the bacterial cells was withdrawn at 2 ml/min from the liquid recirculation loop and fresh nutrient media was added continuously at 2 ml/min to maintain steady state conditions in the bioreactor.

For the total cell recycle mode, a tangential flow filter was in line with the liquid recirculation loop. The product recovery system consisted of a hollow fiber tangential flow membrane filter (Spectrum Co., IL) capable of separating the bacterial cells from the products. The filter consists of a tube bundle consisting of porous fibers 12.5 cm long and capable of processing fluids with suspended solids, particulates matter and microbial cells. The product was filtered by the combined effect of microporous filtration and ultrafiltration. During the operation of the bioreactor a continuous stream of liquid from the bioreactor is recycled through the filter to recover the product from the reactant medium. 2 ml/min of the cell-free permeate was withdrawn from the filter. Fresh nutrient media was added continuously to maintain steady levels in the bioreactor. The

average residence time of the liquid in the bioreactor was 35 hrs (see Chapter 4 for calculations).

The gas flow rate to the bioreactor was 200 ml/min at 5 psig and 25°C, and consisted of CO (25%), CO₂ (15%) and N₂ (60%) blended from individual tanks (Air-Gas Co., Tulsa, OK). Hydrogen uptake by P7 is not discussed in this chapter. To remove any residual oxygen from the gases entering the bioreactor, the gases were passed through an oxygen trap (Fisher Scientific, NJ). The O₂ free gases were fed to the bioreactor through the fritted disc, which dispersed the gases into small bubbles of the order of 1 mm in diameter. The average residence time of the gas phase in the bioreactor was 11 seconds (see Chapter 4 for calculations).

The pH of the media was initially 5.75 and, as the reaction proceeded, was controlled at the lower limit of 5.3 using 1N NaOH solution. In the early stages of the research, the pH was manually controlled. Later, a computer was used to control the pH using a PI (proportional-integral) control algorithm. The reactor temperature was maintained at 37°C using a warm water coil. An electric heater supplied heat through a copper tubing to the circulating water. Warm water was circulated through flexible tubing coiled around the bioreactor. The heater load was manually controlled to maintain the bioreactor temperature.

3.3.4 Analytical Procedure

Cell concentrations in optical density (O.D.) units were determined using a spectrophotometer (Genway Model 6300, Cole Parmer, Vernon Hills, IL). Cell samples

were drawn from the bioreactor using sterile 10 ml syringes. 3 ml of the sample was transferred to 4 ml cuvettes and the O.D. was measured at 660 nm. A standard calibration chart, provided by Ralph Tanner at the University of Oklahoma, was used to estimate the actual cell numbers (Figure 3.2). Samples with an O.D. greater than 0.4 units were diluted to measure the cell concentration within the linear range of calibration, which was from 0 to 0.4 O.D. units.

Gas samples (1 ml) were collected in gas-tight syringes from the inlet and outlet gas streams of the bioreactor. Gas compositions were measured using a gas chromatograph (3800 series, Varian Co., CA) with a Hayesep-DB column (Hayes Separations Inc, Bandera, TX) connected to a thermal conductivity detector using helium as the carrier gas. Standard gas mixes (Airgas Co., Tulsa, OK) were used to develop a calibration chart for the calculation of gas compositions.

Liquid samples (5 ml) from the bioreactor were centrifuged to separate the cells. Two sets of 2 ml of the supernatant liquid were separately collected in two 4 ml capped vials. 0.2 ml from both the samples were transferred to 4 ml septa-capped vials and diluted ten times using 10% phosphate buffer solution. Known amounts of ethanol (0.008 wt. % final), acetic acid (0.004 wt. % final) and butanol (0.004 wt. % final) were added to one vial to be used as standards. Additionally, a blank solution was prepared with 10% phosphate buffer solution and spiked with the same amounts of the analytes to check the area counts of the standards. All vials were allowed to equilibrate at room temperature for at least 2 hours. The vapor-phase of each vial was analyzed for ethanol, butanol and acetic acid by the gas chromatograph using solid phase microextraction (SPME) technique (Supelco Inc., St. Louis, MO). In this technique, an adsorbent

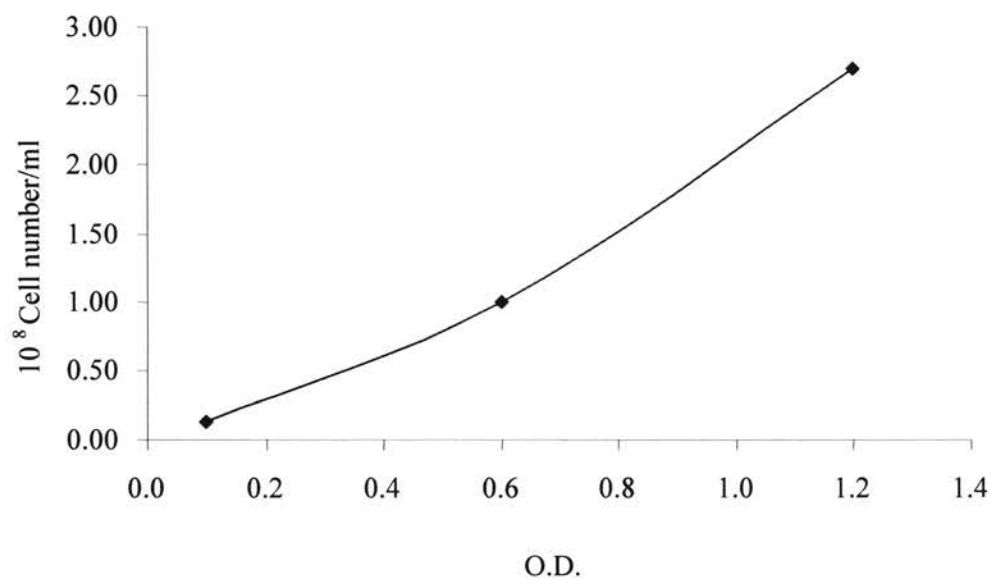


Figure 3.2. Optical density (O.D.) versus cell concentration.

Carboxen/PDMSTM fiber attached to a holder was exposed to the vapor phase inside each vial for a period of 5 min. and then injected into a CarbowaxTM capillary column (Supleco Inc., St. Louis, MO) connected to a flame ionization detector. The difference in area counts of the non-diluted sample and the spiked sample solutions was cross-checked with the area counts of the spiked blank solution for consistency since both area counts should be the same. The standard calibration chart was assumed to be linear (this was validated) with the area count for the spiked blank solution as a single data point. Additionally, the ethanol concentrations were measured with an alcohol assay kit using 0.08 wt.% and 0.16 wt.% standard solutions (ADH enzyme assay kit, Sigma Chemicals, St. Louis, MO). The sulfide concentration in the liquid was measured periodically using a sulfide kit (Sulfide assay kit, Chemetrics, Calverton, VA).

3.4 Results

Several experiments were performed with P7 lasting from one to ten weeks. The results of the runs on cell concentration instability and stability are described below:

3.4.1 Cell instability with total cell recycle

A continuous run with total cell recycle was performed for a 73-day period. Figure 3.3 shows the cell concentration (in O.D. units) during this period. The cells started to grow after a lag phase of 2 days and increased exponentially under batch conditions. The continuous mode of operation was started on Day 3. The cell O.D. was steady at 1.2 for the next 6 days. The O.D. began decreasing on Day 7 and the O.D. dropped to 0.3 units on Day 13. Following this, 3 liters of the bioreactor broth were

drained and replenished with the same volume of fresh sterile nutrients. The cells responded by growing and reaching a maximum O.D. of 1.2 units on Day 18. Cell death again occurred with the O.D. reaching 0.4 units on Day 25. Following this, 3 liters of fresh sterile nutrients were used to replace the same volume of bioreactor media. A similar trend was observed in the next growth-death cycle lasting for 11 days. In the next phase, the pH was not adjusted to investigate the response of the cells. As a result, the pH dropped to less than 4.5. Cell concentration dropped to 0.1 O.D.

On Day 41, 3 liters of bioreactor broth were drained off and replenished with fresh nutrients. The pH was maintained at around 5.5. The cell concentration recovered to a value of 1.4 O.D. The cell concentration dropped yet again to 0.78 on Day 53. Following this, 3 liters of the bioreactor broth were drained off and replenished with the same volume of fresh nutrients. Cell growth and death, similar to the earlier trends was observed. The initial pH of the bioreactor was 5.75. As cells started growing the pH dropped steadily. The pH was controlled manually during the experiment using discrete additions of 1N NaOH solution for every 6 hours. The pH profile shown in Figure 3.4, was very unstable during the experiment. The pH was observed to increase during the cell death phase and decrease during the growth phase.

3.4.2 Cell instability with partial cell recycle

A continuous run was performed without a recycle filter in the recirculation line of the bioreactor. The bioreactor broth was continuously withdrawn at 2 ml/min. Under the batch mode, the cells started growing after a short lag phase, reaching a concentration of 2 O.D. on Day 3, as shown in Figure 3.5. Continuous operation in the chemostat mode

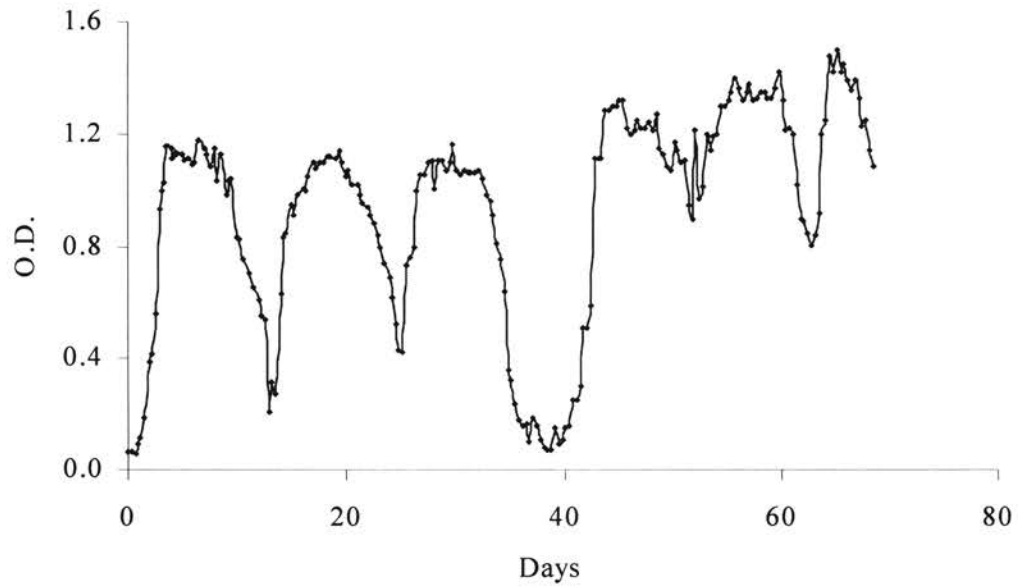


Figure 3.3. Cell instability with total cell recycle. Cell concentration is expressed in O.D. units.

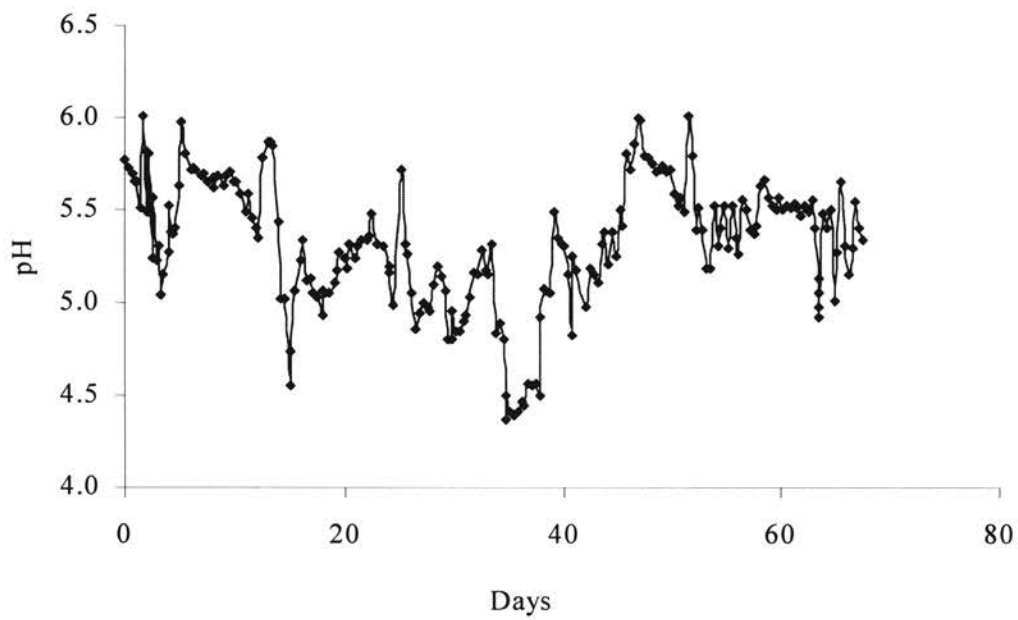


Figure 3.4. pH profile without automatic pH controller. The pH was manually controlled using 1N NaOH solution.

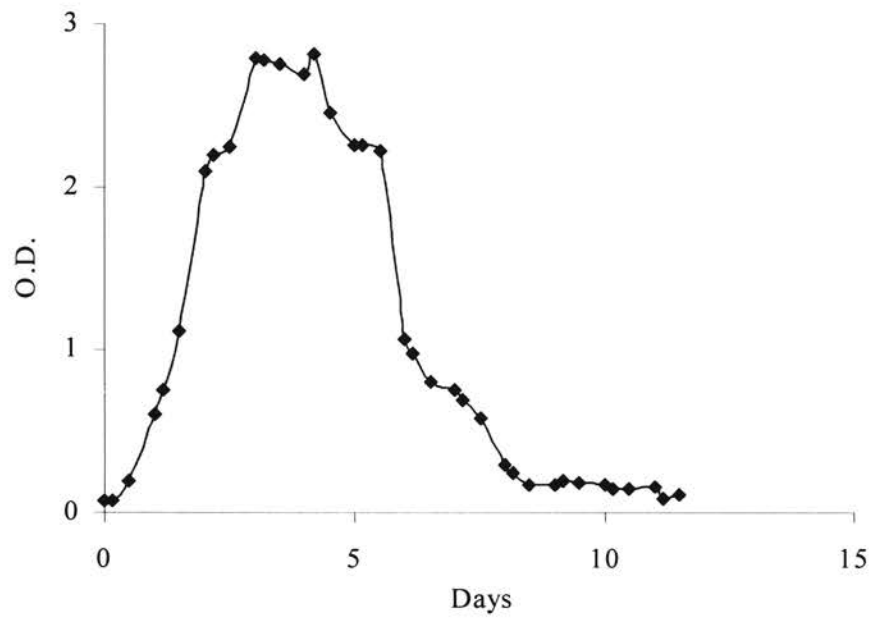


Figure 3.5. Cell instability with partial cell recycle. The cell concentration is expressed in O.D. units.

was initiated following the batch growth phase. The cell concentration reached a steady value of 2.8 O.D. for a period of 1.5 days. Cell death occurred after this steady period with the O.D. dropping to 1.0 unit on Day 6. The experiment was extended for a total period of 12 days after which the cell O.D. was less than 0.3 units during this period of the experiment.

The pH profile shown in Figure 3.6 using a pH controller at the lower pH of 5.3, showed a steady drop from the initial value of 5.75 to 5.3 as the cells started growing. With the initiation of cell death on Day 3, the pH steadily increased to a maximum value of 6.5 on Day 5. The pH values were unsteady following Day 6, possibly due to expulsion of internal cell contents into the media due to the lyses of dying cells.

Measurements of the inlet and outlet concentrations of CO from the bioreactor established the dependence of CO consumption on the cell concentration in the bioreactor. As shown in Figure 3.7, the outlet CO concentration decreased in step with the increasing cell O.D., reaching the minimum value of 7 vol% on Day 2. The inlet CO concentration was maintained at around 25 vol % during the entire period of the experiment. The CO consumption started to decrease at the onset of cell death. Negligible CO consumption was observed following Day 7.

The inlet and outlet CO₂ profiles, as shown in Figure 3.8, showed that the generation of CO₂ also depended on the cell concentration in the bioreactor. For an inlet concentration of 15 vol%, the maximum outlet CO₂ concentration was 27 vol% corresponding to maximum cell O.D. and CO consumption. With the cells dying, CO₂ generation ceased on Day 5.

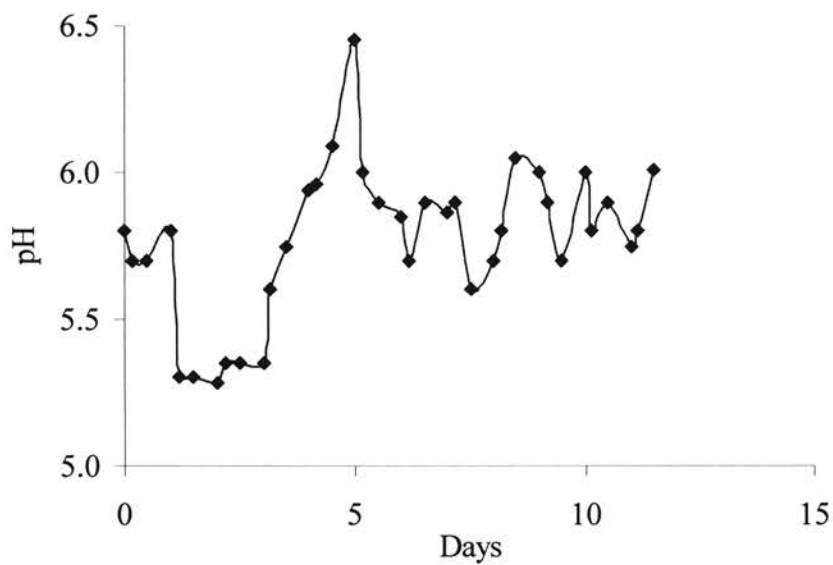


Figure 3.6. pH profile with an automatic controller. A computer based proportional-integral controller was used to control the pH.

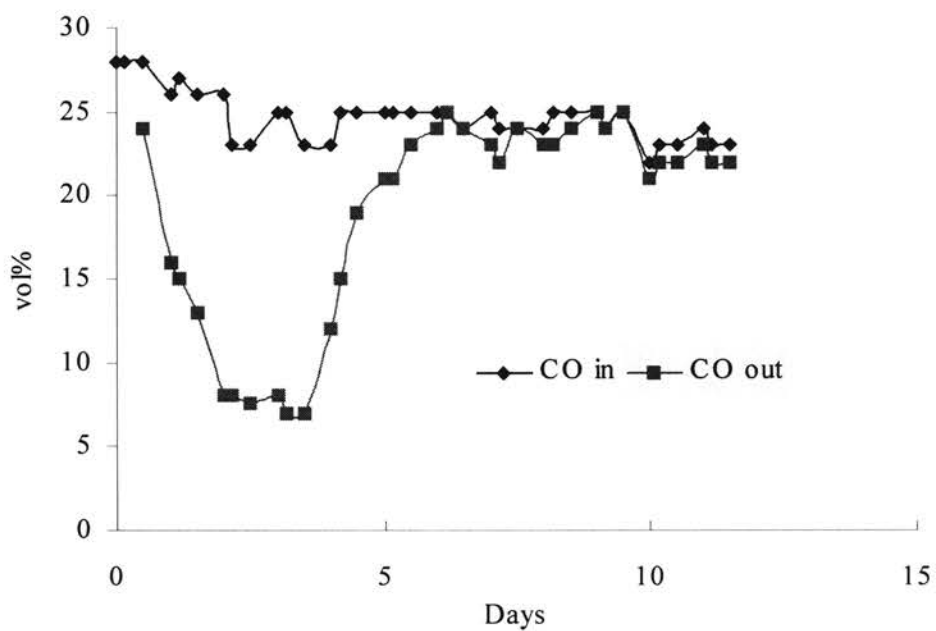


Figure 3.7. CO utilization with partial cell recycle. “CO in” is the vol% of CO in the gas stream entering the bioreactor. “CO out” is the vol% of CO in the gas stream exiting the bioreactor.

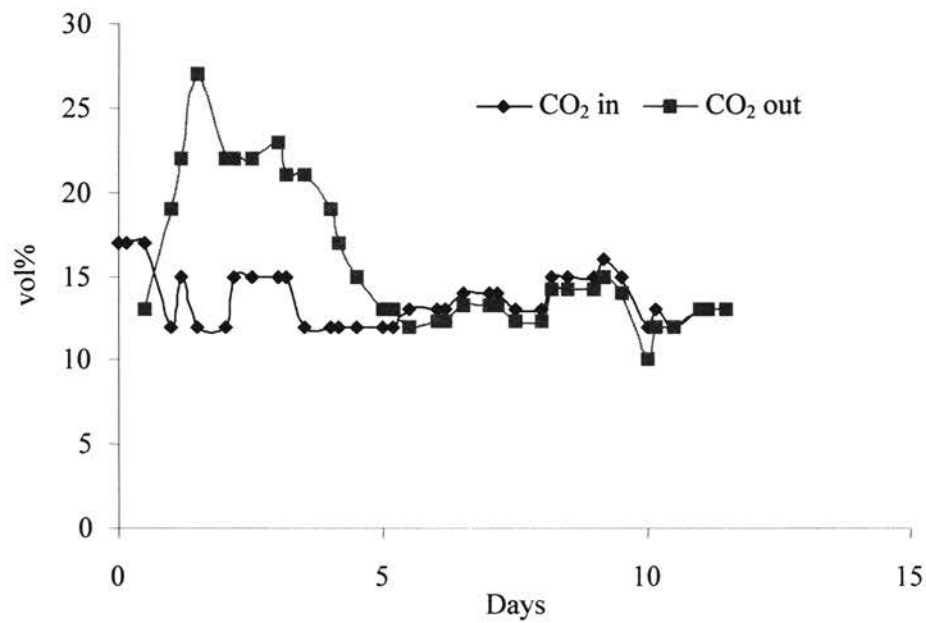


Figure 3.8. CO₂ generation with partial cell recycle. “CO₂ in” is the vol% of CO₂ in the gas stream entering the bioreactor. “CO₂ out” is the vol% of CO₂ in the gas stream exiting the bioreactor.

The ethanol concentration in the product stream of the bioreactor increased to 0.35 wt.% during the cell-growth period (Figure 3.9). At the onset of cell-death, the ethanol concentration decreased sharply to 0.1 wt. % at the end of the experiment. In addition to the above mentioned experiments, several runs were performed on the bioreactor to establish cell stability over a two-week period. Similar to the reported studies, the cell concentration was unstable and the initiation of cell death began after 2-4 days of steady cell O.D. measurements.

3.4.3 Cell Stability with sodium sulfide

During the later phase of the research on cell stability, the concentration of the reducing agent sodium sulfide was monitored closely during discrete intervals of the run using an assay kit. Prior to inoculation, 4.5 L of fresh sterile media was added to the bioreactor containing 4 ml/L of 5 wt.% sulfide solution. As the cell concentration increased, the sulfide concentration was observed to drop to levels less than 0.1 ppm over a period of 1-2 days. Fresh Na_2S was added as a 5 wt.% solution in water using sterilization filters to maintain the sulfide concentration in the bioreactor between 0.1 ppm and 1 ppm using 5 ml of sulfide solution for every 10 hours of the bioreactor operation.

Figure 3.10 shows the cell O.D. in the bioreactor when the sulfide concentration was maintained. The cells were initially grown under batch mode for 2 days with the O.D. reaching 1.3 units on Day 3. Continuous operation with partial cell recycle ensued for the next 7 days. The cell O.D. was stable at 1.7 units.

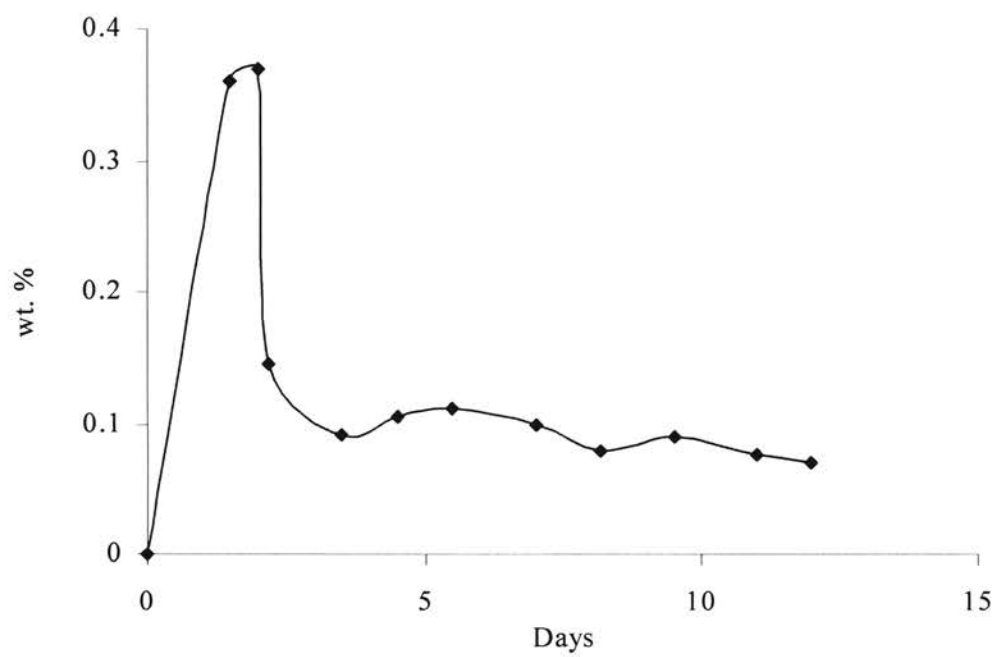


Figure 3.9. Ethanol concentration (wt.%) with partial cell recycle.

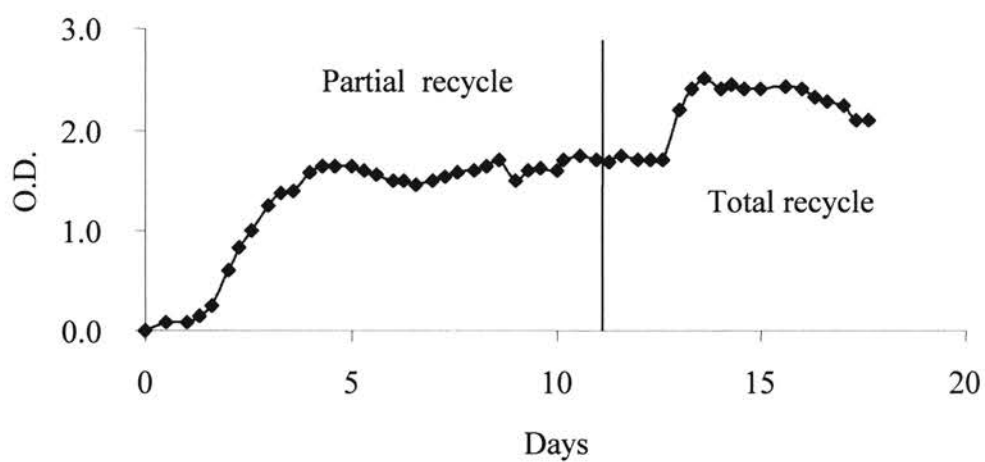


Figure 3.10. Cell concentration (O.D.). On Day 11, the bioreactor was switched from partial recycle mode to total recycle mode. The sodium sulfide concentration was maintained between 0.1-1 ppm.

Total cell recycle using the tangential flow filter was initiated on Day 10. The cell O.D. was stable at 1.7 units for the next 3 days. The concentration of the vitamin solution was increased in the nutrient feed by 50% on Day 12. This resulted in an increase in cell concentration by 0.7 O.D. and was maintained at steady state until filter fouling was detected on Day 16, with reduced flow of permeate through the membrane. CO utilization by the cells in the bioreactor was steady at a value of around 40% throughout the experiment (Figure 3.11).

The concentrations of the products are shown in Figure 3.12. The maximum ethanol concentration was 0.16 wt.% with partial cell recycle and 0.26 wt.% with total cell recycle. The maximum butanol and acetate concentrations were 0.1 wt.% and 0.03 wt.%, respectively. Characteristics of the product synthesis by P7 are discussed in detail in Chapter 4.

An experiment was performed with partial cell recycle for 12 days to assess cell stability due to sodium sulfide in the bioreactor operated with partial cell recycle. The cells were grown under batch mode for a period of 4 days. The nutrient solution contained 50% excess trace metals as compared to the previous experiment. Following a lag phase of 2 days, the cell O.D. started to increase exponentially to 3.1 units, as shown in Figure 3.13. A continuous mode of operation was initiated during the late exponential growth phase. The cell concentration dropped to 2.8 O.D. by the end of Day 5 and stabilized till Day 8. On Day 8, the trace metal concentration was reduced to the original level of 10 ml/L. The cell O.D. increased and stabilized at 3.3 units for the next 4 days. (The experiment proceeded beyond Day 12 with hydrogen in the feed gas. Hydrogen uptake is discussed in later chapters).

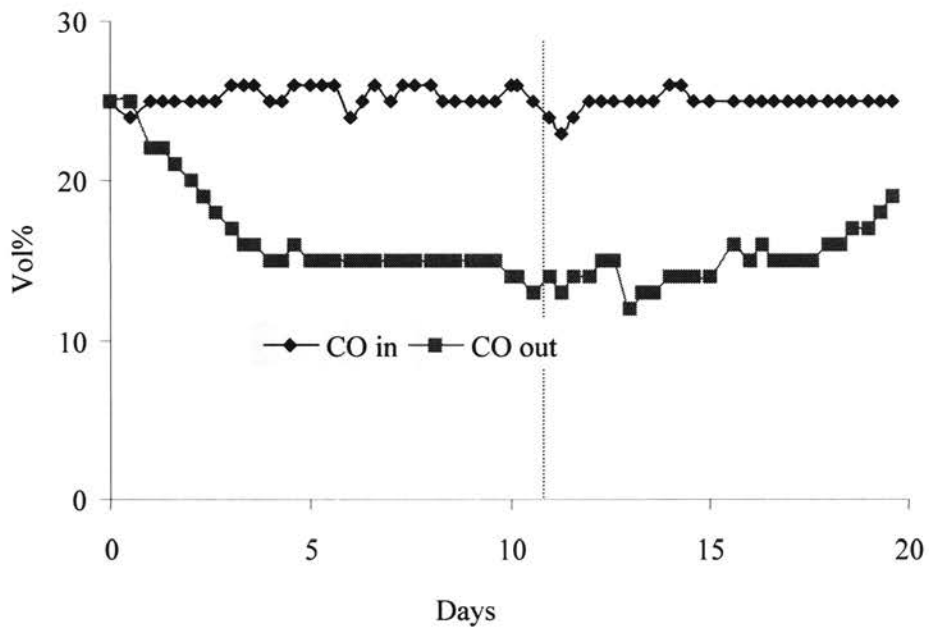


Figure 3.11. CO utilization. On Day 11, the bioreactor was switched from partial recycle mode to total recycle mode. The sodium sulfide concentration was maintained between 0.1-1 ppm. “CO in” is the vol% of CO in the gas stream entering the bioreactor. “CO out” is the vol% of CO in the gas stream exiting the bioreactor.

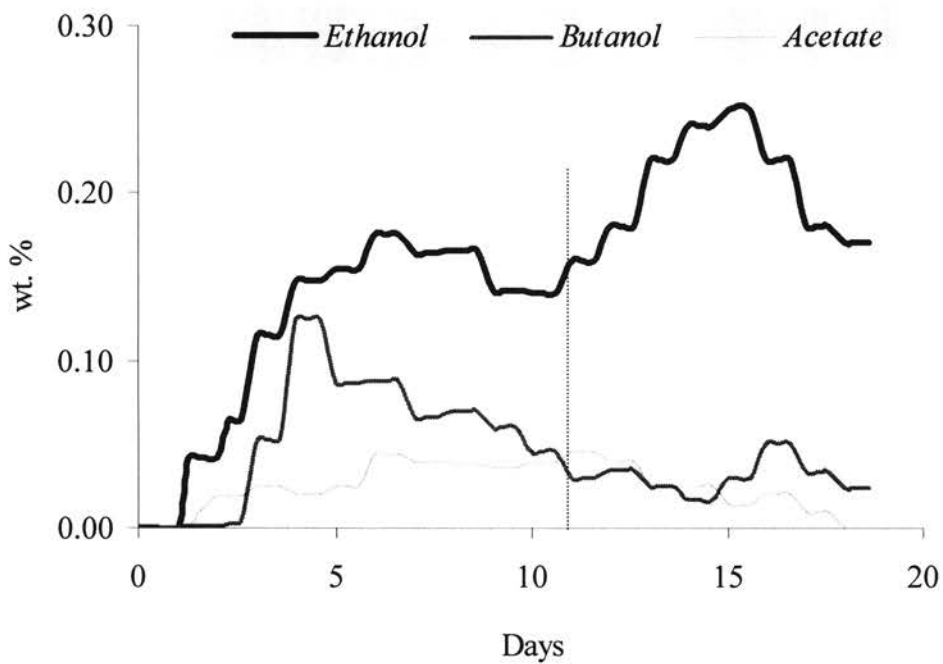


Figure 3.12. Product concentrations (wt.%). On Day 11, the bioreactor was switched from partial recycle mode to total recycle mode. The sodium sulfide concentration was maintained between 0.1-1 ppm.

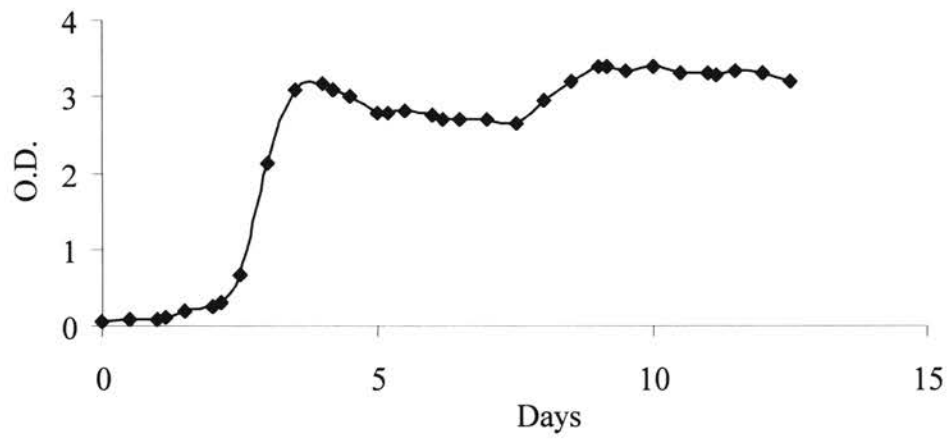


Figure 3.13. Cell concentration with partial cell cycle. The sodium sulfide concentration was maintained between 0.1-1 ppm.

The CO concentration profiles at the inlet and outlet of the bioreactor during the experiment are shown in Figure 3.14. The inlet CO concentration was maintained at approximately 25 % by volume. The outlet CO concentration decreased with a decrease in cell O.D. and stabilized at 17-18% during the entire period of the experiment. The concentrations of the products were not stable during the experiment (Figure 3.15). A maximum ethanol concentration of 0.33 wt. % was achieved during the later phase of the experiment. The acetate and butanol concentrations were both approximately 0.04 wt. % during the period.

3.5 Discussion

Cell instability in the bioreactor was due to limitations on the availability of sodium sulfide in the media during operations with total and partial cell recycle. As the cells started growing, a sharp decrease in the concentration of the reducing agent, sodium sulfide was observed. In the absence of external additions of fresh sodium sulfide, the redox potential of the environment in the bioreactor was not conducive for an active cell growth. Anaerobic bacteria, such as P7, prefer an environment with low redox potential (Rao and Mutharasan, 1988).

The drop in sulfide concentration was likely due to the consumption of sulfide by the cells and/or sodium sulfide stripping as a result of the outflowing gases from the bioreactor. Discrete injections of sodium sulfide sustained an appreciable concentration of sulfide (0.1 to 1 ppm) and facilitated stable cell growth. Reducing agents, such as titanium citrate, have been shown to increase the specific cell growth rate of several anaerobes (Zehnder and Wuhrman, 1976, Smith and Pearson, 1979).

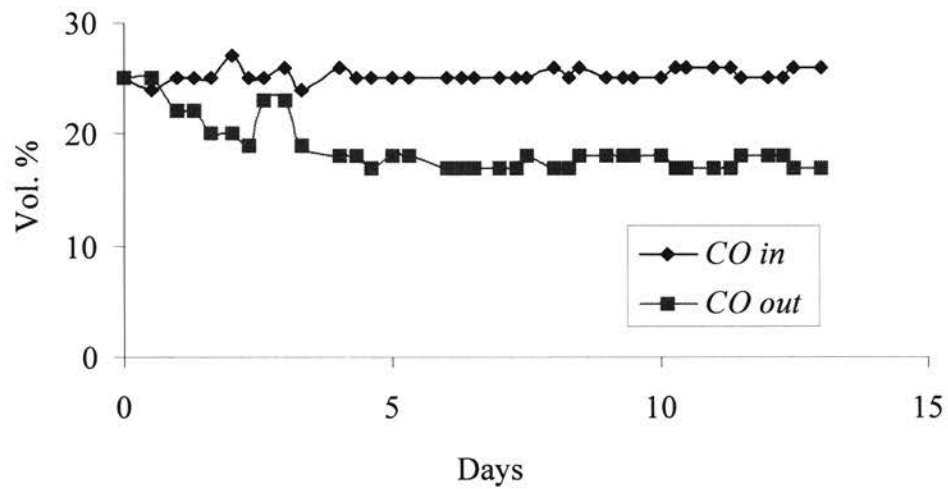


Figure 3.14. CO utilization with partial cell recycle. The sodium sulfide concentration was maintained between 0.1-1 ppm. “CO in” is the vol% of CO in the gas stream entering the bioreactor. “CO out” is the vol% of CO in the gas stream exiting the bioreactor.

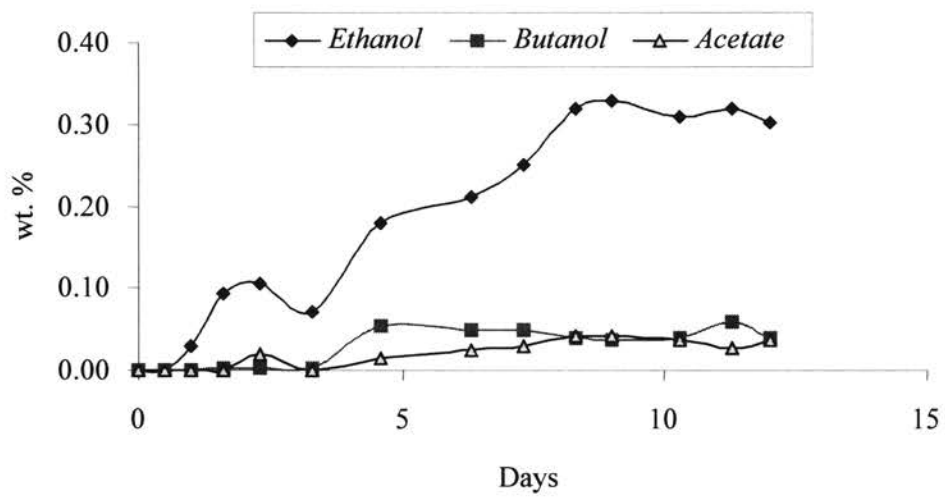


Figure 3.15. Product concentrations (wt.%) with partial cell recycle. The sodium sulfide concentration was maintained between 0.1-1 ppm.

The primary purpose of the reducing agent was to provide an oxygen free media inside the bioreactor. Reducing agents such as sodium sulfide, and sodium dithionate, altered growth rates and electron flow pathways (Rao and Mutharasan, 1988). The reducing agents donate electrons that can reduce a metabolic intermediate resulting in altered electron flow pathways. In addition to affecting cell growth rate, reducing agents were found to affect product distribution in several bacteria. Ethanol was the preferred product of the metabolic activity of *Thermoanaerobacter ethanolicus* under increased reducing agent concentration (Rao et al., 1987). The primary mode of action of reducing agents was reportedly via redox sensitive proteins in the cell membrane that accept or donate electrons to the environment.

3.6 Conclusion

Cell instability was a major problem during the initial phase of experimentation on the bioreactor. Without regular additions of sodium sulfide, experiments conducted with total and partial cell recycle, resulted in steady drops in the cell concentration following a short stable growth period. On the other hand, cell growth was stable in either modes of operations when sodium sulfide concentration was closely monitored and maintained in the range of 0.1 ppm to 1 ppm. The role of reducing agents, such as sodium sulfide, in altering electron flow pathways was reportedly responsible for active cell growth rates and product distributions in several anaerobes similar to P7 (Rao and Mutharasan, 1988, Rao, 1987). The experiments conducted on the bubble column bioreactor established the mandatory requirement of sodium sulfide for stable cell growth conditions under both partial and total cell recycle modes of operation.

CHAPTER 4

CELL GROWTH, SUBSTRATE UTILIZATION AND PRODUCT FORMATION

4.1 Introduction

The bioconversion of the syngas to liquid products by P7 is a complex, heterogeneous process. Bacterial cells suspended in nutrient liquid media in the bioreactor catalyze the conversion of syngas (CO, H₂ and CO₂) to ethanol and other products. Syngas from the bulk gas is transferred to the active sites of the cells through a series of individual steps. Resistance to syngas transfer can be encountered in the following locations (Blanch and Clark, 1997):

- R1. Gas film within the bubble
- R2. Gas-liquid interface
- R3. Liquid film surrounding the gas-liquid interface
- R4. Bulk liquid
- R5. Liquid film surrounding the cells
- R6. Liquid-cell interface
- R7. Intracellular spaces
- R8. Active sites within cells at which the conversion of syngas occurs

The resistances occur in series with only the largest resistance(s) controlling. By comparison to the rate controlling resistances, some of the individual resistances can be

eliminated. Since gas phase diffusivities are typically much higher than liquid phase diffusivities, R1 and R2 can be neglected. Also, since the diffusivities at the liquid cell interface is much higher than that of the liquid phase, R6 can be neglected. Under well-mixed liquid conditions R4 can also be neglected (Blanch and Clark, 1997). Mass transfer resistances (R3, R5 and R7) and reaction rate resistance, R8 can be rate controlling depending on the relative sizes of the cells and bubbles and the rheology of the liquids.

Specific to syngas fermentations, the main resistance for gas transfer to the cells has been observed to be the liquid film surrounding the bubbles, R3 (Vega et al., 1990). Under the mass transfer controlled regime, the dissolved concentration of the limiting syngas component in the liquid approaches zero due to the rapid uptake by the cells (R8 is negligible compared to R3). Under intrinsic kinetic limitations, R3 is negligible compared to R8 and the dissolved syngas concentration is not zero.

Experimental methods to determine process parameters were reported under mass transfer controlled regimes (Vega et al., 1990, Klasson et al., 1992). Parameters such as the volumetric mass transfer coefficient, $K_L a$, intrinsic kinetic parameters such as the specific cell growth rate, μ , specific CO consumption rate, q_{CO} , yields, Y , and product selectivities were determined.

For this study, CO is targeted as the syngas component for the assessment of mass transfer/kinetic limitations. Unfortunately, under kinetic limitations, efforts to characterize simultaneous mass transfer and reaction rates are complicated by the lack of a convenient and a reliable liquid phase CO assay (Worden et al., 1989). Intrinsic

kinetics controlled by the enzymatic activities inside the cells are influenced by several media components, such as minerals, trace metals, vitamins and reducing agents.

The limiting step for the overall CO bioconversion process and specific kinetic parameters of P7 related to cell growth, CO utilization and product formation are discussed in this chapter.

4.2 Objectives of the study

The specific objectives addressed in this chapter focus on the following:

- Identify the rate controlling mechanism and the limiting reactant(s) for the microbial catalysis of CO/CO₂ in the bubble column bioreactor.
- Estimate the kinetic parameters of cell growth, CO utilization and product formation for comparison with previous studies with other CO-consuming bacteria.

4.3 Materials and Methods

4.3.1 Microorganism

The bacterium P7, used in the study, was isolated and provided by Dr. Ralph Tanner, University of Oklahoma. The inoculum was prepared as per the procedure described in Chapter 3. Fresh inoculum (100 ml) that was grown on CO and CO₂ was used for initiating each experiment.

4.3.2 Bioreactor media

The anoxic media was prepared as described in Chapter 3. Initially, the bioreactor was filled with 4.5 L of the sterile media and inoculated for initiating cell growth under batch conditions. The gases were continuously bubbled as described below. Under the continuous mode, two 20 L glass tanks were used alternately to provide a continuous flow of anoxic media to the bioreactor. Several media compositions were used for different runs on the bioreactor. For simplicity, media containing ‘x’ ml/L mineral solution, ‘y’ ml/L vitamin solution and ‘z’ ml/L trace metal solution is denoted by “Media x-y-z” in this chapter. The composition of each solution is discussed in Chapter 3.

4.3.3 Bioreactor operation

All the experiments were performed in the 4.5-L bubble column bioreactor, described in Chapter 3. In the chemostat mode, the product stream containing the bacterial cells was withdrawn from the liquid recirculation line and fresh nutrient media was added continuously at the same rate to maintain steady state conditions in the bioreactor.

The gas flow rate to the bioreactor was 200 ml/min at 5 psig and 25°C. Gas compositions used for specific studies varied as described below. The gases were sterilized using a microporous membrane filter (0.2 μm) prior to entering the bioreactor. Analytical methods for measuring concentrations of cells, products (ethanol, butanol and acetate) and reactant gases (CO and CO₂) are mentioned in Chapter 3.

4.3.4 Methodology

4.3.4.1 Rate limiting mechanism

Previous studies have identified the mass transfer rate of the gaseous reactant across the liquid film surrounding the bubble (R3) as the limiting step of the overall process (Klasson et al., 1991, Phillips et al., 1994, Worden et al., 1997). However, due to the smaller size of the bubbles generated by the porous disc in the 4.5 L bubble column bioreactor, as compared to traditional sparging, suggest that intrinsic kinetics of the bacterial cells could be the rate controlling step.

The experimental technique for identifying the overall rate controlling step is illustrated as follows. For intrinsic kinetic limitations, the liquid nutrient compositions are varied and the response of the cell concentration is monitored. If cell growth and CO utilization rates are affected by changes in a specific liquid nutrient composition, then the bioreactor is limited by the intrinsic kinetics of the bacteria. On the other hand, if changes in the CO concentration in the feed gas stream affect cell growth, nutrient uptake and product formation rates, then the bioreactor is limited by the mass transfer rates of CO to the cells.

4.3.4.2 Kinetic parameters

Cell growth rates

The rate of increase of cell concentration (R_X) in the bioreactor is proportional to the concentration of the cells (X) such that,

$$R_X = \mu X \quad 4.1$$

For a well mixed batch system, the material balance for cells gives

$$\frac{dX}{dt} = R_X \quad 4.2$$

The value of μ varies according to the operating conditions of the bioreactor. For a constant μ during the growth phase, integration of Eq. 4.2 with $X = X_0$ at $t = t_0$,

$$\ln \frac{X}{X_0} = \mu (t - t_0) \quad 4.3$$

where, X_0 is the initial cell concentration at the onset of the exponential growth phase at time, t_0 , (usually zero) X is the cell concentration in O.D. units at time, t . The plot of $\ln(X/X_0)$ versus $(t - t_0)$ yields a straight line with a slope equal to μ , the specific cell growth rate. Another parameter of interest for batch cell growth is the doubling time, t_D , defined as the time required for the cell concentration to double. Based on Eq. 4.3, t_D is

$$t_D = \ln \frac{2}{\mu} \quad 4.4$$

When the death rate of the cells is significant, μ is a combination of the actual cell growth rate, μ^* and the specific cell death rate (k_d).

In the chemostat mode, the product stream containing the bacterial cells is continuously withdrawn from the bioreactor and fresh nutrient media is added continuously at the same rate to maintain steady state conditions in the bioreactor. Under steady state conditions and a sterile, cell-free feed, the cell balance gives,

$$\frac{dX}{dt} = -DX + R_x \quad 4.5$$

where D is the reactor liquid volume divided by the liquid flow rate. Thus at steady state, $\mu = D$. Again, μ can be comprised of μ^* and k_d and is directly calculated from the nutrient flow rate and the media volume in the bioreactor.

% CO utilization

With CO as the sole carbon source, the conversion of CO is estimated from the molar flow rates of CO measured at the inlet and outlet of the bioreactor. Using the ideal gas law, the volumetric flow rates of CO are converted to molar flow rates. The difference in the molar flow rates of CO-in and CO-out equals CO-consumed by the bacteria such that,

$$CO_{in} = \left(\frac{PVy}{RT}\right)_{in} \quad 4.6$$

$$CO_{out} = \left(\frac{PVy}{RT}\right)_{out} \quad 4.7$$

$$\% CO \text{ utilization} = \frac{(CO_{in} - CO_{out})}{CO_{in}} * 100 \quad 4.8$$

where CO_{in} and CO_{out} are expressed in moles/min., V is the total volumetric flow rate of the gas in ml/min, y is the volume fraction of CO, R is the gas constant, and T is the gas temperature in K. V was measured using a turbine flowmeter (Cole Parmer, Vernon Hills) accurate to ± 6 ml/min, as provided by the instrument manufacturer. y was measured using a GC as described in Chapter 3 precise up to $\pm 1\%$ (3800 series, Varian Co., CA). T was measured using a J-type thermocouple (Cole Parmer, Vernon Hills) accurate to $\pm 0.4\%$. P was measured using a high accuracy pressure gauge accurate to $\pm 1\%$. The accuracy data are based on manufacturer information.

Yield of CO₂

The theoretical yield of CO₂ from CO is 0.67 mole C/mole C, when ethanol is the sole-product of the bioconversion process, as shown by equation 2.1 in Chapter 2. The actual yield of CO₂ will be different than the theoretical value due to the formation of by-products such as acetic acid and butanol. The yield of CO₂ is calculated as

$$Y_{\text{CO}_2/\text{CO}} = \frac{(\text{CO}_{2,\text{out}} - \text{CO}_{2,\text{in}})}{(\text{CO}_{\text{in}} - \text{CO}_{\text{out}})} \quad 4.9$$

where CO_{in} and CO_{out} are molar CO flow rates in moles/min., and $\text{CO}_{2,\text{in}}$ and $\text{CO}_{2,\text{out}}$ are molar flow rates of CO_2 expressed in moles/min. The molar flow rates of CO_2 were measured as that of CO described earlier.

Yields of products

The theoretical maximum yield of ethanol from CO as the sole carbon source is 0.33 mole C/mole C, as previously shown by equation 2.1 in Chapter 2. The maximum, possible yields of the by-products acetic acid and butanol are 0.5 mole C/mole CO and 0.67 mole C/mole CO (Worden et al., 1994). The product (P) yields are calculated as,

$$Y_{\text{P/CO}} = (\text{moles of C in product formed/min.})/(\text{CO}_{\text{in}} - \text{CO}_{\text{out}}) \quad 4.10$$

$(\text{CO}_{\text{in}} - \text{CO}_{\text{out}})$ was determined as described earlier. The molar product flow rates were obtained from the flow rate of the product stream from the bioreactor, F_L , and the concentration of the specific product in the product stream. F_L was directly measured from liquid samples collected over a period of time. The actual molar flow rate of carbon in the products was determined from the molar flow rates and theoretical carbon contents in ethanol (2 C moles/mole), butanol (4 C moles/mole) and acetate (2 C moles/mole). The concentrations of ethanol, butanol and acetate in the product stream were measured using solid-phase microextraction (SPME) technique on a GC as described in Chapter 3. The liquid analysis was accurate to $\pm 10\%$ as observed from multiple measurements using standard analytes.

Yield of cells

The experimental yields of cells from CO are calculated as,

$$Y_{X/CO} = (\text{g cells formed/min.})/(\text{CO}_{in} - \text{CO}_{out}) \quad 4.11$$

$(\text{CO}_{in} - \text{CO}_{out})$ was determined as described earlier. The actual growth rate (R_X times reactor volume) of the cells was estimated from measured cell concentrations, X in g cells/ml, and the flow rate of the product stream, F_L in ml/min, since the actual growth rate is equivalent to the mass flow rate (see Eq. 4.5). To calculate X in g cells/ml, the cell number/ml were first calculated from O.D. measurements of the sample using the standard calibration chart, shown in Figure 3.3. The cell number/ml was converted to g cells/ml using reported values of bacterial cell mass, (10^{-12} g/cell, Schuler and Kargi, 1992). Also, bacterial cells reportedly contain 50% carbon on a mass basis (Schuler and Kargi, 1992). Based on this data, the actual molar flow rate (12 g/mole C) of carbon in the cells was determined.

Specific CO uptake rate

The specific CO uptake rate (q_{CO}) is defined as the amount of CO consumed per unit time per unit mass of cells, such that

$$q_{CO} = (\text{CO}_{in} - \text{CO}_{out})/(\text{g cells in the bioreactor}) \quad 4.12$$

$(CO_{in} - CO_{out})$ was determined as described earlier. The actual grams of cells in the bioreactor was determined from the cell concentration, X in g cells/ml, multiplied with the liquid volume, V_L in ml, in the bioreactor.

Specific ethanol formation rate, q_{EtOH}

The specific product formation rate is the ratio of the molar production rate of the specific product per unit mass of cells in the bioreactor. For ethanol,

$$q_{EtOH} = (\text{moles of C in ethanol formed/min.})/(\text{g cells in the bioreactor}) \quad 4.13$$

The moles of C in ethanol/min. were determined as described earlier.

Residence time

The gas residence time in the bioreactor was measured from the gas hold-up, V_G , in the bioreactor and the volumetric gas flow rate, F_G . For the gas,

$$t_G = \frac{V_G}{F_G} \quad 4.14$$

The liquid residence time was calculated from the liquid hold-up, V_L and the liquid flow rate, F_L . For the liquid,

$$t_L = \frac{V_L}{F_L} \quad 4.15$$

The total volume of the aerated liquid, V , was measured directly from the liquid height and inner diameter of the bioreactor. The gas flow rate was then cut-off and the volume of the bubble-free liquid, V_L , was measured. The actual gas hold-up, V_G , was equal to $V - V_L$.

4.4 Results

4.4.1 Rate controlling step

A continuous experiment was carried out for over a two-week period. The gas flow rate was 200 ml/min at 25 °C and 5 psig, containing 25% CO, 60% N₂ and 15% CO₂. Media 20-10-5 was initially used. The effect of doubling the trace metal concentration using media 20-10-10 on cell growth, CO utilization and product formation is discussed as follows:

4.4.1.1 Cell growth

Following inoculation, the cells grew under batch conditions for a period of 3 days in the bioreactor as shown in Figure 4.1. The cells started growing after a lag phase of one day. Continuous mode of operation was started on Day 4 with a dilution rate of 0.027 hr⁻¹ (Phase I). The cell concentration at steady state was around 1.15 O.D. At the end of six days, the trace metal concentration in the bioreactor feed was doubled from 5 ml/liter to 10 ml/liter (Phase II). After 24 hours, the cell concentration increased to 2.3 O.D. On Day 10, the temperature of the bioreactor decreased due to equipment failure from 37°C to 25°C for a day and was then restored, as shown in Figure 4.2. The cell concentration dropped to 1.7 O.D. and recovered to 2.3 O.D. when the temperature was restored to 37 °C. On Day 14, the iron content in the liquid feed was reduced to 50% of

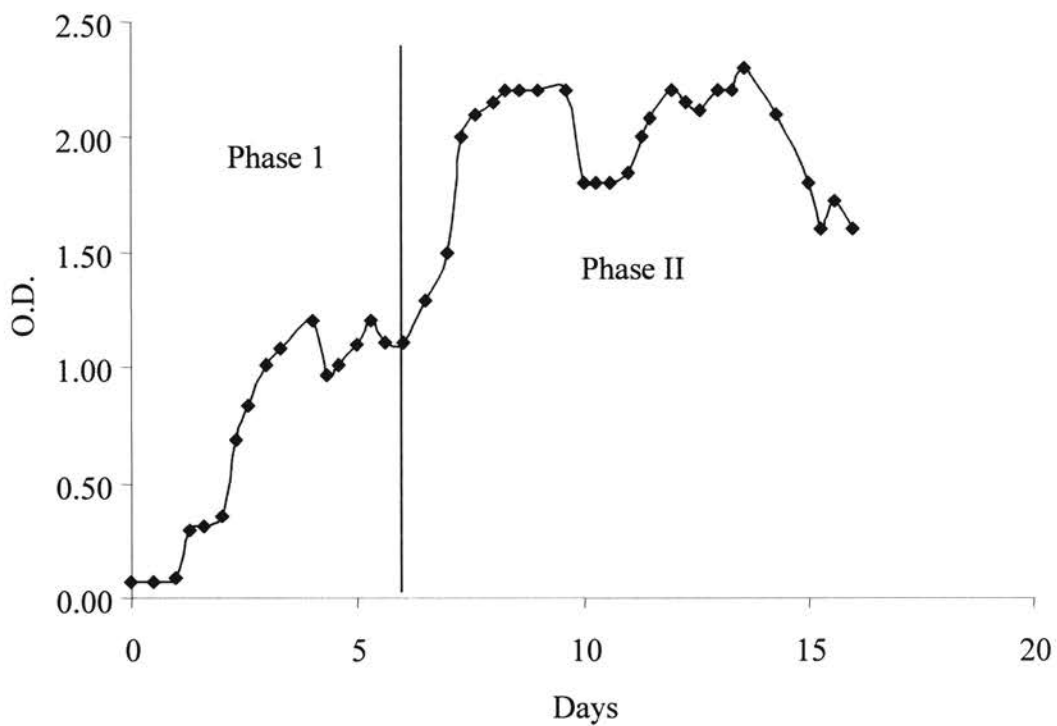


Figure 4.1. Effect of trace metal concentrations on cell growth. During phase I, the trace metal concentration was 5 ml/L of media. During phase II, the trace metal concentration was increased to 10 ml/L.

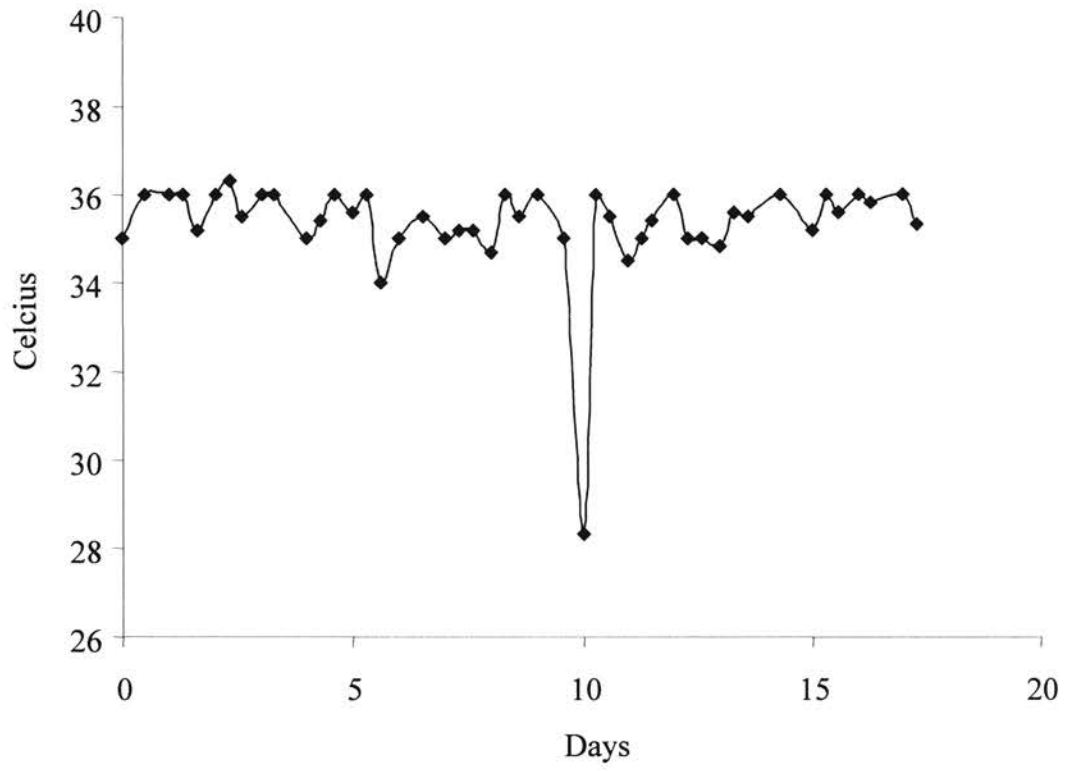


Figure 4.2. Temperature profile versus time.

the original composition. The cell concentration showed a steady decline until Day 16 when the experiment was terminated.

4.4.1.2 CO utilization

Following the lag phase, CO utilization increased with cell concentration in the bioreactor, as shown in Figure 4.3. During Phase I, the CO utilization stabilized at 30% on a molar basis. As the trace metal concentration was doubled during Phase II, the CO utilization approximately doubled to 60% establishing that the uptake rate of CO was not limited by the mass transfer rate, but the intrinsic kinetics of the microbial catalysts. CO utilization dropped temporarily to less than 50%, due to the sudden drop in the temperature of the bioreactor. Following the cell recovery from the temperature shock, CO utilization settled at 55%. Cell death, due to the 50% decrement in iron content of the media, lowered the CO utilization to less than 40%. As expected, the specific CO uptake rate of the cells, q_{CO} , remained more or less unaffected by the change in trace metals concentration (i.e. CO utilization was directly proportional to cell concentration). The steady state value q_{CO} was approximately 0.9 moles CO consumed/(min·g cells). The CO₂ yield from CO was in the range of 55% to 65% over the entire period of the experiment.

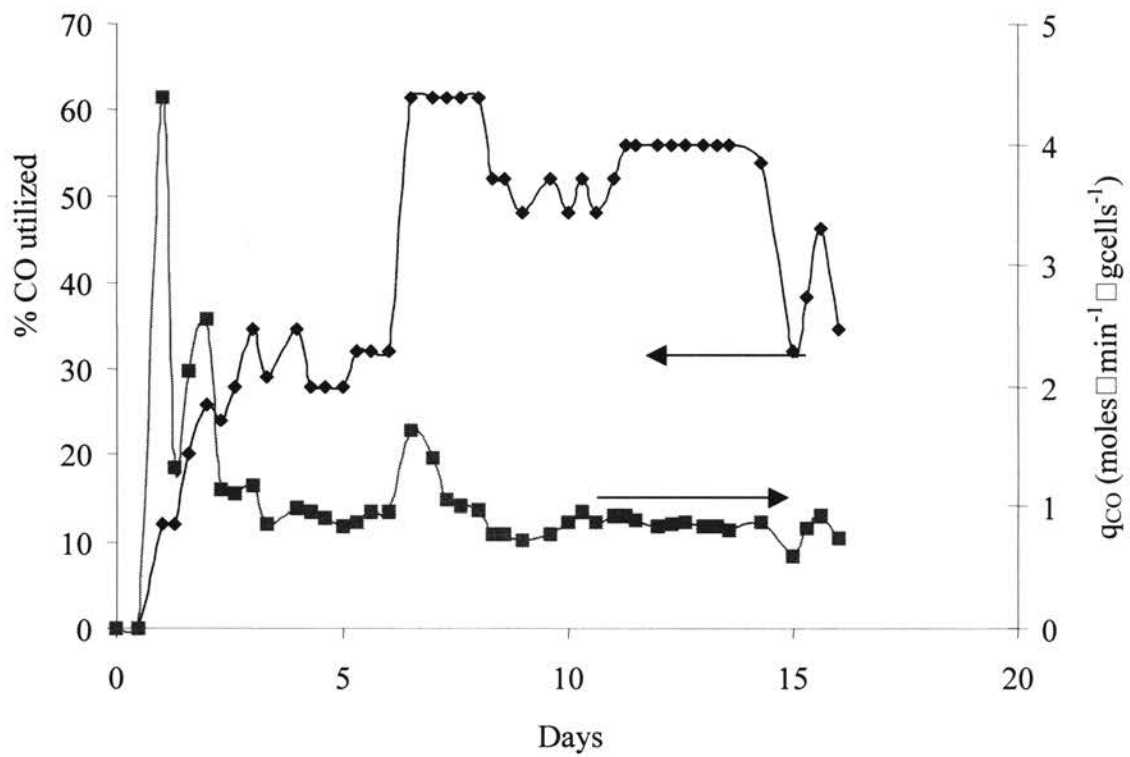


Figure 4.3. CO utilization and specific CO uptake rate (q_{CO}) by P7. CO utilization was calculated using Eq. 4.8. q_{CO} was calculated using Eq. 4.12.

4.4.2. Kinetic parameters

Average liquid and gas residence times

The total volume of the aerated liquid in the bioreactor was 4.5 L. The gas hold-up, directly measured from aerated and non-aerated liquid volumes, was 50 ml. At a total gas flow rate of 200 ml/min, 1.3 atm and 25°C, the average gas residence time in the bioreactor at 37°C and one atm was 11 seconds. The average liquid residence time was 35 hours and 14 hours at 2ml/min and 5 ml/min, respectively.

Specific cell growth rates

The concentration of cells, X (in O.D. units) measured from liquid samples over the period of each experiment was used to calculate μ , the specific cell growth rate during the batch growth phase. The value of μ was different for different runs depending on the operating conditions and potential inoculum differences of the bioreactor. A plot of $\ln(X/X_0)$ versus time for a typical experiment is shown in Figure 4.4. The slope of the graph gave the value of μ as 0.11 hr^{-1} .

Similarly, μ was calculated for other runs with different operating conditions in the bioreactor as listed in Table 4.1. For Trial-1, the media 20-10-5 provided μ of 0.05 hr^{-1} . During Trial-2, the media 25-10-10 resulted in μ of 0.11 hr^{-1} . During Trials 3 and 4, both media 25-15-15 and media 30-10-10 resulted in μ of 0.066 hr^{-1} . Notably, Trials 1 through 4 were performed without a recycle filter in the 4.5 L bubble column bioreactor. Trial 5 with media 30-10-10 was performed with a recycle filter. The value of μ , during

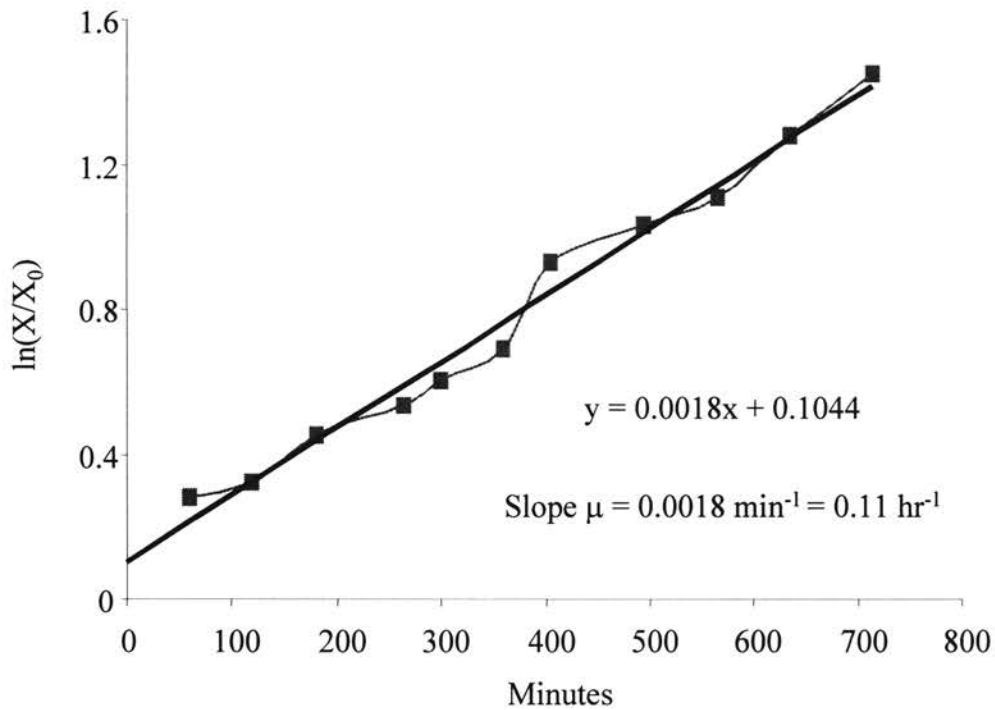


Figure 4.4. Batch growth curve of P7. X_0 is the cell concentration in O.D. units at time $t_0 = 0$. X is the cell concentration in O.D. units at any time, t . The plot of $\ln(X/X_0)$ versus time is a straight line with the slope = μ (see Eq. 4.3). Error analysis in the estimation of μ is shown in Appendix II.

Trial #	Media	Mode	μ (hr ⁻¹)	t_D (hours)
1	20-10-5	No Filter	0.050	14
2	25-10-10	No Filter	0.110	6
3	25-15-15	No Filter	0.066	11
4	30-10-10	No Filter	0.066	11
5	30-10-10	Filter	0.030	23

Table 4.1. Growth rate (μ) and doubling times (t_D) for P7. μ was calculated as shown in Figure 4.4. $t_D = 0.693/\mu$.

the initial batch mode was 0.03 hr^{-1} . Clearly, the presence of the recycle filter decreased the effective cell growth rate. The phenomena will be addressed in the future.

The doubling time, t_D , was the lowest for media 25-10-10 at 6 hrs and the highest for media 20-10-5 at 14. With the recycle filter, t_D increased further to 23 hrs, as shown in Table 4.1. The results showed that cells multiplied at a slower rate (over longer time intervals) due to the presence of the recycle filter.

During the chemostat mode of operation (which occurred after the initial batch mode) μ is equal to D , the dilution rate as shown in Eq. 4.5. Trials 1, 3 and 4 were performed in a chemostat mode with the liquid flowing at 2 ml/min, corresponding to a μ of 0.027 hr^{-1} . During Trial 2, three different liquid flow rates were used, 2 ml/min, 3.2 ml/min, and 5 ml/min. Correspondingly, the values of μ equal to D during steady state were 0.027 hr^{-1} , 0.043 hr^{-1} and 0.066 hr^{-1} .

% CO utilization

As shown in Table 4.2, the % CO utilization was dependent on the operating conditions of the bioreactor. Media 20-10-5 provided a maximum CO utilization of 32% at steady state conditions. As the trace metal concentration was doubled it increased to 62%. Media 25-10-10 provided up to 80% CO utilization and media 30-10-10 provided up to 75% CO utilization. However, per unit cell, CO utilization was independent of the type of media, as described below.

Trial #	Media	Mode	% CO utilized	$q_{CO} * 10^3$	$Y_{X/CO}$	$Y_{CO_2/CO}$
1a	20-10-5	No Filter	24-32	0.8-1.1	0.42-0.53	0.57-0.65
1b	20-10-10	No Filter	47-62	0.8-1.0	0.47-0.59	0.60-0.65
2	25-10-10	No Filter	50-80	0.7-1.7	0.40-0.58	0.65-0.70
3	25-15-15	No Filter	50-75	0.6-0.9	0.49-0.56	0.57-0.68
4	30-10-10	No Filter	40-45	0.7-1.0	0.43-0.55	0.60-0.65
5	30-10-10	Filter	40-50	0.8-1.2	N	0.55-0.63

Table 4.2. CO utilization, specific CO uptake rate (q_{CO}), cell yield from CO ($Y_{X/CO}$) and CO₂ yield from CO ($Y_{CO_2/CO}$) for P7. q_{CO} is in moles CO/(min□g cells) and $Y_{X/CO}$ in in g cells/mole CO.

Specific CO uptake rate (q_{CO})

Steady state values of q_{CO} for different operating conditions of the bioreactor are shown in Table 4.2. For all the trials, the experimental values of q_{CO} were within the range of 0.7 mmoles CO/min.g cells and 1.7 mmoles CO/min.g cells. Thus, CO consumption was clearly a function of the cell concentration and not the media composition.

Cell yield from CO ($Y_{X/CO}$)

Interestingly, for all the operating conditions of the bioreactor, the experimental values of $Y_{X/CO}$, were approximately in the range of 0.45 - 0.59 g cell/mole CO (Table 4.2). The generation rate of the cells in the bioreactor influenced the utilization rate of CO, and hence, the average yield, $Y_{X/CO}$ was 0.5 g cells/mole CO.

Product yields from CO (Y_P/CO)

As shown in Table 4.3, the yields of ethanol, butanol and acetate were not stable even during steady state conditions of the other variables, such as, cell concentration, liquid level in the bioreactor and CO consumption and CO₂ production rates. The yield of ethanol varied between 0.10 mole C/mole CO to 0.28 mole C/mole CO. Butanol yield varied between 0.02 and 0.16 mole C/mole CO, while that of acetate varied between 0 and 0.07 mole C/mole CO.

Trial #	Media	Mode	$Y_{\text{EtOH}/\text{CO}}$	$Y_{\text{BuOH}/\text{CO}}$	$Y_{\text{Ace.}/\text{CO}}$	$q_{\text{EtOH}} * 10^3$
1a	20-10-5	No Filter	0.18-0.2	0.03-0.05	0.015-0.020	0.12-0.20
1b	20-10-10	No Filter	0.18-0.22	0.02-0.04	0.015-0.020	0.15-0.25
2	25-10-10	No Filter	0.18-0.28	0.02-0.05	-	0.15-0.30
3	25-15-15	No Filter	0.10-0.24	0.05-0.16	0.020-0.070	0.09-0.20
4	30-10-10	No Filter	0.10-0.19	0.05-0.13	0.013-0.030	0.08-0.13
5	30-10-10	Filter	0.11-0.15	0.01-0.06	0.005-0.015	0.13-0.15

Table 4.3. Product yields from CO and the specific ethanol production rate for P7. Ethanol yield, $Y_{\text{EtOH}/\text{CO}}$, butanol yield, $Y_{\text{BuOH}/\text{CO}}$ and acetate yield, $Y_{\text{Ace}/\text{CO}}$ are expressed in mole C/mole CO. The specific ethanol production rate, q_{EtOH} is expressed in (mole C in ethanol)/(min \times g cells).

Yield of CO₂ from CO ($Y_{CO_2/CO}$)

The yield of CO₂ from CO was approximately in the range of 0.55 to 0.70 for all the experiments as shown in Table 4.2. The theoretical yield of CO₂ from CO is 0.67 with ethanol or butanol as the sole-product, and 0.50 if acetate is the sole-product of the bioconversion of CO, based on the stoichiometry shown in Chapter 2. Evidently, the yield of CO₂ depended on the generated products during the bioconversion process.

Specific production rate of ethanol (q_{EtOH})

The specific ethanol production rate, expressed as the rate of production of ethanol as mmoles C per gram of cells per min was in the range of 0.12 to 0.2 for the media 20-10-5 and 0.15 to 0.25 for the media 20-10-10 as shown in Table 4.3. For media 25-10-10, q_{EtOH} increased from 0.15 at a dilution rate of 0.027 hr⁻¹ to 0.25 at a dilution rate of 0.066 hr⁻¹. For all the trials, values of q_{EtOH} were in the range of 0.08 to 0.2. Evidently, high dilution rates enhanced the specific production rate of ethanol by the bacterial cells in the bioreactor, perhaps by raising the nutrient composition in the bioreactor (i.e. fresh feed was added at a faster rate). This agrees with the earlier observations in that media composition was the limiting factor for CO utilization.

Discussions

The limiting step for the biological production of ethanol from P7 with the current bioreactor configuration is not the mass transfer rate of the gaseous reactants to the cells, but rather, the intrinsic kinetic rate of the cells. The cell concentration and CO utilization approximately doubled when the trace metal concentration was doubled. The fine size of

the bubbles (less than 1 mm) generated by the fritted disc has expectedly increased the mass transfer surface area, (a), resulting in sufficient volumetric mass transfer coefficient ($K_L a$) to eliminate a mass-transfer controlled regime, as explained below.

The transport of CO from the gas phase to the liquid phase is given by,

$$\text{CO transport rate} = \frac{K_L a}{H} (P^G - P^L) V_L \quad 4.16$$

where P^G is the average partial pressure of CO in the gas phase in atm, P^L is the partial pressure of CO in equilibrium with the CO concentration in the bulk liquid phase in atm, $K_L a$ is the overall mass-transfer coefficient (hr^{-1}), and H is the Henry's law constant in $\text{atm m}^3/\text{mol CO}$, V_L is the liquid volume in the bioreactor in m^3 . In the liquid phase, the CO uptake rate is a function of the cell concentration, X , and the specific CO uptake rate, q_{CO} , such that,

$$\text{CO consumption rate} = q_{\text{CO}} X V_L \quad 4.17$$

where V_L is the liquid volume in the bioreactor. For a system under mass transfer limitations, the CO uptake rate by the cells is faster than the CO transport rate resulting in $P^L = 0$. At steady state, the CO uptake rate is equal to the CO transport rate,

$$\frac{K_L a}{H} V_L P^G = q_{\text{CO}} X V_L \quad 4.18$$

Therefore, under mass transfer limitations, the cell concentration in the bioreactor is a function of the average CO partial pressure in the bulk gas. However, the results from the bioreactor, as shown in Figure 4.1, demonstrated that the cell concentration was limited by the media composition and not the gas composition. Thus, bioreactor

performance was not limited by the mass transfer rate of CO, but by the intrinsic kinetics of the bacterial cells or the mass transfer of the liquid nutrients to the cells.

As shown in Figure 4.3, the CO uptake increased from 30% to 60%, as cell concentration doubled during phase II of the run. This is again consistent with kinetic limitations on the utilization of CO.

One of the limiting nutrients identified for cell growth was iron in the trace metal solution. The cell concentration doubled with the doubling of the trace metal concentration, as shown in Figure 4.1. On Day 14, as the iron content was decreased to 50% of the original composition, the cell concentration dropped from 2.3 O.D. units to 1.5 O.D. units. Obviously, cell growth was limited by the iron content in the medium.

Results of the experiments performed on the bioreactor showed that the cell growth, CO uptake and product formation rates of P7 were influenced by the media compositions and operating conditions of the bioreactor.

During the chemostat mode, the specific cell growth rate was the highest for media 25-10-10 and lowest for media 20-10-5 establishing a strong dependence of cell growth on media composition. The addition of the recycle filter resulted in decreased growth rates of P7. This is expectedly due to the increase in specific death rates, k_d , due to a possible shearing environment in the filter. For a given media composition, the actual growth rate, μ^* is generally dependent only on the limiting nutrient, as described by Monod's growth model (Blanch and Clark, 1997). Under such conditions, the observed cell growth rate, $\mu = \mu^* - k_d$, is influenced by the death rate, k_d , of the cells.

CO utilization was affected by both the dilution rate, D , and the cell concentration, X , in the bioreactor under a chemostat mode of operation. CO utilization

essentially doubled during Trial 1 when X doubled due to the increment in trace metals. On the other hand, Trial 2 showed that as D was increased from 0.027 hr^{-1} to 0.066 hr^{-1} , the cell concentration decreased while the % CO utilization was unaffected (thus, the specific CO uptake rate, q_{CO} increased). q_{CO} was estimated at 0.67 to 0.8 mmole CO/(min· g cells) at $D = 0.027 \text{ hr}^{-1}$ and 1.7 mole CO/min· g cells at $D = 0.066 \text{ hr}^{-1}$. This demonstrated that CO utilization not only depended on X but also on D (i.e., the rate of CO utilization depended on the production rate of the cells in the bioreactor). Also the yield of cells, measured as the production rate of cells over the consumption rate of CO, was approximately 0.5 g cells/ mole CO for all the experiments in the bioreactor.

The yields of products from CO were not stable during the experiment. Specifically, unstable ethanol yields resulted in unstable specific ethanol production rates, q_{EtOH} , in the bioreactor. Additional details on metabolic pathway responsible for the production of ethanol, acetate and butanol are required to explain this phenomenon. Also, the activities of the enzymes, the concentration profiles of the metabolic intermediates, such as acetyl-CoA, and the carbon and electron flows during the process need investigation.

The yield of ethanol from CO as compared to acetate and butanol is higher by 6 and 2 times respectively, establishing a high level of product selectivity and specificity of P7. However, as much as 60% of CO was utilized for CO_2 production during both phases, as expected for growth on CO alone. By introducing hydrogen, the utilization of carbon for the production of ethanol can potentially be increased.

As a comparison, the results of a similar fermentation study using batch-grown *C. ljungdahlii* showed yields of 0.062 for $Y_{\text{EtOH}/\text{CO}}$ and 0.094 for $Y_{\text{Acetate}/\text{CO}}$ on a molar carbon

basis, and a cell yield, $Y_{X/CO}$ of 1.378 g/mol (Phillips et al., 1994). P7 showed yields up to 0.28 for $Y_{EtOH/CO}$ and 0.02 for $Y_{Acetate/CO}$ on a molar carbon basis, and a cell yield, $Y_{X/CO}$ of 0.59 g/mol. Obviously, P7 provided a higher ethanol selectivity and yield on CO, while *C. ljungdahlii* showed a higher cell yield on CO. Therefore, P7 shows good potential for ethanol conversion since the organism has only been studied for the last two years as compared to over a decade for *C. ljungdahlii*.

Finally, the residence time was 11 seconds for the gas phase and 14 hrs to 35 hrs for the liquid phase in the 4.5 L bubble column bioreactor. A similar bioconversion process performed on a CSTR utilized a gas residence time of 14.7 min and a liquid residence time of 30.4 hrs (Putsche et al, 1999).

4.5 Conclusions

The five liter bubble column bioreactor is currently limited by the intrinsic kinetics of the bacterial cells (nutrient limitations) and not by the mass transfer rate of CO from the bulk gas phase to the cells. The fine size of the bubbles dispersed by the porous fritted disc provided sufficient mass transfer area for CO transfer.

As a result of the kinetic limitations, the metabolic activities of P7 are sensitive to changes in nutrient levels in the bioreactor. Therefore, optimization of nutrient requirements to maximize the metabolic activities of P7 is required

The estimates of the kinetic parameters showed that the cell growth, CO uptake and product formation characteristics of P7 were influenced by the media compositions and operating conditions of the bioreactor. The results of CO conversion using P7 were compared to that of a similar fermentation using *C. ljungdahlii*. P7 provided a higher

ethanol selectivity and yield on CO, while *C. ljungdahlii* showed a higher cell yield on CO.

CHAPTER 5

EFFECTS OF PROCESS PERTURBATIONS

5.1 Introduction

The production of ethanol from CO, CO₂ and H₂ in the bubble column bioreactor requires continuous operations at nearly stable conditions prior to scale-up and commercialization. Industrial scale operations of the bioreactor are susceptible to process variations such as pH, temperature, flow rates and compositions of nutrients that may result in cell death and/or loss of microbial activity. The ability of the bacterium P7 to recover from process shocks due to changes in process conditions are discussed in this chapter.

Process variations in the bubble column bioreactor considered for this study includes changes in nutrient flow rates and composition, pH, temperature and changes in feed gas compositions. Responses of P7 to both intentional and unintentional disturbances (due to equipment breakdowns) are included in this chapter.

The nutrient flow rate influences the productivities of the products. As reported in Chapter 3 of this research work, the 4.5 L bubble column bioreactor is currently limited by the intrinsic kinetics (nutrient limitations) of the bacterium-P7. Variations in nutrient compositions were introduced to estimate the performance of the bacteria.

Under no gas phase mass transfer limitations, changes in gas composition were not expected to affect the performance of the cells. Specific experiments on the

bioreactor performed with CO as the sole carbon source were expected to be unaffected by the CO₂ composition in the feed gas. Metabolic requirement of CO₂ for P7 was expected to be provided by the conversion of CO to CO₂ as shown by Eq. 3.1 (see chapter 3).

Process shocks such as the operating pH and temperature were expected to result in loss of enzyme-activities and/or cell death. Experimental verification was required to assess the ability of the cells to recover from process shocks and maintain normal activities for cell growth and product synthesis.

5.2 Objectives of the study

The specific objectives of this study are listed as follows:

1. Determine the effect of dilution rate of liquid nutrients on cell growth, CO utilization and product formation.
2. Determine the effects of nutrient compositions on cell growth and product yields from CO.
3. Determine the effects of eliminating CO₂ from the feed gas such that only CO and N₂ were present.
4. Determine the effects of pH and temperature shocks on the stability of the cells in the bioreactor.

5.3 Materials and methods

5.3.1 Microorganism

The bacterium-P7 was provided by Dr. Ralph Tanner, University of Oklahoma. Isolation and culture techniques for the bacterium are discussed in Chapter 3.

5.3.2 Media

A defined medium containing Pfenning's minerals and trace metals, vitamins, and reducing agents was used to prepare the inocula and cultivate cells in the bioreactor. The compositions of the stock solutions are provided in Chapter 3. Individual studies described in this chapter were performed with different compositions of the minerals, vitamins and trace metals and are mentioned in the respective studies. Commonly, the media contained (per liter) 5 g MES, 0.5 g yeast extract, 5 ml of 4% cysteine-sulfide solution and 0.1 ml of 0.1% resazurin solution.

5.3.3 Bioreactor design and operation

All the experiments were performed in the 4.5-L bubble column bioreactor, described in Chapter 3. In the chemostat mode, the product stream containing the bacterial cells was withdrawn from the liquid recirculation line and fresh nutrient media was added continuously at the same rate to maintain steady state conditions in the bioreactor. Nutrient feed preparation for the experiments are explained in Chapter 3.

The gas flow rate to the bioreactor was 200 ml/min at 5 psig and 25°C. Gas compositions used for specific studies are mentioned under the respective sections. The

gases were sterilized via a microporous membrane filter (0.2 μm). Analytical methods for measuring concentrations of cells, products and reactant gases are mentioned in Chapter 3.

5.3.4 Process perturbations

For this study, the following process disturbances were considered:

- Changes in dilution rate, D
- Changes in trace metal composition
- CO_2 cut-off in the feed gas
- Shocks in operating temperature and pH

The effects of the above mentioned disturbances on process parameters such as the specific cell growth rate (μ), % CO utilization, yields (Y) of products and CO_2 from CO, and specific CO uptake rate (q_{CO}) are described. The parameters were calculated as shown in Chapter 4.

5.4 Results

5.4.1 Effect of dilution rate on bioreactor performance

Initially, 100 ml of inoculum was transferred under sterile conditions into 4 liters of anoxic media containing 25 ml/l minerals, 15 ml/l vitamins and 10 ml/l of trace metals. The initial pH was maintained at 6.3. The flow rate of the nutrient solution was varied from 2-5 ml/min, as shown in Figure 5.1. The effects of varying the nutrient feed rates on the concentrations of cells and products, CO utilization and productivities of the bioreactor are discussed in the following sections.

5.4.1.1 Cell growth

Cells were grown under batch mode for a period of 2 days (Figure 5.2). The initial pH was 6.3 and was controlled at a lower value of 5.2, as shown in Figure 5.3. After a lag phase of 1 day, the cells started growing. At a cell concentration of 2.5 O.D., fresh nutrient solution at a pH of 5.5 was initiated at a flow rate of 2 ml/min. The pH of the bioreactor increased due to the incoming nutrient solution followed by a drop in cell concentration to 1.65 O.D. on Day 4. Fresh nutrients with a pH of 5.35 were started on Day 4. The cell concentration recovered and reached a steady value of 3.2 O.D.

The liquid flow rate was increased to 3.2 ml/min on Day 7. The cell concentration started to decrease due to the higher dilution rate. Under steady state conditions, the cell concentration was stable at around 2.3 O.D. The flow rate was further increased to 5 ml/min on Day 9. The cell concentration dropped to 1.7 O.D. However, due to the non-availability of a nutrient, the bioreactor was run in a batch mode for a period of one day. During this period, the cell concentration increased from 1.7 to 3.3 O.D., as expected from the batch growth conditions.

Following the temporary batch phase, fresh feed was initiated at 5 ml/min on Day 12. The cell O.D. dropped to 1.7 units, as observed earlier for a flow rate of 5 ml/min.. Following a steady state period of 2 days, the nutrient flow rate was restored to 2 ml/min. The experiment was terminated following a stable cell concentration of 3.3 O.D, similar to the earlier observations for 3 ml/min from Days 4 -7.

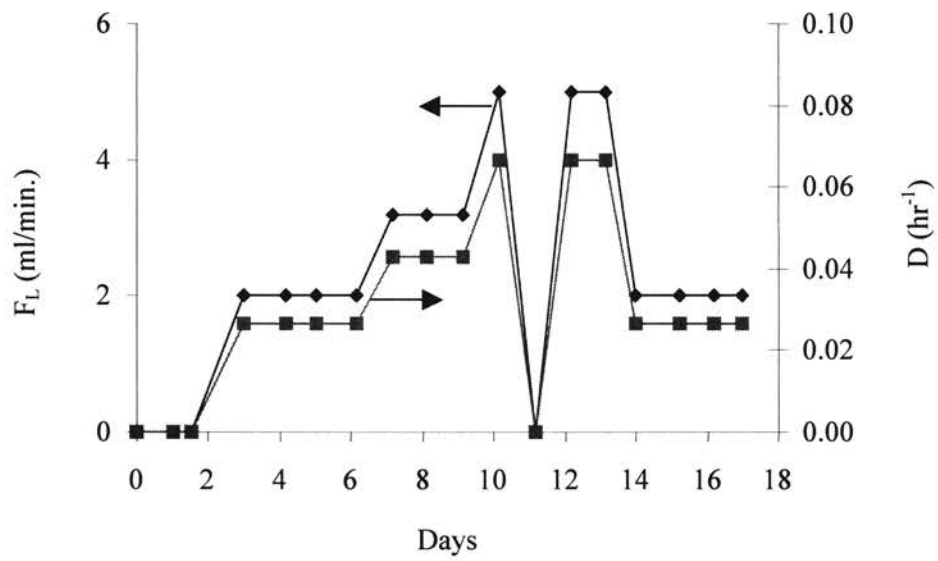


Figure 5.1. Perturbations in the flow rate of nutrients. The nutrient flow rate F_L and the total liquid volume, V_L , in the bioreactor were used to calculate the dilution rate, $D = F_L/V_L$.

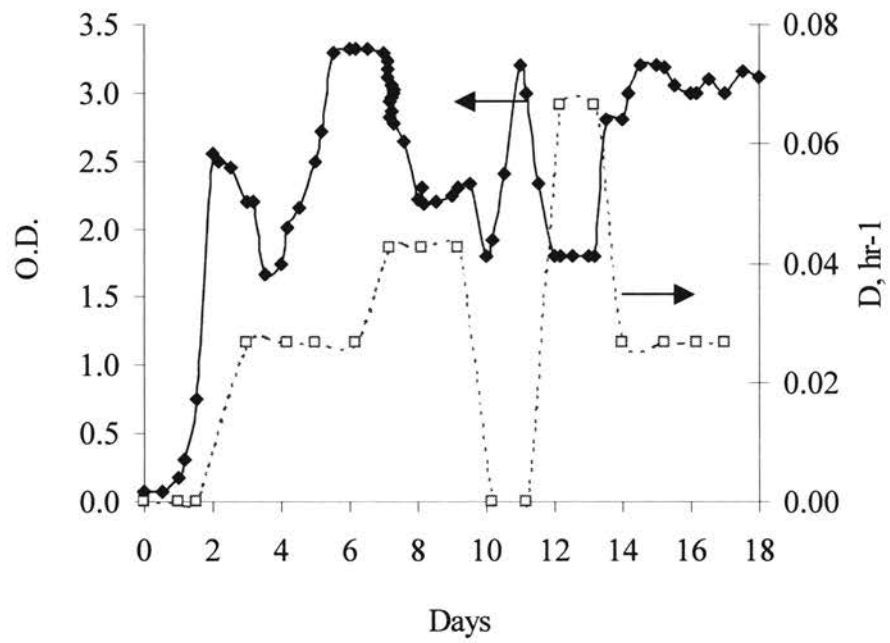


Figure 5.2. Cell concentration (O.D.) in the bioreactor for different dilution rates, D (hr^{-1}).

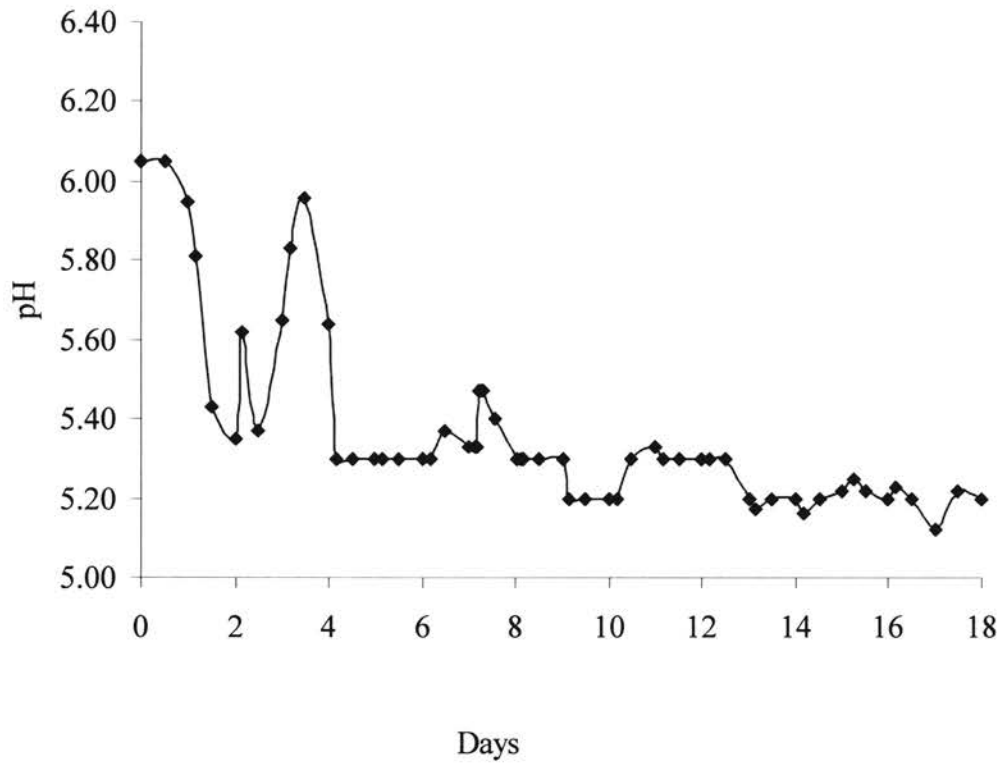


Figure 5.3. pH profile in the bioreactor. pH increased from 5.4 to 5.95 from Day 2 to 3 due to high pH of the nutrient feed.

The specific growth rate of the cells during the initial batch phase was estimated to be 0.11 hr^{-1} . During the chemostat mode, the specific growth rate is equal to the dilution rate, D , calculated as the ratio of the liquid flow rate to the liquid volume of the bioreactor. D was 0.027 hr^{-1} at 2 ml/min , 0.043 hr^{-1} at 3.2 ml/min , and 0.066 hr^{-1} at 5 ml/min

5.4.1.2 CO utilization

The percentage utilization of CO by the bacterial cells in the bioreactor increased following the lag phase to 60% (Figure 5.4). During the initial decrease in cell O.D. due to the high pH of the nutrient feed, the CO utilization dropped to less than 40%. However, the value stabilized at around 80% during the later phase of the experiment. The average specific rate of CO consumption by the cells, q_{CO} , was $1 \text{ mmole-CO}/(\text{g-cells}\cdot\text{min.})$ at 2 cc/min. , $1.2 \text{ mmole-CO}/(\text{g-cells}\cdot\text{min.})$ at 3.2 cc/min. and $1.7 \text{ mmol-CO}/(\text{g-cells}\cdot\text{min.})$ at 5 cc/min. (Figure 5.4).

5.4.1.3 Product formation

Ethanol and butanol were the predominant products formed in the bioreactor. Acetate was not produced by the cells in detectable amounts. Ethanol and butanol concentrations and production rates varied with the dilution rates, as shown in Figures 5.5 and 5.6. At 2 ml/min , the maximum ethanol concentration was 0.56 wt. \% corresponding to a production rate of 0.8 mol-C/min . Butanol concentration was 0.064 wt. \% with a corresponding production rate of $0.1 \cdot 10^{-3} \text{ mol-C/min}$. At 3.2 cc/min. , the ethanol dropped to 0.38 wt. \% and production rate decreased to $0.05 \cdot 10^{-3} \text{ mol-C/min}$.

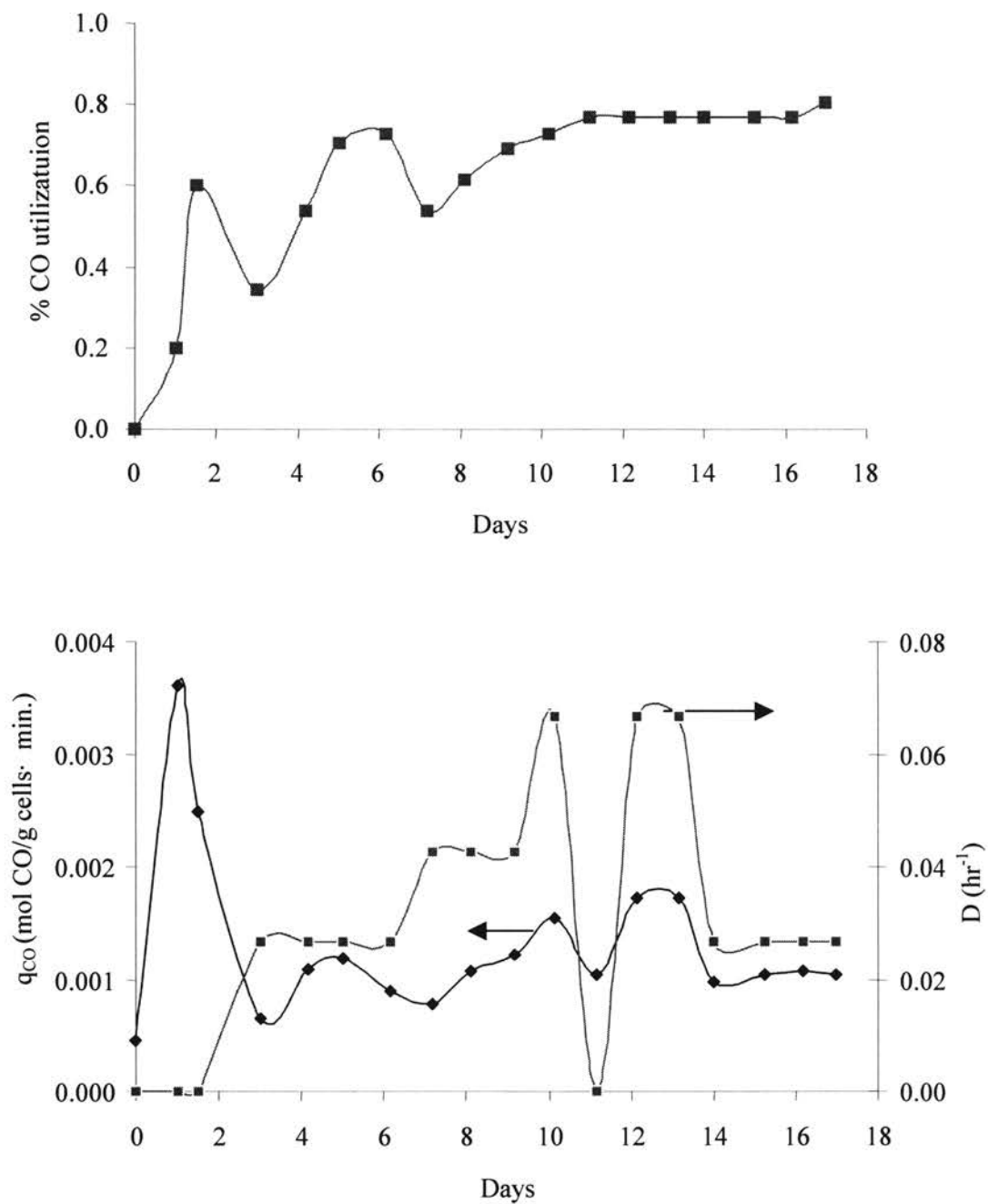


Figure 5.4. Percentage CO utilization and specific CO utilization, q_{CO} , for different values of dilution rate, D . On Day 11, under batch mode, $D = 0$, no product was withdrawn.

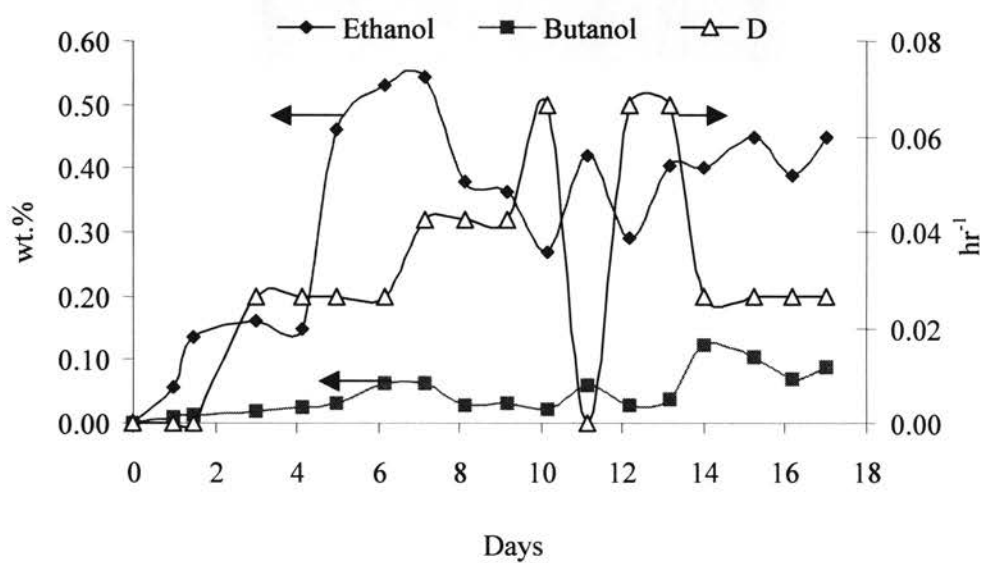


Figure 5.5. Concentrations of ethanol and butanol (wt.%) for different values of dilution rate, D (hr^{-1}). On Day 11, under batch mode, $D = 0$, no product was withdrawn.

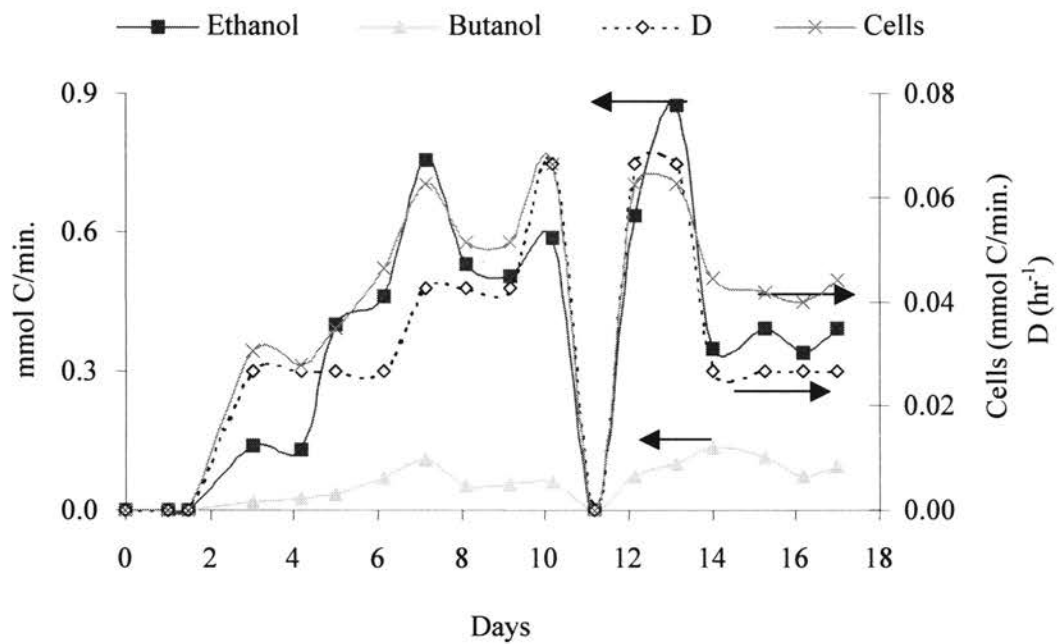


Figure 5.6. Production rates of ethanol, butanol and cells (mmol C/min.) for different values of D (hr⁻¹). On Day 11, under batch mode, D = 0, no product was withdrawn.

Butanol concentration was 0.033 wt.% and production rate was $0.05 \cdot 10^{-3}$ mol-C/min. At 5 cc/min, the ethanol concentration dropped to 0.3 wt. % but the production rate increased to $0.87 \cdot 10^{-3}$ mol-C/min. Similarly, the butanol concentration dropped to 0.028 wt.% but the production rate increased to $0.07 \cdot 10^{-3}$ mol-C/min. On Day 11, the bioreactor was temporarily operated in a batch mode. The products accumulated in the bioreactor resulting in higher concentrations than that during the continuous mode. The production rate (product concentration times flow rate) was zero as no product stream was withdrawn during the batch growth phase.

The yields of ethanol and butanol were not steady during the experiment (Figure 5.7). Ethanol yield varied between 0.15 to 0.3 mol. C/(mol. CO) during stable cell growth conditions. The maximum butanol yield was 0.057 mol. C/(mol. CO). The yield of CO₂ from CO was in the range of 0.6 to 0.65 mol. C/(mol. CO).

The moles of carbon utilized for the generation of the cells, products and CO₂ from CO was estimated. The difference in CO entering and exiting the bioreactor was also calculated. From the two estimated quantities, the carbon balance around the bioreactor was determined. As shown in Figure 5.8, the carbon balance included the products, CO₂ and cells and accounted for over 90% of the utilized carbon.

5.4.1.4 Discussion on dilution rate

Changes in dilution rate, $D (= F_L/V_L)$, of the liquid nutrients affected the production rates of cells and products. The steady state cell concentration, X_{SS} , in the bioreactor operating in a chemostat mode can be described as (Blanch and Clark, 1997),

$$X_{SS} = Y_{X/S} (S_0 - DK_S/(\mu_m - D)) \quad 5.1$$

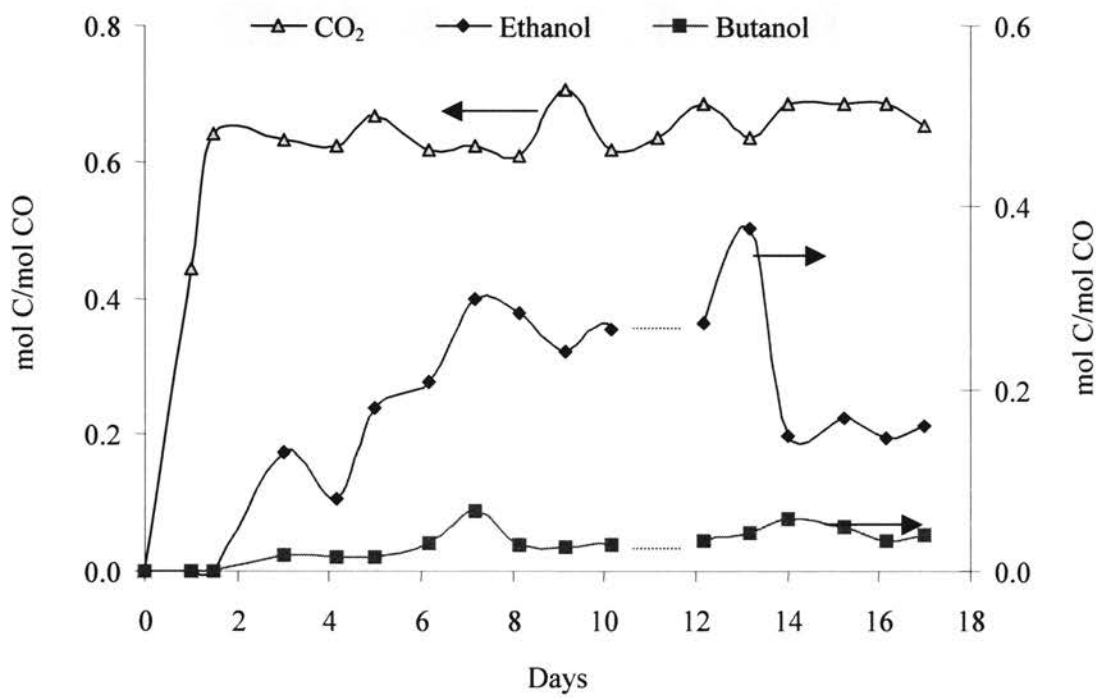


Figure 5.7. Yields of ethanol, butanol and CO₂ from CO. Yields were calculated as the ratio of the moles of carbon in products (mol C) to mole CO.

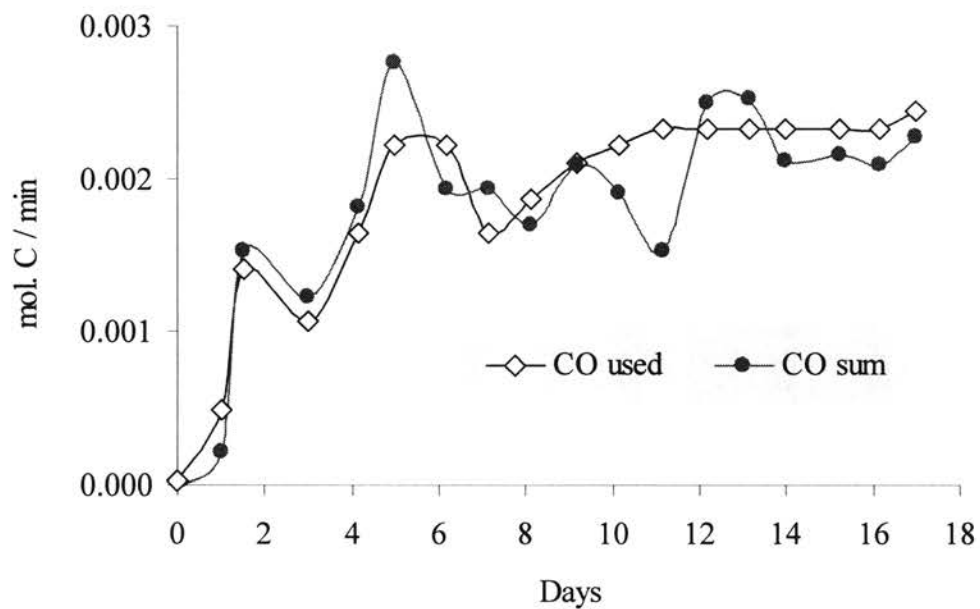


Figure 5.8. Carbon balance for the bioreactor. “CO used” equals the difference in moles/min CO at inlet and outlet of the bioreactor. “CO sum” equals the sum of carbon utilized in cells, CO₂, ethanol and butanol.

where, $Y_{X/S}$ is the cell yield from the limiting nutrient, S_0 is the inlet concentration of the limiting nutrient, K_S is the half-velocity constant in the Monod growth model and μ_m is the maximum cell growth rate.

The production rate of the cells increases (DX_{SS}) with D until washout occurs when $D > \mu_M$. Prior to washout, the specific growth rate of the cells in the chemostat equals the dilutions rate, D . At D greater than μ_M more cells are lost in the effluent stream than can be produced in the bioreactor (Blanch and Clark, 1997).

The following summarizes the results of the study on the effects of dilution rates:

- An increase in the dilution rate increased the production rates of cells and ethanol.
- CO utilization rates were not affected appreciably by changes in the dilution rate.
- The yields of ethanol and butanol were not steady during the experiment. The ethanol yield varied between 0.15 to 0.3 mol. C/(mol. CO) during stable cell growth conditions. The maximum butanol yield was 0.057 mol. C/(mol. CO). The yield of CO₂ from CO was in the range of 0.6 to 0.65 mol. C/(mol. CO).

5.4.2. Effects of trace metal composition

A continuous experiment was carried out for over a two-week period. The gas flow rate was 200 ml/min at 25 °C and 5 psig, containing 25% CO, 60% N₂ and 15% CO₂. The nutrient media initially contained 20 ml/L mineral salt solution, 10 ml/L vitamin solution and 5 ml/L trace metal solution. The effect of doubling trace metal concentration on cell growth, CO utilization and product formation are discussed as follows:

5.4.2.1 Cell growth

Following inoculation, the cells grew under batch conditions for a period of 3 days in the bioreactor as shown in Figure 5.9. The cells started growing after a lag phase of 1 day. Continuous mode of operation was started on Day 4 with dilution rate at 0.027 hr^{-1} (Phase I). The cell concentration at steady state was around 1.15 O.D. At the end of 6 days, the trace metal concentration in the bioreactor feed was doubled from 5 ml/liter to 10 ml/liter (Phase II). After 24 hours, the cell concentration increased to 2.3 O.D. On Day 11, the temperature of the bioreactor was decreased from $37 \text{ }^{\circ}\text{C}$ to $25 \text{ }^{\circ}\text{C}$ for a day and restored. The cell concentration dropped to 1.7 O.D. and recovered to 2.3 O.D. when the temperature was restored to $37 \text{ }^{\circ}\text{C}$. On Day 14, the iron content in the liquid feed was reduced to 50% of the original composition. The cell concentration showed a steady decline until Day 18 (Phase III).

Following the lag phase, the cell concentration (O.D. units) growing under batch conditions was monitored frequently, to estimate the specific growth rate (μ). The estimated μ was 0.05 hr^{-1} . During steady, continuous operations in the chemostat mode, μ was 0.0027 hr^{-1} (also equal to the dilution rate).

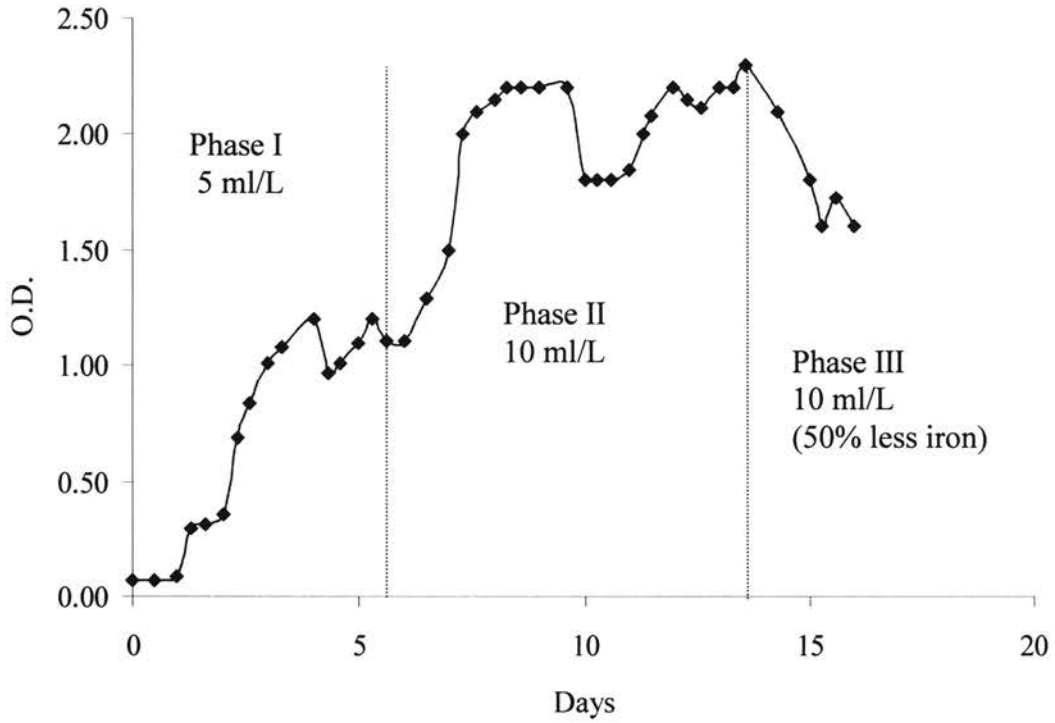


Figure 5.9. Effect of trace metals composition on cell growth. Trace metal content in the media (per liter) was 5 ml/L during Phase I, 10 ml/L during Phase II and 10 ml/L (with 50% less iron than that during Phase I) during Phase III.

5.4.2.2 CO utilization

Following the lag phase, CO utilization increased with cell concentration in the bioreactor, as shown in Figure 5.10. During Phase I, the CO utilization stabilized at 30%. As the trace metal concentration was doubled during Phase II, CO utilization almost doubled to 60% establishing that the uptake rate of CO was not limited by the mass transfer rate, but the intrinsic kinetics of the microbial catalysts (as discussed in Chapter 4). On Day 10, the CO utilization dropped temporarily to less than 50%, due to the sudden drop in the temperature of the bioreactor. Following the cell recovery from the temperature shock, CO utilization returned to 55%. As a result of the cell death due the 50% decrement in iron content of the media, the CO utilization decreased to less than 40%. As expected, the specific CO uptake rate of the cells(q_{CO}) remained more or less unaffected by the change in trace metals concentration. The steady state value of q_{CO} was approximately, 0.9 moles CO consumed/(min· gcells). The CO_2 yield from CO was in the range of 55% to 65% over the entire period of the experiment.

5.4.2.3 Product formation

During phase I, the ethanol concentration reached a steady value of 0.18 wt.%, as shown in Figure 5.11. The corresponding acetate and butanol concentrations were less than 0.03 wt.%. During phase II, the ethanol concentration increased to 0.35 wt.%, while butanol and acetate concentrations increased to 0.075 wt.% and 0.035 wt.%, respectively.

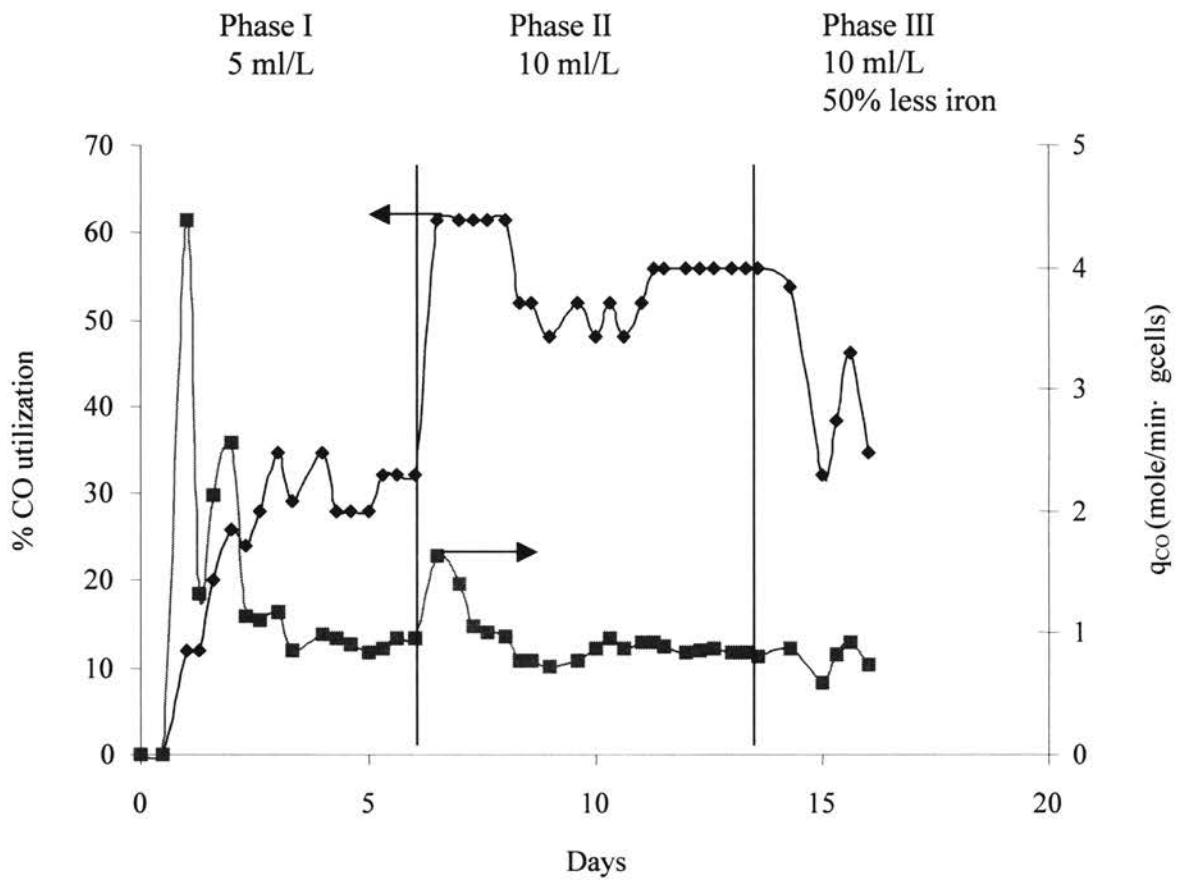


Figure 5.10. CO utilization and specific uptake rate (q_{CO}) by P7 for changes in trace metal compositions. The total trace metal concentration is shown for each phase.

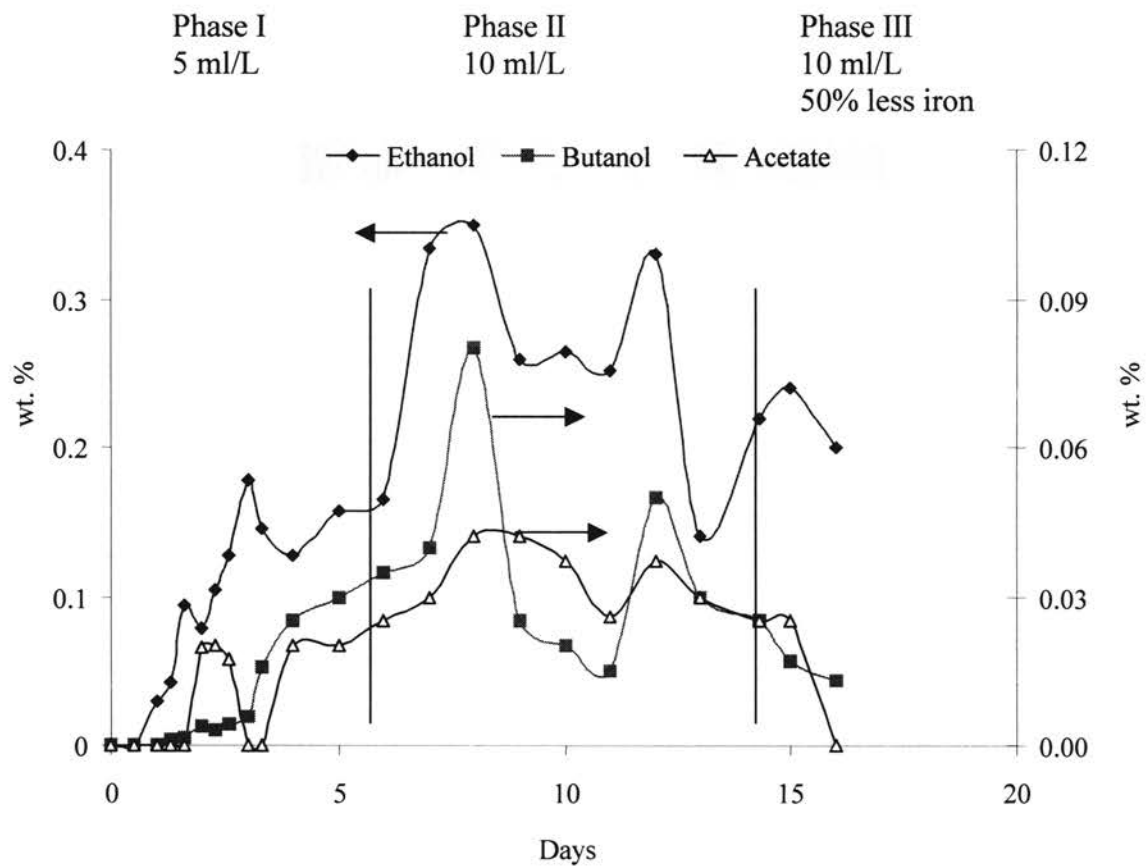


Figure 5.11. Product concentration (wt.%) for changes in trace metal concentration. The total trace metal concentration is shown for each phase.

An increase in the trace metal concentration did not affect the yields of cells and ethanol significantly. Apparent yields, $Y_{EtOH/CO}$, $Y_{Butanol/CO}$ and $Y_{Acetate/CO}$ were 0.33, 0.03 and 0.04 respectively on a molar basis (Figure 5.12) and yield of cells, $Y_{X/CO}$ was 0.25 g/mol at steady state. The yield of ethanol from CO as compared to acetate and butanol is higher by 8 and 11 times respectively, establishing a high level of product selectivity and specificity of the new acetogen.

5.4.2.4 Discussion on trace metal composition

One limiting nutrient for cell growth is iron in the trace metal solution. The cell concentration doubled with the doubling of the trace metal content, as shown in Figure 5.9. On Day 14, as the iron content was decreased to 50% of the original composition, while the remaining trace metals were maintained at double concentrations, the cell concentration dropped from 2.3 to 1.5 O.D. units. Evidently, cell growth was affected by the decrease in iron content in the medium.

CO utilization doubled from 30% to 60% as the trace metal concentration was doubled. However, the CO utilization per unit cell mass was not significantly affected as shown in Figure 5.10. Obviously, doubling the trace metal, doubled the cell concentration that in turn doubled CO utilization. As explained in Chapter 4, the CO utilization was not limited by the mass transfer rate of CO but rather by the intrinsic kinetics (nutrient limitations) of the cells.

Ethanol concentration increased from 0.18 wt.% during Phase I to 0.35 during Phase II. The yield of ethanol from CO was not significantly affected by trace metal

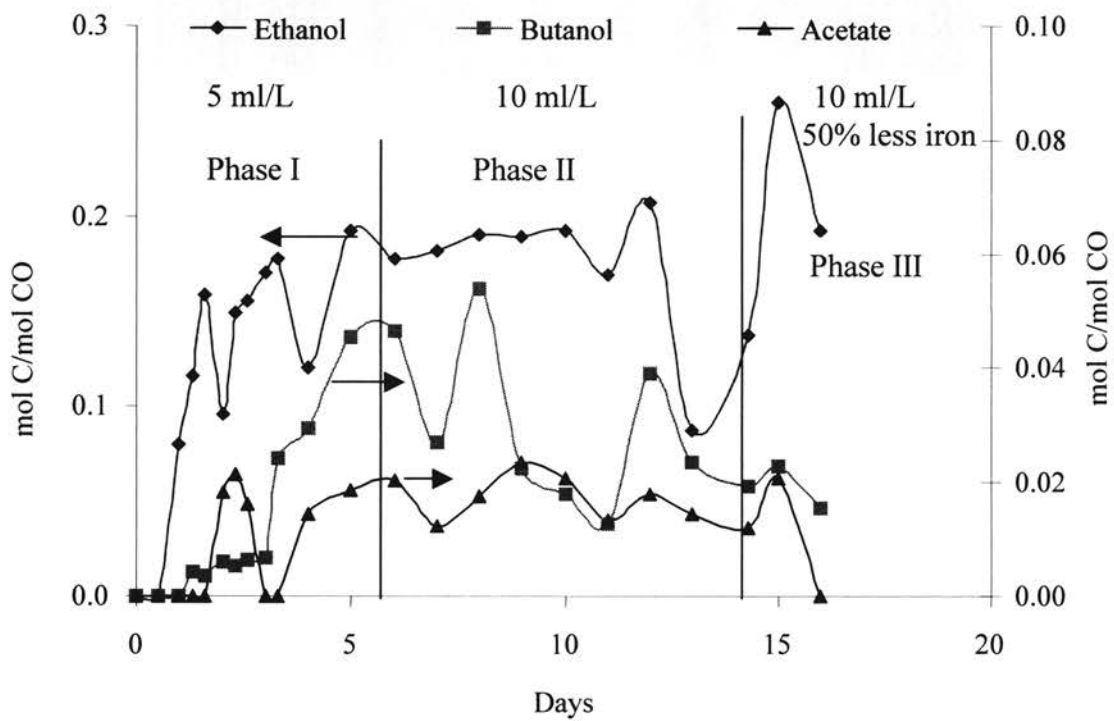


Figure 5.12. Yields of products from CO for changes in trace metal composition. The total trace metal concentration is shown for each phase.

composition, showing that the net increase in cell concentration resulted in a net increase in ethanol concentration. In the future, the effects of individual of trace metal solution constituents on ethanol yield from CO need to be investigated.

5.4.3 Cell recovery from temperature shock

The ability of P7 to recover from the temporary temperature shock is industrially significant, as similar shocks are likely to occur in a commercial scale operation. The optimum temperature for P7 determined from culture tube experiments at the University of Oklahoma was 37°C. Enzyme activities, responsible for normal metabolic functions of the cells are sensitive to changes in the process temperature. As shown in Figure 5.9, a decrease in cell concentration ensued following the sudden drop in the bioreactor temperature to 25°C. However, as the normal operating temperature was restored, cell growth, substrate uptake and product synthesis were reestablished in the bioreactor within one day. Evidently, this result establishes that P7 is capable of withstanding shocks in temperature. However, temperature shocks greater than 37°C need to be evaluated.

5.4.4 Response to CO₂ cut-off

Several experiments were performed on the bubble column bioreactor without CO₂ in the feed gas stream (CO and N₂ only). For such a case, as the cells were expected to utilize CO₂ produced from CO (see Eq. 2.1). The gas composition was 75% N₂ and 25% CO. No cell growth was observed during the experiments even after a one-week batch mode of operation.

Another experiment was performed for over a period of 12 days. The run was started with 4 liters of anoxic media containing 20 ml/l minerals, 10 ml/l vitamins and 5 ml/l of trace metals. The gas flow rate was 200 ml/min with 60% N₂, 25% CO and 15% CO₂. The initial pH was 5.8. Anoxic 1 N sodium hydroxide solution was used to control the lower limit of the pH at 5.3.

Initially, 100 ml of raw inoculum was transferred aseptically to the bioreactor. Cells started to grow after a lag-phase of 0.5 days. Batch-growth was terminated at the end of 3 days by continuous feed of liquid at 2 ml/min. The cell concentration at the end of batch growth was 1.6 O.D. (Figure 5.13).

A continuous mode of operation was initiated on Day 3 with 4 ml/min of product/feed flow rate. The cell O.D. dropped gradually over the next 4 days to 0.9 O.D. On Day 8, the pH of the bioreactor increased from 5.35 to 6.1 due to a technical failure in the pH control system (Figure 5.14). Excessive frothing was observed in the bioreactor implying cell death and subsequent extrusion of proteins from the lysed cells. The cell O.D. immediately dropped to 0.5 O.D. However, the pH was restored to 5.3 by the cells without any external effects and cell growth resumed. The cell O.D. recovered to 1.4 O.D following a 2 day period.

On Day 13, the CO₂ supply (15% of 200 ml/min) to the bioreactor was cut-off and replaced with the same flow rate of N₂ (only CO and N₂ were present). The cell concentration dropped to 0.8 O.D. in the next 2 days signifying cell death. The experiment was terminated on Day 15.

The CO utilization remained in the range of 35% to 40% during the experiment. With the CO₂ cut-off, CO utilization dropped to less than 10%, as shown in

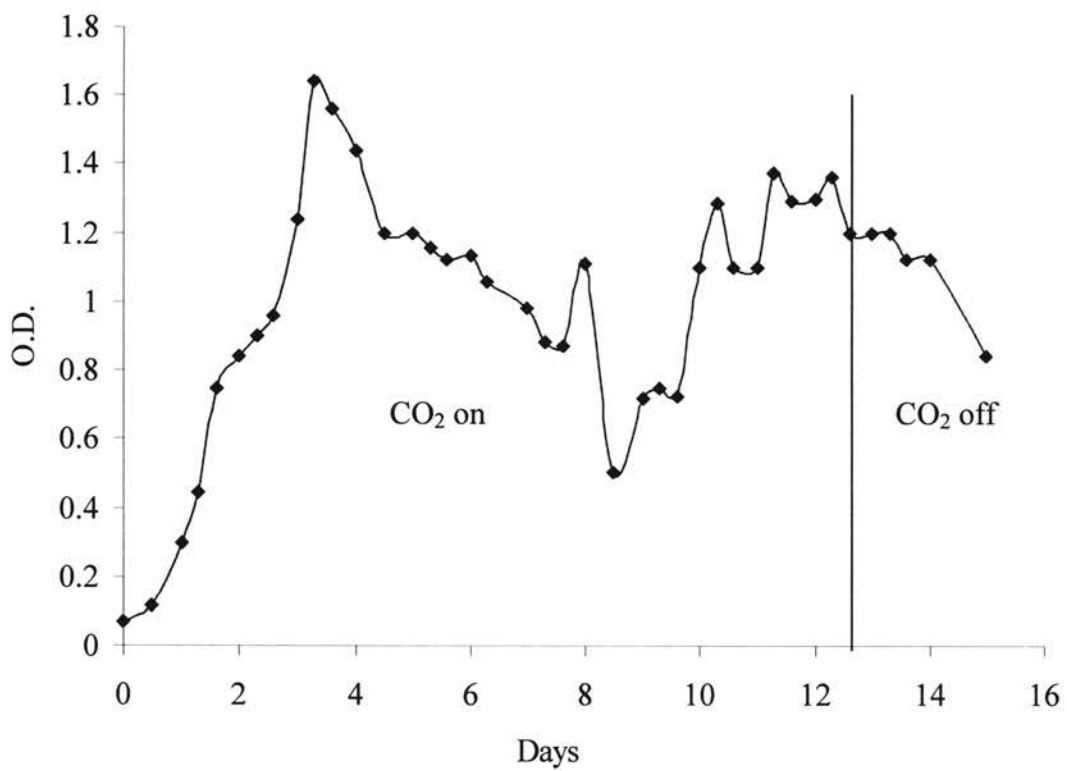


Figure 5.13. Effects of CO₂ cut-off in the feed stream.

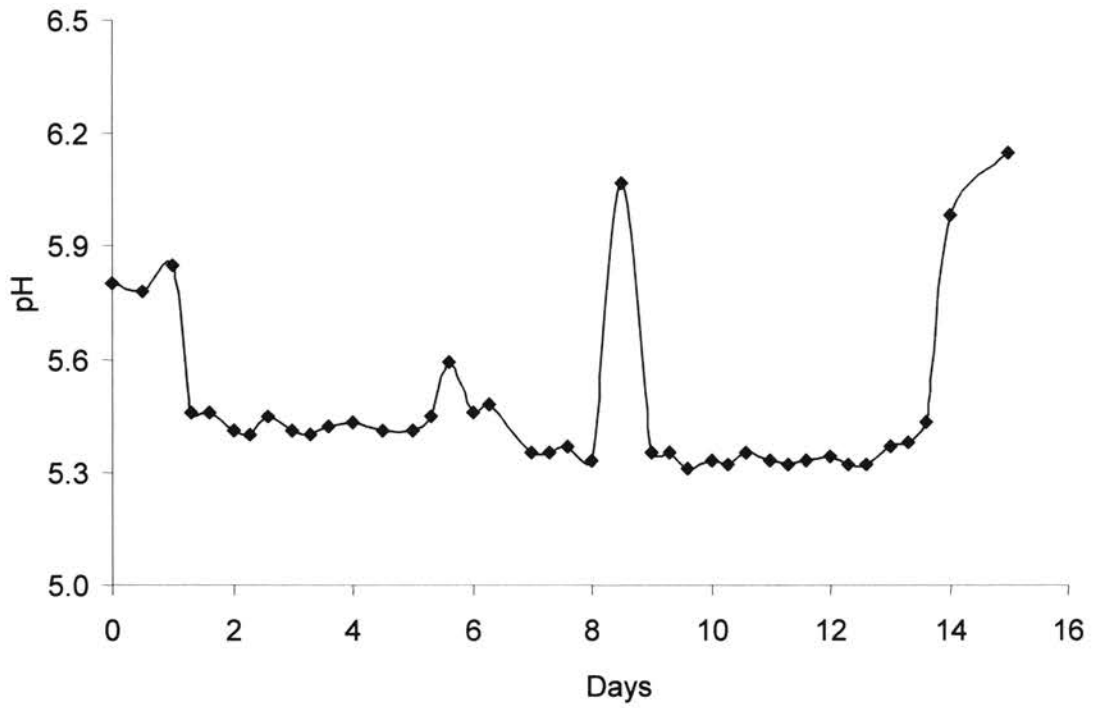


Figure 5.14 pH profile showing sudden spike on Day 8 (Equipment failure occurred on Day 8).

Figure 5.15. Steady state ethanol concentration remained around at 0.5 wt. %, as shown in Figure 5.16.

5.4.4.1 Discussions on CO₂ cut-off

The central metabolic pathway for the synthesis of ethanol, acetate and butanol from the bacterium-P7 is expected to follow the acetyl-CoA pathway described in chapter 3. CO₂ is the precursor to the formation of a methyl group responsible for the formation of the acetyl-CoA intermediate. The key characteristics of the pathway are the formation of the methyl moiety from the CO₂, transfer of the methyl moiety to carbon monoxide dehydrogenase (CODH) via a corrinoid enzyme and a CODH-catalyzed condensation of the methyl group with a CO-derived carbonyl and coenzyme A to form a acetyl-CoA intermediate. Acetyl-CoA is hydrolyzed to acetic acid and subsequently to ethanol, butyrate and butanol (Phillips et al., 1994). The distinctive feature in the pathway is the mechanism by which CO₂ is utilized for the total synthesis of an organic compound from which succeeding anabolic reactions proceed.

Interestingly, with CO as the carbon source, the CO can serve as the electron donor generating CO₂ in the process (Wood et al., 1984). The CO₂ generated from CO was expected to form the methyl moiety. H₂ is required as a source of energy and electrons only when the bacteria grow on CO₂. However, results from the experiments on P7 without CO₂ in the feed gas showed that no cell growth occurred in the bioreactor. The inability of P7 to utilize CO₂ generated from CO for the synthesis of products and cell materials using the acetyl-CoA pathway requires additional experiments to determine activities of the enzymes involved in the process. The results from the experiments on

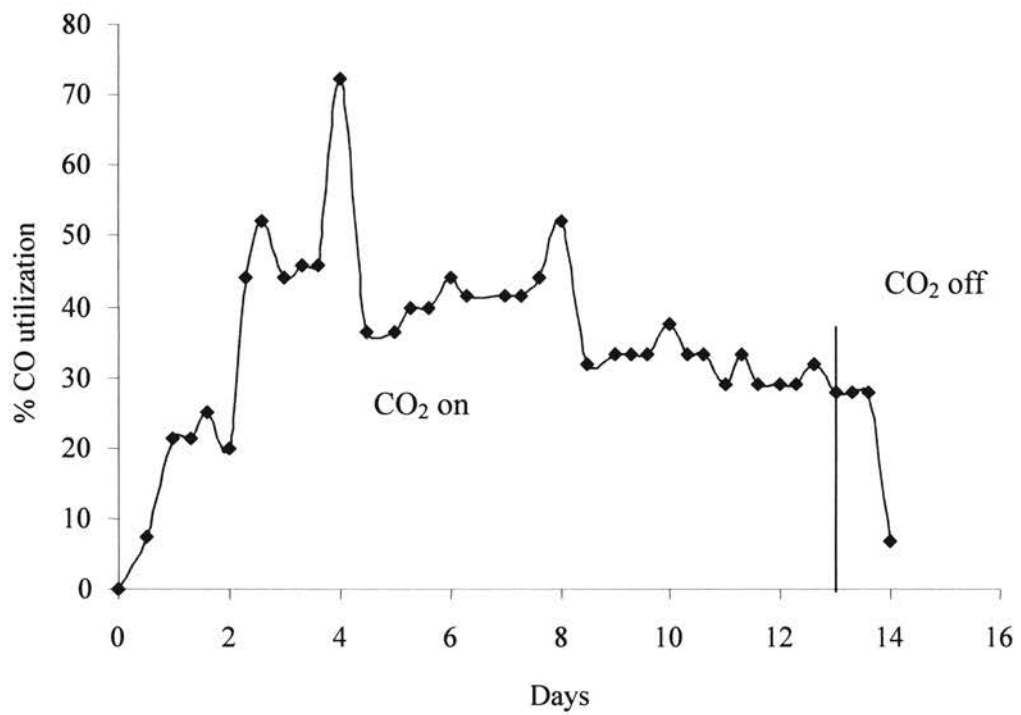


Figure 5.15 CO utilization (%) as a function of CO₂ in the feed stream.

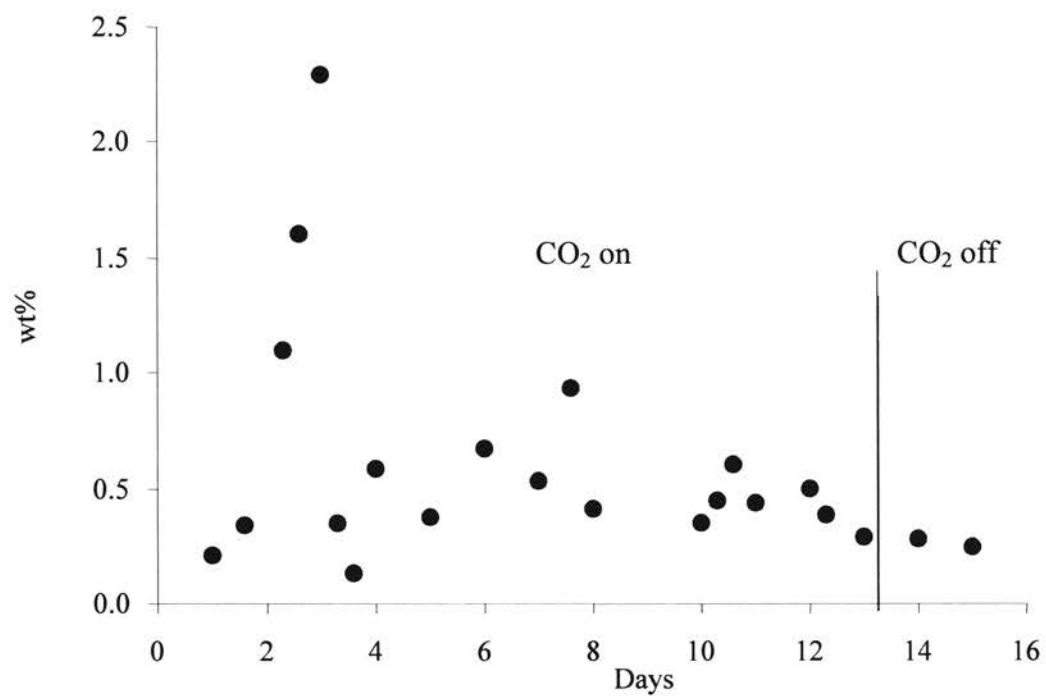


Figure 5.16. Ethanol concentration as a function of CO₂ in the feed gas stream.

CO₂ are useful in identifying future research on the biochemistry, microbiology and enzymology of the syngas conversion process.

5.4.5 Response to pH shock

As described in Section 5.4.3, the pH of the bioreactor spiked from 5.35 to 6.1 due to a technical failure in the pH control system (Figures 5.13 & 5.14). Excessive frothing was observed in the bioreactor implying cell death and subsequent extrusion of proteins from the lysed cells. The cell O.D. immediately dropped to 0.5 O.D. However, the pH was restored to 5.3 by the cells without any external effects and cell growth resumed. The cell O.D. recovered to 1.4 O.D following a 2 day period. This showed that the cell death, and possibly damage of cell constituents caused by an unfavorable pH, was not permanent and normal cell growth resumed once favorable pH conditions were restored.

Sudden changes in the operational conditions are expected to occur in any industrial scale bioreactor. P7, being a living organism, was expected to be very sensitive to sudden pH changes in the bioreactors. The activities of the enzymes, responsible for the synthesis of products and cell materials, are maximal only at optimal pH conditions. Loss in enzyme activities under unfavorable pH conditions leads to cell death. Hence, the results of the experiment are significant in establishing the robustness of P7 to recover from pH shocks in the process.

5.5. Conclusions

The response of P7 to changes in process conditions have been experimentally investigated in this chapter. The effects of changes in dilution rates of the nutrients, trace metal compositions, CO₂ cut-off in the feed gas stream and process disturbances (namely pH and temperature) have been determined.

Higher dilution rates favored the production rates of cells and ethanol. The bioreactor is limited by the intrinsic kinetics of the cells, influenced directly by the nutrient compositions in the media. Increasing trace metal content in the bioreactor increased cell and product concentrations and the CO uptake without affecting the yields of products. CO₂ is required for initiating and sustaining cell growth in the bioreactor even though CO₂ is a by-product of the conversion of CO by P7. Sudden spikes in pH and temperature temporarily affected cell growth and metabolic activities. However, the cells rapidly recovered from pH and temperature shocks and performed normal metabolic activities once normal operating conditions were restored. The results show that P7 is tolerant to some process shocks likely to occur in industrial scale bioreactors.

CHAPTER 6

PROCESS IMPROVEMENT TECHNIQUES

6.1 Introduction

The productivity and yield of ethanol from the components of syngas need to be improved from the current values to improve the process economics. The maximized productivity of ethanol, measured as the rate of ethanol production per unit volume of the bioreactor, is desired to minimize the reactor size and operating cost of the equipment. The maximum yield of ethanol from moles of carbon (CO and CO₂) utilized is desired to improve the utilization of the biomass carbon to useful products.

Some of the methods to increase the productivity and yield of ethanol in syngas fermentations include optimization of nutrients, cell recycle to increase the net cell concentration, hydrogen utilization, and mass transfer improvements. A detailed literature study on these process enhancement methods is provided in Chapter 2.

This chapter discusses studies aimed at improving the performance of the process by incorporating H₂ in the feed gas, recycling cells to improve cell concentrations in the bioreactor, and screening nutrients affecting cell growth and ethanol yield. The bubble column bioreactor used in this research work has been shown in Chapter 5 to be operating under nutrient limitations and not currently gas mass transfer limitations. Thus, the bioreactor design with regards to gas utilization is not the limiting criterion on the

overall economics of the process. Hence, improvement in bioreactor design is not considered in this study.

6.1.1 Hydrogen utilization

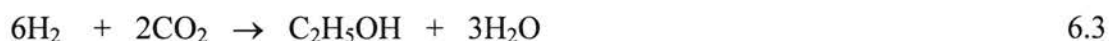
The overall carbon utilization towards the production of ethanol by P7 can be improved by the use of H₂ in the feed gas. As described in Chapter 3, the theoretical yield of ethanol with only CO and CO₂ in the feed gas is 0.33 moles of carbon in ethanol per mole of CO reacted. The remaining carbon is expended on generating electrons required for ethanol production with CO₂ formed as the by-product.



With H₂ in the feed gas, the electrons required for the process can be derived from H₂ as,



CO₂, generated from CO, can potentially be utilized for ethanol production as,



Evidently, the theoretical yields of ethanol from the available moles of carbon in syngas can be doubled by the use of an equimolar quantity of H₂ and CO in the feed gas. In an equimolar CO and H₂ mixture, as much as, 67% of CO can be directed towards the production of ethanol. Also, as shown in Eq. 6.3, a 3:1 ratio of H₂ and CO₂ could result in 100% conversion of CO₂ to ethanol. Obviously, the syngas composition can result in a varied theoretical conversion to ethanol. Thus, all enzymatic pathways must be optimized to obtain the highest conversion.

As all previous experiments in the five liter bioreactor utilized only CO and CO₂ in the feed, H₂ uptake by P7 required experimental verification at the scale of the bubble

column bioreactor. Culture isolation studies at the University of Oklahoma, Norman demonstrated that P7 could utilize H₂ although the cell growth was lower than with a CO/CO₂ feed.

6.1.2 Cell recycle system

The productivity of ethanol from the 4.5 L bubble column bioreactor can potentially be enhanced by using a cell recycle system by increasing the net cell concentration in the bioreactor. With recycle, cells essentially grow in a batch mode, although the liquid and gas may be in a continuous mode. Assuming the yield of ethanol from cells remains the same, an increase in cell concentration will lead to an increase in the ethanol concentration and hence, the production rate of ethanol from the bioreactor.

Hollow fiber membrane filters, ceramic and stainless steel fritted tubes, and plate and frame filters are some of the currently used filters for increasing cell concentrations of yeast and bacteria. Syngas fermentations with *C. ljungdahlii* were found to provide better cell and ethanol concentrations with the use of a hollow fiber membrane filter (Klasson et al., 1993).

In this chapter, experiments performed on a 4.5 L bubble column bioreactor with a hollow fiber membrane filter is used to achieve total cell recycle. The effect of cell recycle on the cell and ethanol concentrations was assessed by comparison of runs with and without the filter.

6.1.3 Media optimization

The conversion of CO to ethanol by the bacterium P7 is a complex process involving several nutrients. The level of nutrients available for the cells significantly influences cell growth and ethanol yield as shown in Chapter 4. Determination of the optimum nutrient levels in a biochemical process is a multivariable problem and requires initial screening of factors prior to a more rigorous analysis. In the present work, the screening of factors that significantly affect cell concentrations and ethanol yields in the biochemical conversion of CO to ethanol is discussed.

Factorial design and response surface analysis are commonly performed for the optimization of nutrient levels in biochemical processes (Kalil et al., 2000). An initial screening design such as the methodology of Plackett-Burman significantly reduces the number of experiments to be performed by identifying potentially influential factors prior to a factorial experiment (Plackett and Burman, 1946). Reportedly, Plackett-Burman designs require fewer runs than fractional factorial designs (Kalil et al., 2000).

Specific to P7, the biochemical process currently requires 30 nutrients in the liquid phase for cell growth. In order to minimize the experimental effort, ten variables are chosen based on earlier research works by Vega et al. (1991) and knowledge of the key enzymes. For instance, methyl viologen was chosen as a variable based on its reported effect in enhancing ethanol yields from CO (Phillips et al., 1992) while cobalt chloride is chosen as it is a promotor for the corrinoid enzyme (Ljungdahl, 1986). A full factorial design with 10 variables would require 2^{10} (1024) trials at two levels of each nutrient. Using a Plackett-Burman screening design, it is possible to identify the most influential factors with only a small number of trials. Once the significant factors are

identified, a more rigorous factorial design can be performed to obtain additional information about the process. Finally, response surface methodology can be employed to determine optimum levels of the screened factors.

6.2 Objectives of the study

- Enhance the yield of ethanol from CO by incorporating hydrogen in the feed gas stream.
- Increase the production levels of ethanol by increasing the cell concentration in the bioreactor using a cell recycle system.
- Identify the most significant factors affecting cell concentration and ethanol yields for the bioconversion of CO to ethanol by P7. A Plackett-Burman design is used to screen significant factors affecting cell concentration and ethanol yield from cells by performing experiments on small batch bioreactors.

6.3 Materials and Methods

6.3.1. Microorganism

The microorganism used for all the studies was P7, supplied by Ralph Tanner, University of Oklahoma. Isolation and culture techniques for the bacterium are discussed in Chapter 3.

6.3.2 Media

A defined medium containing Pfenning's minerals and trace metals, vitamins, and

reducing agents was used to prepare the inoculum and cultivate cells in the bioreactor. The exact compositions of the stock solutions are provided in Chapter 3. Individual studies described in this chapter were performed with different compositions of the minerals, vitamins, trace metals, and other nutrients. The exact compositions of the nutrients are mentioned in the respective studies. Unless specifically mentioned, the media also contained (per liter) 5 g MES (N-Morpholinoethane sulfonic acid), 0.5 g yeast extract, 5ml of 4% cysteine-sulfide solution and 0.1ml of 0.1% resazurin.

6.3.3 Experimental set-up

6.3.3.1 Hydrogen utilization and cell recycle in a bubble column bioreactor

All the cell recycle and some of the hydrogen experiments were performed in the 4.5-L bubble column bioreactor as described in Chapter 3. The nutrient media contained (per liter) 25 ml mineral, 15 ml vitamin, and 10 ml trace metals solutions in addition to the chemicals listed in section 6.3.2. In the chemostat mode, the product stream containing the bacterial cells was withdrawn from the liquid recirculation line and fresh nutrient media was added continuously at the same rate to maintain steady state conditions in the bioreactor. For the total cell recycle mode, a tangential flow filter was placed in the liquid recirculation line. Flow rates of the fresh nutrient feed and the permeate from the filter were equal (2-4 ml/min) to maintain steady liquid levels in the bioreactor. The total gas flow rate to the bioreactor was 200 ml/min at 5 psig and 25°C. Gas compositions used for specific studies are mentioned under the respective result sections. To remove any residual oxygen from the gases prior to the bioreactor, the gases

were de-oxygenated by adsorption in a packed column oxygen trap (Fisher Scientific, NJ). The gases were sterilized via a microporous membrane filter (0.2 μm). Analytical methods for measuring concentrations of cells, products and reactant gases are mentioned in Chapter 3. Unless noted, all other operations of the bioreactor are similar to those mentioned in Chapter 3.

6.3.3.2 Hydrogen utilization (one-liter flask)

Additionally, hydrogen utilization was studied in a semi-batch bioreactor. The experimental set-up consisted of a one-liter glass flask with a butyl rubber stopper. The working volume of the batch liquid was 400 ml. The liquid was maintained at a constant temperature of 37°C in an incubator. The liquid composition was similar to that described in the previous section. The liquid was steam sterilized at 121°C for 30 minutes. Prior to inoculation, a gas stream containing 70% H₂ and 30% CO₂ was continuously bubbled through the liquid at 200 ml/min and room conditions, until the liquid was deoxygenated. The gases were filter sterilized as explained in Chapter 3. Only the cell concentration and pH of the liquid were monitored. The inlet and outlet gas compositions were essentially the same due to the fast flow rate and hence, only discretely measured during the experiment.

6.3.3.3 Screening experiments

All the screening experiments were performed in 200 ml glass bottles with 150 ml batch liquid media and a continuous gas flow rate of 25 ml/min per bottle. Gas tight

conditions were provided by butyl rubber stoppers. The feed gas consisted of CO (25%), CO₂ (15%) and N₂ (60%) from a single tank (Air-Gas Co., Tulsa, OK). Hydrogen uptake by P7 was not considered for this study. To remove any residual oxygen from the gases prior to entering the bioreactor, the gases were de-oxygenated by adsorption in a packed column oxygen trap (Fisher Scientific, NJ). The O₂ free gases were sparged into the batch-bioreactors through 22 gauge, six-inch long needles. The total gas flow rate was split evenly (25 ml/bottle) using a swagelok-union (OKC Valves and Fittings, Oklahoma). The bioreactors were kept in an incubator at 37° C as shown in Figure 6.2 (three bottles/batch). The first set of experiments was performed with three bottles/batch. Subsequently, the number of bottles/batch was increased to five to minimize the experimental time. A control run was selected for all the experiments to account for process variations during different trials. The control run was performed during every batch of experiments along with other runs. The control run should give similar results during all the batches. Thus, the results from the control run provide some measure of the process variations during different batches.

Following media preparation, each bottle was autoclaved at 121°C for 30 minutes. The media was deoxygenated under a continuous bubbling of N₂. Sodium sulfide (one of the factors being investigated) as required by individual batches was added prior to inoculation using a sterile syringe filter. The supply of the gas mix was started after the media turned colorless after which 5 ml of raw inoculum was added to each bottle using a sterile disposable syringe. The experiments lasted between 7-10 days. Liquid samples were analyzed for cell and ethanol concentrations and pH for every 24 hours. Details of the analytical methods used for the study are provided in Chapter 3. For analyzing H₂

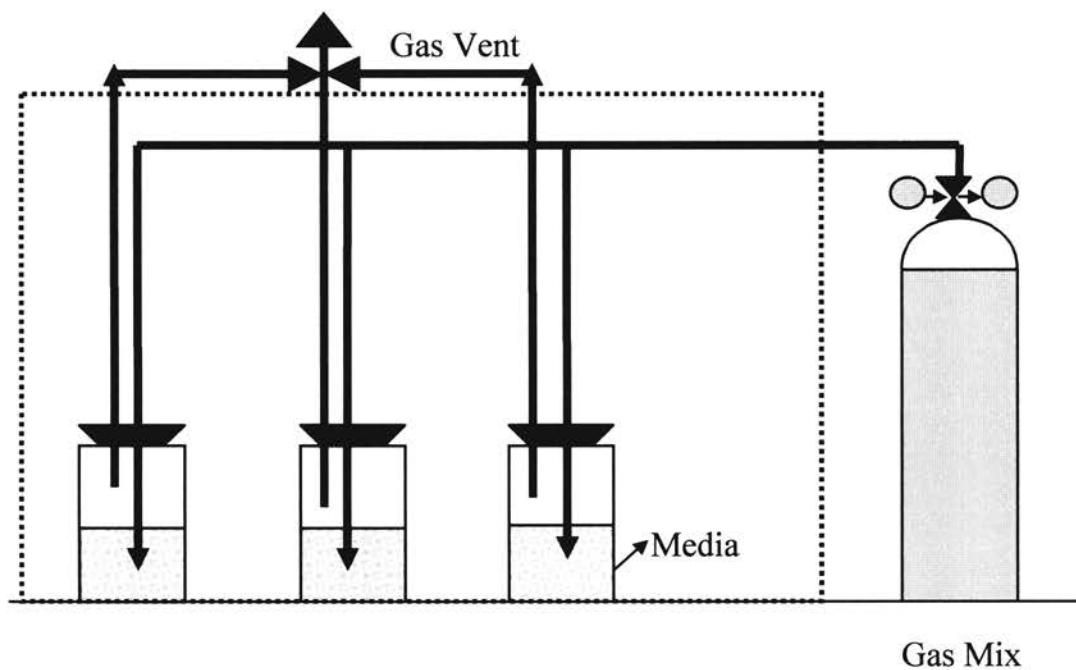


Figure 6.1. Experimental set-up for the screening design of nutrients affecting cell concentration and ethanol yield from CO.

along with the CO, CO₂ and N₂ using the GC, argon was used instead of helium as the carrier gas. The analytical procedure was exactly similar to that described in Chapter 3.

6.4 Results and discussions

6.4.1 Hydrogen utilization

The results of the runs with H₂ in the 4.5 L bubble column and the one-liter flask are individually discussed as follows:

6.4.1.1 Hydrogen utilization (bubble column bioreactor)

Several experiments were performed using the 4.5 L bubble column bioreactor to assess H₂ uptake by P7. During the first trials, P7 grown under CO and CO₂ were used to inoculate the bioreactor. The gas feed was initiated with 25% H₂, 15% CO₂ and 60% N₂ at a flow rate of 200 ml/min and at room conditions. No cell growth was observed even after one week following inoculation. Similarly, experiments were initiated with inoculum cultured on H₂ and CO₂ with the same the feed gas composition and no cell growth was again observed in the bioreactor.

In one of the experiments, 100 ml of inoculum, grown on CO and CO₂, was used to initiate cell growth in the bioreactor with 25% CO, 15% CO₂ and 60% N₂ in the feed gas. As shown in Figure 6.2, the cells started growing after a lag phase of 2 days. With

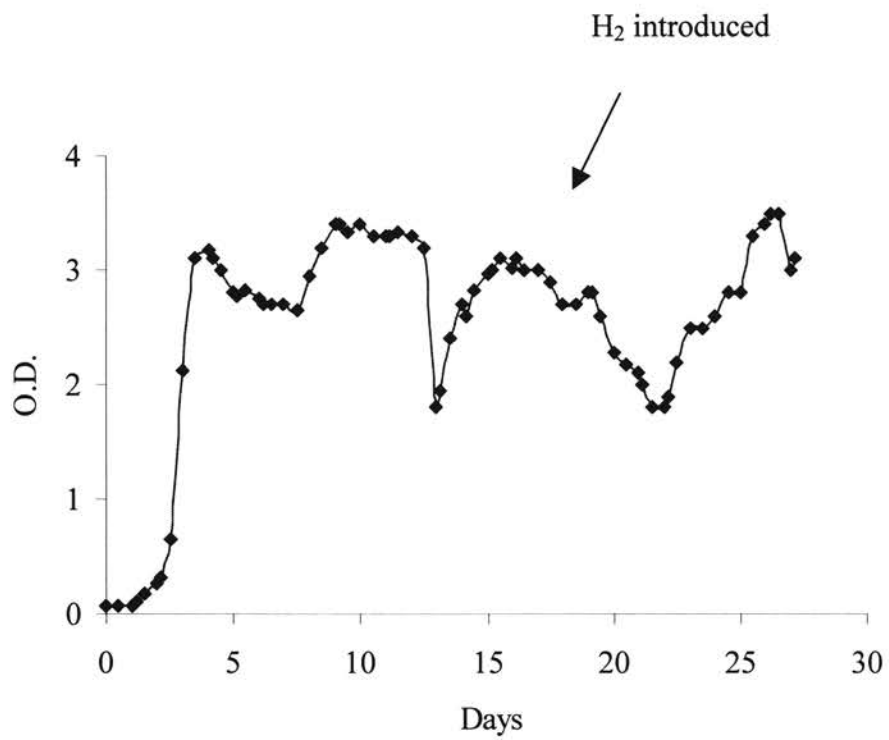


Figure 6.2. Cell concentration (O.D.) during the hydrogen utilization experiment with the bubble column bioreactor.

the cell O.D. at 3.3 units, batch growth phase was terminated and a continuous flow of feed at 2 ml/min was initiated. The cell concentration dropped initially but stabilized at 3.3 units till Day 13. Due to equipment failure, the temperature of the bioreactor dropped to less than 25°C on Day 13. Cell death ensued, dropping the O.D. to less than 1.8 units. The cells recovered from the temperature shock once normal conditions were restored. On Day 17, N₂ flow to the bioreactor was reduced by 20 ml/min and replaced with the same quantity of H₂. Cell concentration dropped continuously to 1.8 O.D. until Day 22. However, the cell concentration started to increase on Day 22 without any process changes and reached 3.5 O.D. units on Day 27. The cell concentration again started to drop on Day 28, after which the experiment was terminated. The causes for the cell growth and death during this phase of the experiment will be investigated in future.

The CO utilization rate was affected by the cell concentration in the bioreactor. At 3.3 O.D., approximately 75% of the incoming CO was utilized by the cells, as shown in Figure 6.3. Due to the temperature shock, the CO utilization dropped to 55% with the cell O.D. at 1.8. With the introduction of H₂ and the subsequent cell death, CO utilization dropped to as low as 40%. The inlet and outlet H₂ concentrations were essentially the same demonstrating that no H₂ was utilized by the cells during the experiment. The CO₂ yield from CO remained approximately in the range of 60-70% throughout the experiment. The introduction of H₂ in the feed gas did not affect the yield of CO₂. The steady state ethanol concentration, as shown in Figure 6.4, was 0.3 wt.%. However, the introduction of H₂ resulted in a decrease in ethanol production due to the drop in cell O.D. (which may or may not be attributed to H₂).

In another experiment, 100 ml of inoculum, grown on H₂ and CO₂, was used to

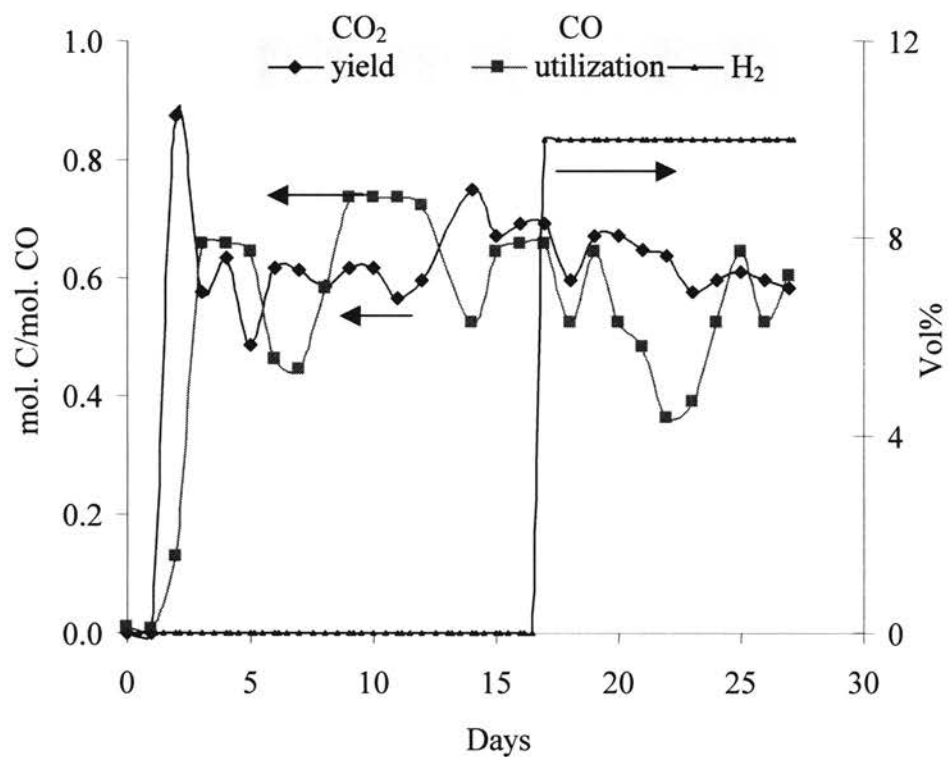


Figure 6.3. CO utilization, CO₂ yield and H₂ feed composition during the hydrogen utilization experiment with the bubble column bioreactor. The inlet and outlet H₂ concentrations were essentially equal during the experiment.

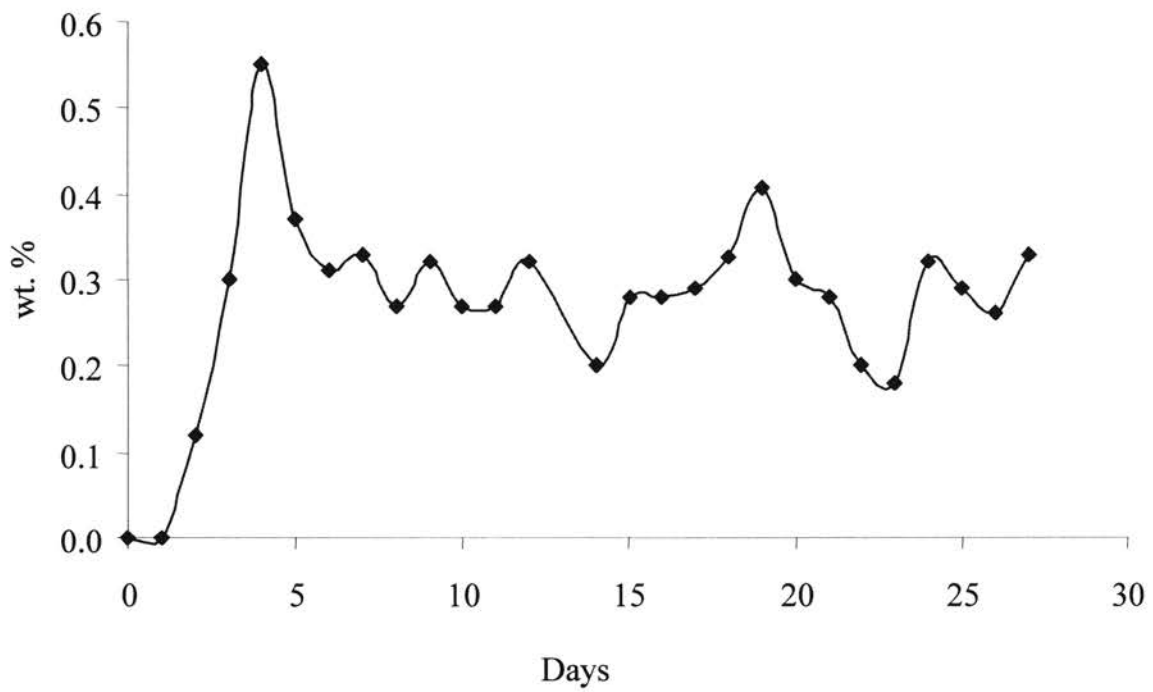


Figure 6.4. Ethanol concentration during the hydrogen utilization experiment with the bubble column bioreactor.

initiate cell growth in the bioreactor with 25% CO, 15% CO₂ and 60% N₂ in the feed gas. Steady growth and concentrations of the cells were achieved over 7 days. H₂ was introduced in the feed gas (25% CO, 15% CO₂, 10% H₂ and rest N₂) on Day 7. No H₂ was utilized by the cells. Cells continued to grow on CO alone and maintained a steady O.D. of 1.7 to 1.8 units for over six days.

Also, an experiment performed with 70% H₂ and 30% CO₂ feed gas using cells grown on H₂ and CO₂ showed no cell growth for the entire one week run. However, when the H₂ flow was cut-off and the gas stream was changed to 25% CO, 60% N₂ and 15% CO₂, the cells started growing as observed in previous studies. The maximum cell concentration reached at the end of the batch phase was 2.5 O.D. Thus, for all the experiments using the 4.5 L bioreactor, H₂ was not utilized.

6.4.1.2 Hydrogen utilization (one-liter flask)

25 ml of cells, grown on H₂ and CO₂, was used to inoculate 400 ml of sterilized media in the one-liter flask under a continuous gas flow rate of 200 ml/min at standard room conditions. The gas composition was 70% H₂ and 30% CO₂. Cells started growing following a lag phase of 3 days, as shown in Figure 6.5. As mentioned earlier, only the cell O.D. and the pH were monitored on a daily basis for the run.

The cell O.D. reached a maximum value of 0.7 units on Day 5, remained essentially stable for the remainder of the run. The liquid volume decreased to less than 300 ml on Day 7, due to the continuous stripping action of the gas stream. Any change in cell concentration due to the decrease in liquid volume was not considered for the run.

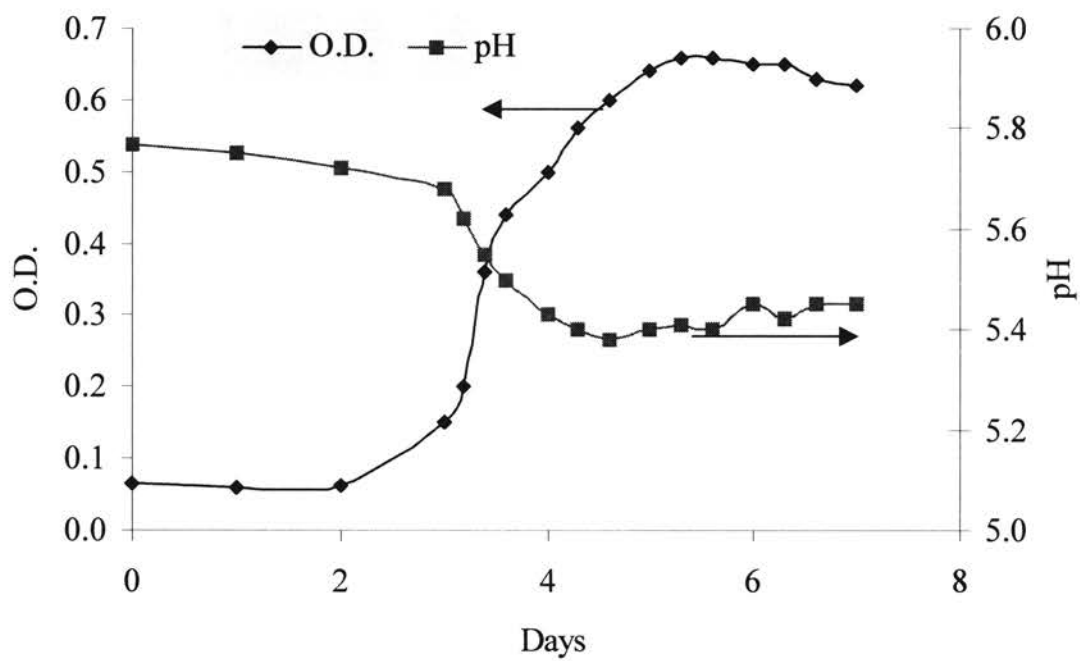


Figure 6.5. Cell concentration and pH profiles for hydrogen utilization experiment in a 1-L flask.

Finally, the run was terminated due to the low liquid level in the flask. The initial pH was 5.75 and as the cells started growing, dropped to 5.3. The pH was stabilized at 5.3 by adding anoxic 0.1N NaOH solution to the media. The pH marginally increased beyond Day 6, as shown in Figure 6.5. The temperature of the flask was maintained at 37°C during the entire period of the experiment.

6.4.1.3. Discussions on H₂ utilization

The results of the experiments performed on the 4.5 L bubble column and the 1-L flask showed that the cells utilized H₂ at the small scale only. Both the bioreactors were operated under a batch-liquid and continuous-gas mode during the batch growth phase. The quantity of inoculum added and the flow rate of the gases per unit volume of media were higher for the 1-L flask. The liquid in the bubble column was recirculated continuously through external tubing (Tygon, Cole Parmer, Vernon, IL), possibly resulting in very low amounts of oxygen transferred into the bioreactor that can affect the H₂ utilizing enzyme, hydrogenase (Adams et al., 1981). However, the resazurin indicator always showed a deoxygenated solution.

Hydrogen uptake by acetogens, similar to P7, is found due to the enzyme hydrogenase (Menon et al., 1996, Adams et al., 1981). The active site of the enzyme has iron-sulfur centers known as “H cluster” (Bennett et al., 2000). The enzyme reversibly catalyzes the uptake or the synthesis of hydrogen.

The inability of the cells to utilize hydrogen in the presence of CO could likely be due to the inhibition of hydrogenase by the CO. Experimental studies performed on *C.*

pasteurianum showed that CO inhibited hydrogenase activity irreversibly (Bennett et al., 2000). Additionally, experiments performed at the University of Oklahoma, on batch cultures, showed that the cell yields with H₂/CO₂ were ten times less than that of CO. Evidently, CO was preferred over hydrogen as substrate for cell growth. This was evident from the lack of hydrogen utilization by the cell in some of the experiments performed with both CO and H₂ in the bioreactor. Similarly, when CO was cut-off in one of the experiments and replaced with H₂, the cells were unable to grow on the new substrate and subsequently died. In the future, specific studies will be performed to target each of the following issues related to H₂ uptake by P7:

- Hydrogenase activity in the bioreactor
- Metabolic engineering of P7 to promote hydrogenase production

6.4.2 Cell recycle system for bubble column bioreactor

Several runs were performed seeking to enhance the cell concentration and ethanol production in the 4.5 L bubble column bioreactor using a total cell recycle system. The results of two illustrative runs are discussed as follows:

In the first trial, the cells were initially grown in the chemostat mode (partial cell recycle). The recycle filter was subsequently connected and the effect of total cell recycle on the cell concentration was assessed. The experiment was initiated with 100 ml of inoculum grown on CO and CO₂. The growth media contained per liter, 30 ml of mineral solution, 10 ml of vitamin solution and 10 ml of trace metal solution. As shown in Figure 6.6, the cells started growing in a batch mode after a 2 day lag period, to a concentration of 1.5 O.D.

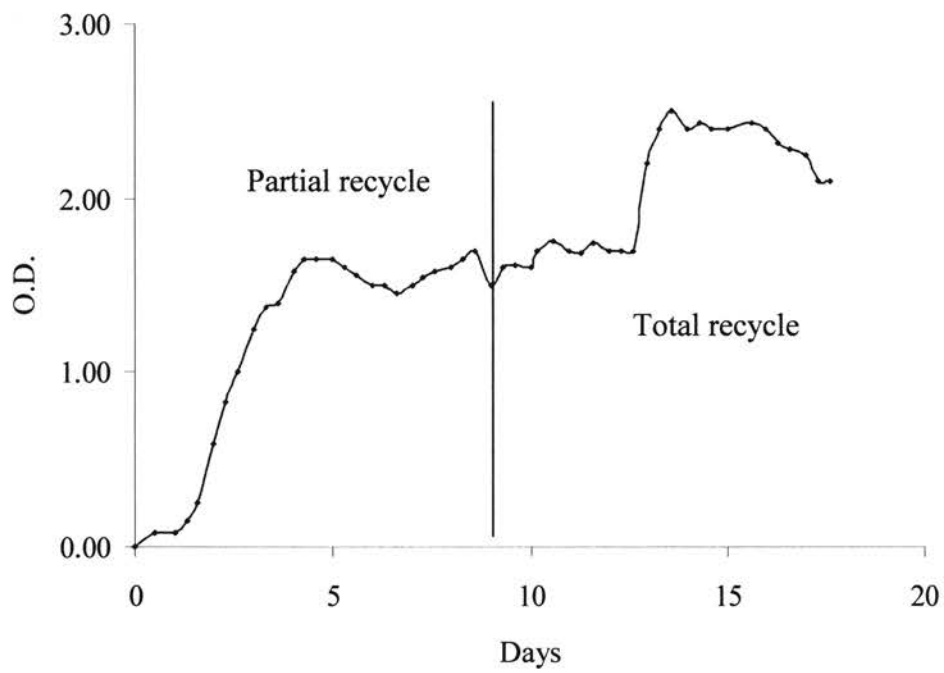


Figure 6.6. Effects of total cell recycle on cell concentration in the bubble column bioreactor. Total cell recycle was started on Day 9.

A chemostat mode of operation with 2 ml/min of fresh nutrients to the bioreactor was started on Day 3. The cell O.D. increased to 1.7 units and was stable for the next 5 days. The tangential flow recycle filter was connected to the liquid recirculation line on Day 9. The cell concentration was not affected by the total cell recycle. The cell O.D. was stable at 1.7 units. On Day 11, a fresh nutrient solution with a composition of 25 ml/L mineral solution, 15ml/L vitamin solution and 10 ml/L trace metal solution was continuously fed at 2 ml/min. The cell O.D. increased to 2.4 units and stabilized at this concentration for the next 3 days. The flow rate of the nutrients was increased to 3 ml/min on Day 16. No increase in cell O.D. was observed. On the contrary, the cell O.D. started to decrease and dropped to less than 1.5 O.D. beginning on Day 16. The recycle filter was observed to be increasingly fouled due to the continuous bioreactor operation and the permeate from the filter ceased to flow on Day 18. Following this, the experiment was terminated.

CO utilization was approximately 40% for both the partial and total cell recycle operations until Day 12. As the cell concentration increased due to the new media composition on Day 12, the CO utilization increased to 50% as shown in Figure 6.7. Due to cell death, CO utilization dropped to less than 40% on Day 18 (not shown). The CO₂ yield from CO was around 60-70% as theoretically expected.

The maximum product concentrations during the chemostat mode were 0.17 wt.% ethanol, 0.1 wt.% butanol and 0.03wt. % acetate, as shown in Figure 6.8. During the initial recycle mode, the ethanol concentration dropped to 0.12 wt.%. With higher cell concentration during the total cell recycle mode, the ethanol concentration increased to 0.24 wt.% before cell death began to control.

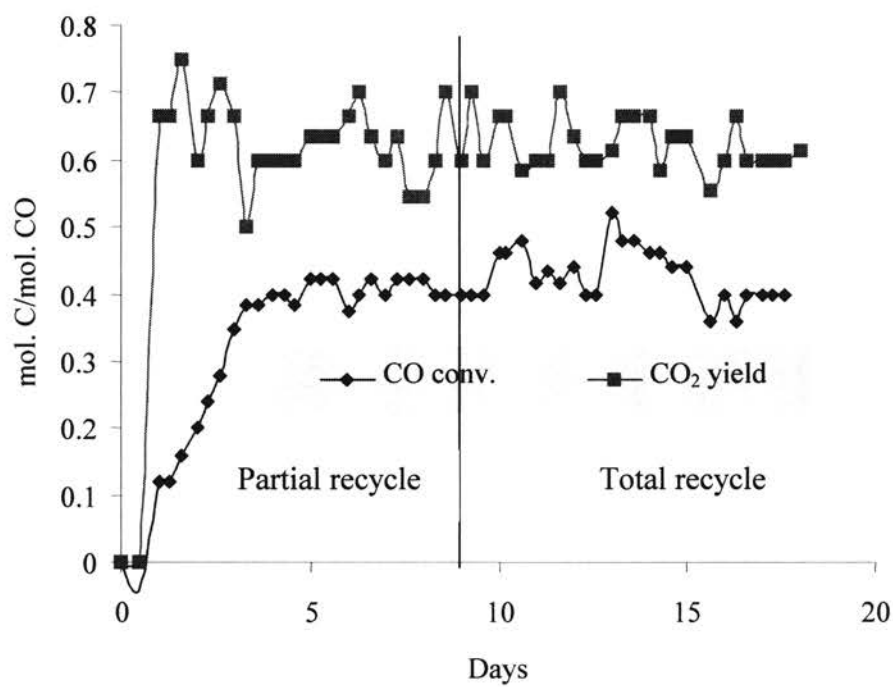


Figure 6.7. CO utilization and CO yield in the experiment with total cell recycle beginning on Day 9.

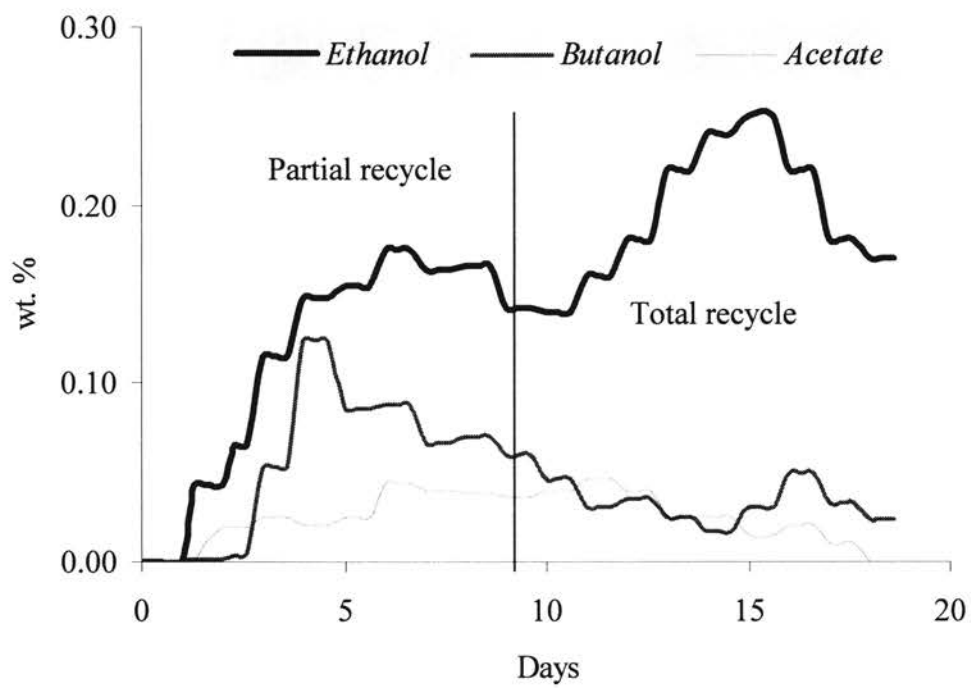


Figure 6.8. Product concentrations for the experiment with total cell recycle beginning on Day 9.

In a similar experiment, the recycle system was operational during the entire experiment. The growth media contained per liter, 30 ml of mineral solution, 10 ml of vitamin solution and 10 ml of trace metal solution. As shown in Figure 6.9, the cell started growing in a batch mode after a 3 day lag period. The initial value of μ , estimated from the batch growth phase was 0.03 hr^{-1} . A continuous mode of operation was started with 2 ml/min fresh nutrient solution on Day 5. The cell O.D. increased to 2 O.D. over the next 2 days. The flow rate of the nutrients was increased to 4 ml/min on Day 7. The cell O.D. increased to 2.3 over the next two days. Filter clogging (no permeate flow) was noticed on Day 9. At this point, the cell concentration started to decrease on Day 10. The experiment was terminated when the cell concentration dropped to less than 1.7 O.D.

Maximum CO utilization was 40% at 2 ml/min and 45% at 4 ml/min. The average yield of CO_2 from CO was in the range of 60-65%. The maximum ethanol yield from CO was 0.27 mol. C/mol. CO. The maximum product concentrations were 0.24 wt.% ethanol, 0.06 wt.% acetate and 0.08 wt.% butanol as shown in Figure 6.10.

6.4.3 Discussions on cell recycle

Results of the cell recycle experiments showed that the cell concentration in the bioreactor was not enhanced due to the total cell recycle. Results from the run started with the recycle filter showed that the specific cell growth rate, μ , was much lower than that from the run started without the filter. The initial value of μ was 0.03 hr^{-1} with the filter and 0.066 hr^{-1} without the filter (see Chapter 4).

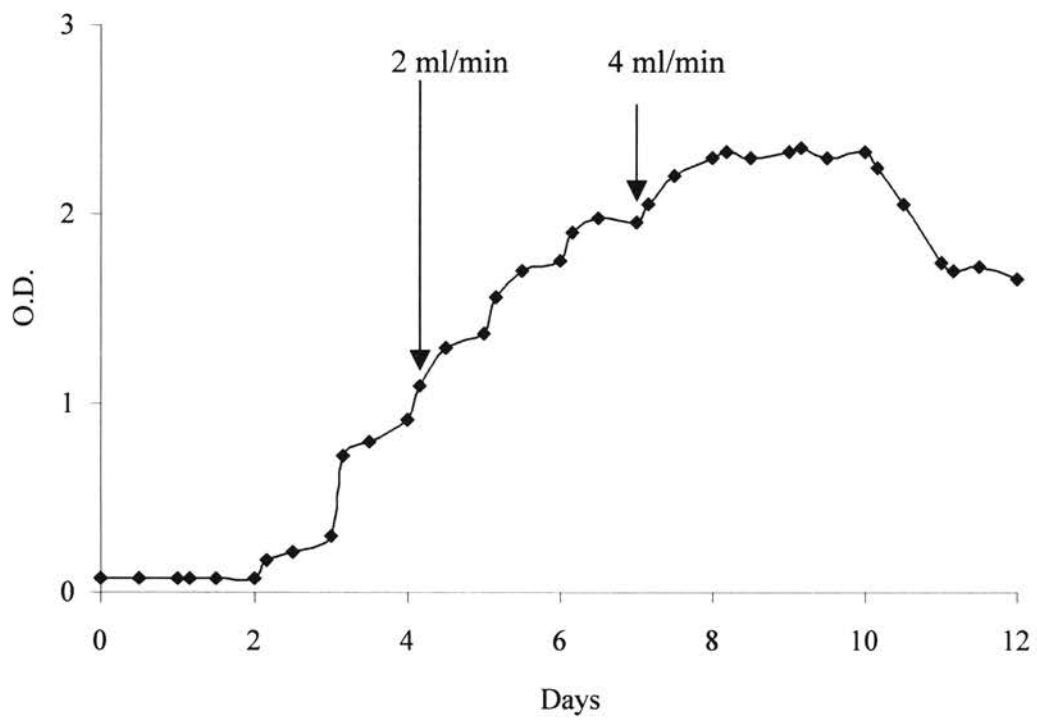


Figure 6.9. Cell concentration profile with total cell recycle during the entire period. Nutrient flow rates (ml/min) during the experiment are shown.

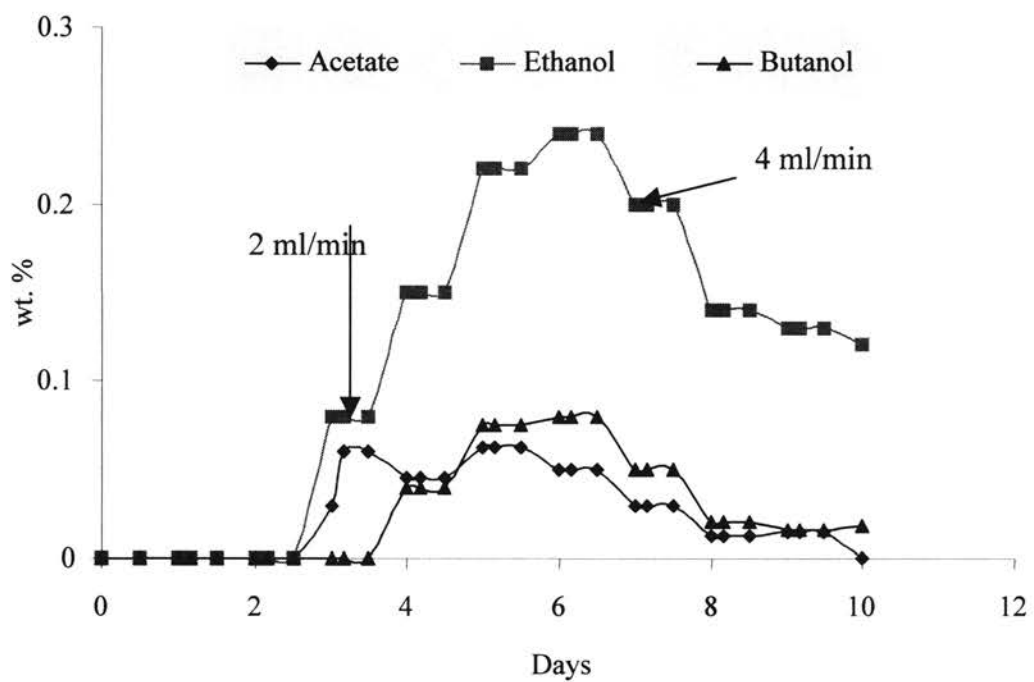


Figure 6.10. Product concentrations with total cell recycle. The filter began to clog on Day 9.

Evidently, cell growth was affected by the introduction of the recycle filter to the bioreactor. Shear stresses experienced by the cell within the lumens of the recycle filter could result in higher death rates of the cells. Bacteria are generally resistant to shear due to the presence of thick cell walls. However, the cell-resistance of P7 to shear needs to be assessed. With an increase in the vitamin concentration during the recycle mode, the cell concentration increased. This effect also needs to be investigated further, but again demonstrates that nutrient limitations currently control the bioreactor performance.

6.4.4 Nutrient screening

6.4.4.1 Design of Experiment

The experimental design involving 23 trials for 10 nutrient at two concentrations was used for the study as shown in Table 6.1. The elements '+1' and '-1' represent the two different concentrations of the independent variables under investigation, as shown in Table 6.2. The design was based on the standard Plackett-Burman (PB) design with 20 trials. The methodology assumes that important main effects will be much larger than two-factor interactions (i.e. two nutrient interact to affect a significant response). The PB design is a fraction of the two-factorial design allowing investigation of up to N-1 variables from N trials. The responses Y1 and Y2, representing cell concentration (O.D. units) and ethanol yield (wt.%/ cell O.D.), respectively, were measured for each trial. The ranges of the variables were chosen based on the original media composition for the cell culture. Once experiments were performed, multiple regression analysis was

TRIALS	X1	X2	X3	X4	X5	X6	X7	X8	X9	X10	Y1	Y2
1	1	1	-1	-1	1	1	-1	1	-1	1	0.42	0.15
2	1	-1	-1	1	1	1	-1	-1	1	-1	0.59	0.23
3	1	-1	1	1	1	1	1	1	-1	1	0.20	0.16
4	-1	1	1	1	1	-1	-1	-1	1	-1	0.47	0.14
5	1	1	1	1	-1	1	1	1	-1	-1	0.11	0.00
6	1	1	-1	-1	1	-1	-1	-1	-1	-1	0.51	0.18
7	1	1	-1	1	-1	1	1	-1	-1	-1	0.74	0.25
8	1	-1	1	-1	1	-1	1	-1	-1	1	0.00	0.00
9	-1	1	-1	1	-1	-1	1	-1	1	1	0.31	0.19
10	1	-1	1	-1	-1	-1	1	1	1	-1	0.10	0.00
11	-1	1	-1	-1	-1	-1	-1	1	-1	1	0.36	0.09
12	1	-1	-1	-1	-1	1	-1	-1	-1	1	0.33	0.32
13	-1	-1	-1	-1	1	1	1	1	1	-1	0.20	0.16
14	-1	-1	-1	1	1	-1	-1	1	-1	-1	0.29	0.34
15	-1	-1	1	1	-1	1	-1	-1	-1	1	0.25	0.32
16	-1	1	1	-1	1	1	1	-1	1	1	0.36	0.34
17	1	1	-1	1	1	-1	1	1	1	1	0.21	0.11
18	1	-1	1	1	-1	-1	-1	1	1	1	0.31	0.28
19	-1	1	1	-1	-1	1	-1	1	1	-1	0.41	0.28
20	-1	-1	-1	-1	-1	-1	1	-1	-1	-1	0.40	0.24
3*	1	1	1	1	-1	1	1	1	-1	-1	0.21	0.07
5*	1	-1	1	-1	-1	-1	1	1	1	-1	0.20	0.07
17*	1	1	-1	1	1	-1	1	1	1	1	0.21	0.08

Table 6.1. Plackett-Burman design for screening nutrients.
Y1 - Cell concentration (O.D.); Y2 - Ethanol yield (wt.%/O.D.);
See Table 6.2 for definitions of X1 through X10.
Some replicates were performed as denoted by *.

Factors	Nutrient	Level 1	Level -1
X1	Fe. Amm. Sulfate	2.4 mg	1.2 mg
X2	Nickel chloride	0.06 mg	0.03 mg
X3	Cobalt chloride	0.6 mg	0.03 mg
X4	4% sulfide solution	1.5 ml	0.75 ml
X5	Cellobiose	7.5 mg	0 mg
X6	Yeast extract	7.5 mg	0 mg
X7	MES buffer	75 mg	37.5 mg
X8	Methy viologen	4.5 mg	0 mg
X9	Media concentration	double	regular
X10	Vitamin B12	0.0075 mg	0.00375 mg

double = 40 ml/L minerals, 20 ml/L vitamins and 10 ml/L trace metal solutions.

regular = 20 ml/L minerals, 10 ml/L vitamins and 5 ml/L trace metal solutions.

Table 6.2. Factors and ranges selected for the Plackett-Burman design

performed to correlate the independent variables (X1 through X10) to each response (Y1 and Y2) according to a linear model described as,

$$Y = A + B X_1 + C X_2 + D X_3 + \dots + K X_{10} \quad 6.5$$

where Y is the response and A, B, C... K are the coefficients of the linear model and X's are the factors.

6.4.4.2 Results

Each response, namely cell concentration in O.D. and ethanol yield in wt.% / (O.D.), was individually analyzed from outcomes of the PB experiment performed (Table 6.1). A total of 23 runs were performed with trial 20 as the control repeated for each experiments (Cell grew in Trial 20 to 0.47 O.D. units that was higher than that in the other bottles during the first batch of experiments. Hence, Trial 20 was chosen as the control and repeated during every successive batch). Trials 3, 5 and 17 had shown poor cell growth and hence replicated by Trials 21, 22 and 23.

Cell concentration (Y1) was affected significantly at a 95% confidence level (p-value < 0.05) by X1, X7 and X8, as shown by Table 6.3. The negative coefficients indicated that cell concentration was not favored at the higher levels of the corresponding nutrients namely, cobalt chloride (X1), MES buffer (X7) and methyl viologen (X8). The remaining seven nutrients appeared not to significantly affect cell concentration in the experiments. However, the screening design considered only the main effects of the factors. Hence, a more extensive factorial design is required to account for possible interactions between individual factors.

<i>Coeff</i>	<i>Value</i>	<i>S.E.</i>	<i>t Stat</i>	<i>P-value</i>	<i>Lower 95%</i>	<i>Upper 95%</i>
A	0.3233	0.0258	12.5288	0.0000	0.2671	0.3795
B	0.0168	0.0272	0.6168	0.5489	-0.0424	0.0759
C	0.0471	0.0256	1.8361	0.0912	-0.0088	0.1030
D	-0.0658	0.0275	-2.3904	0.0341	-0.1257	-0.0058
E	0.0159	0.0255	0.6241	0.5442	-0.0396	0.0713
F	-0.0149	0.0260	-0.5731	0.5772	-0.0715	0.0417
G	0.0334	0.0260	1.2837	0.2235	-0.0233	0.0901
H	-0.0638	0.0257	-2.4862	0.0286	-0.1198	-0.0079
I	-0.0652	0.0264	-2.4687	0.0296	-0.1228	-0.0077
J	0.0287	0.0270	1.0619	0.3092	-0.0302	0.0875
K	-0.0455	0.0253	-1.7942	0.0980	-0.1007	0.0097

ANOVA

	<i>df</i>	<i>SS</i>	<i>MS</i>	<i>F-value</i>	<i>Significant F</i>
Regression	10	0.4425	0.0443	3.1168	0.0330
Residuals	12	0.1704	0.0142		
Total	22	0.6129			

df - degrees of freedom, SS - sum of squares, and MS - mean square value.

<i>Regression Statistics</i>	
Multiple R	0.850
R Sq.	0.722
Adj. R Sq.	0.490
Std. Error	0.119
Observations	23

Table 6.3. Regression analysis for cell concentration (Y1) using Eq. 6.5.

The ANOVA table for cell concentration showed a correlation coefficient of 0.85. The F-value showed that the model was reliable since the calculated F value (3.1168) was 94 times higher than the listed value (0.0330) for 95% of confidence. (Practically, a model has statistical significance when the calculated F value is at least 3-5 times greater than the listed value, Steel at al., 1997). The predicted values of cell O.D. (Y1) by the linear model (Eq. 6.5) were compared to the actual values and residual were determined to verify the accuracy of the linear model Eq. 6.5 (Table 6.4 and Figure 6.15).

The ethanol yield per unit cell mass was not significantly affected by any of the factors at a 95% confidence level (Table 6.5). However, ferrous ammonium sulfate (X1) and yeast extract (X6) appeared to have higher effects on ethanol yield than any other nutrient. The ANOVA table showed a correlation coefficient of 0.77. The F-value calculated for the model was 1.78 and was higher than the listed value (0.1693) by at least 10 times showing that the model was reliable. The model predictions were compared with the actual observations and residuals were determined (Table 6.6 and Figure 6.16).

6.4.4.3. Discussions on screening

The ten factors for the PB design were chosen based on reported literature on the effects of nutrients (Vega et al., 1987, Klasson et al., 1991, Sudha Rani et al., 1992) and enzymatic pathways in syngas fermentation (Wood, 1984). The varying effects of each nutrient shown by the design were based on the assumption that only main effects, and not the interactions between nutrients, were dominant.

Cell concentration was shown to be influenced by cobalt chloride (X1), MES

<i>Trials</i>	<i>Predicted Y1</i>	<i>Observed Y1</i>	<i>Residuals</i>
1	0.3800	0.4196	0.0396
2	0.5963	0.5894	-0.0069
3	0.0584	0.2002	0.1418
4	0.4586	0.4686	0.0100
5	0.2733	0.1113	-0.1620
6	0.5346	0.5138	-0.0208
7	0.5353	0.7397	0.2044
8	0.0903	0.0000	-0.0903
9	0.4014	0.3086	-0.0928
10	0.1379	0.1012	-0.0367
11	0.3094	0.3600	0.0506
12	0.4460	0.3320	-0.1140
13	0.2730	0.2002	-0.0728
14	0.3082	0.2893	-0.0189
15	0.3128	0.2500	-0.0628
16	0.2751	0.3550	0.0799
17	0.2747	0.2130	-0.0617
18	0.2064	0.3100	0.1036
19	0.3930	0.4066	0.0136
20	0.3090	0.4022	0.0932
21	0.2733	0.2125	-0.0608
22	0.1379	0.1956	0.0577
23	0.2064	0.2124	0.0060

Table 6.4. Residuals from the regression analysis for cell concentration. Experimental values (observed Y1) were compared with predicted Y1 from the linear model (Eq. 6.5).

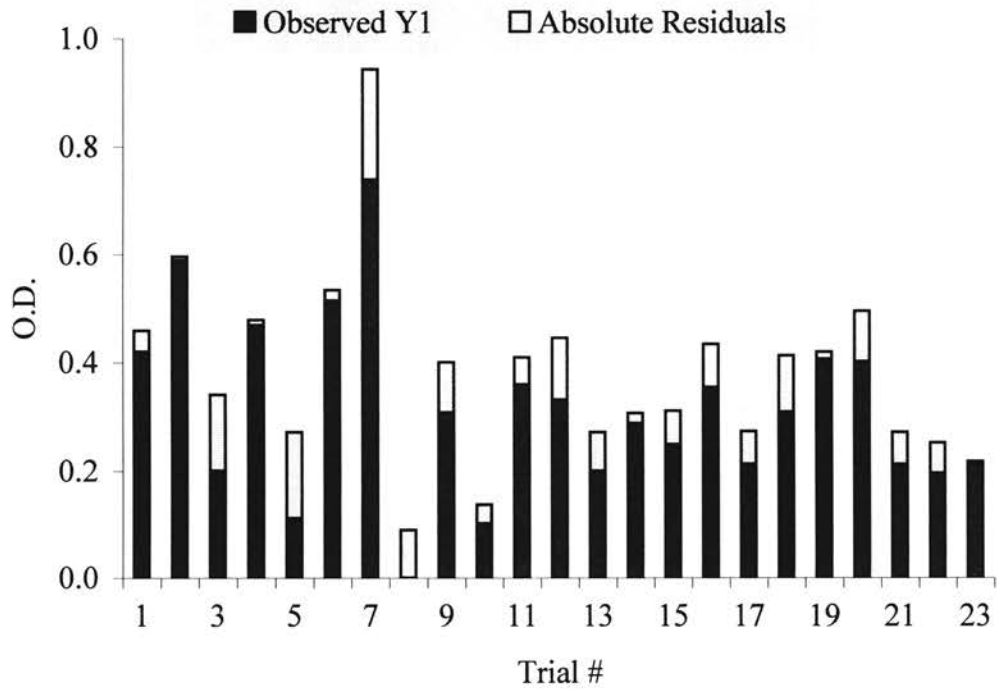


Figure 6.15. Experimental cell O.D. (Y1) and absolute residuals from the regression of Eq. 6.5.

<i>Coeff.</i>	<i>Value</i>	<i>S.E.</i>	<i>t Stat</i>	<i>P-value</i>	<i>Lower 95%</i>	<i>Upper 95%</i>
A	0.1901	0.0205	9.2729	0.0000	0.1454	0.2347
B	-0.0417	0.0216	-1.9346	0.0770	-0.0888	0.0053
C	-0.0228	0.0204	-1.1171	0.2858	-0.0671	0.0216
D	-0.0259	0.0219	-1.1867	0.2583	-0.0735	0.0217
E	0.0127	0.0202	0.6295	0.5408	-0.0313	0.0568
F	-0.0059	0.0206	-0.2842	0.7811	-0.0508	0.0391
G	0.0407	0.0207	1.9701	0.0723	-0.0043	0.0858
H	-0.0338	0.0204	-1.6559	0.1236	-0.0782	0.0107
I	-0.0274	0.0210	-1.3056	0.2162	-0.0731	0.0183
J	0.0109	0.0214	0.5067	0.6215	-0.0359	0.0576
K	0.0110	0.0201	0.5485	0.5934	-0.0328	0.0549

ANOVA

	<i>df</i>	<i>SS</i>	<i>MS</i>	<i>F-value</i>	<i>Significant F</i>
Regression	10	0.1600	0.0160	1.7862	0.1693
Residuals	12	0.1075	0.0090		
Total	22	0.2675			

df - degrees of freedom, SS - sum of squares, and MS - mean square value.

<i>Regrn. Statistics</i>	
Multiple R	0.773
R Sq.	0.598
Adj. R Sq.	0.263
Std. Error	0.095
Observations	23

Table 6.5. Results of regression analysis for ethanol yield (Y2) using Eq. 6.5.

<i>Trials</i>	<i>Predicted Y2</i>	<i>Observed Y2</i>	<i>Residuals</i>
1	0.1802	0.1531	-0.0271
2	0.3056	0.2274	-0.0782
3	0.1317	0.1608	0.0290
4	0.2102	0.1358	-0.0744
5	0.0759	0.0000	-0.0759
6	0.1314	0.1813	0.0498
7	0.1825	0.2450	0.0625
8	0.0796	0.0000	-0.0796
9	0.2284	0.1917	-0.0367
10	0.0362	0.0000	-0.0362
11	0.1939	0.0917	-0.1023
12	0.2922	0.3221	0.0299
13	0.2413	0.1608	-0.0805
14	0.2311	0.3405	0.1094
15	0.3493	0.3200	-0.0293
16	0.2208	0.3380	0.1172
17	0.0784	0.1128	0.0344
18	0.1513	0.2824	0.1311
19	0.2232	0.2809	0.0577
20	0.2046	0.2435	0.0389
21	0.0759	0.0706	-0.0053
22	0.0362	0.0685	0.0323
23	0.1513	0.0847	-0.0666

Table 6.6. Residuals from the regression analysis for ethanol yield. Experimental values (observed Y2) were compared with predicted Y2 from the linear model (Eq. 6.5).

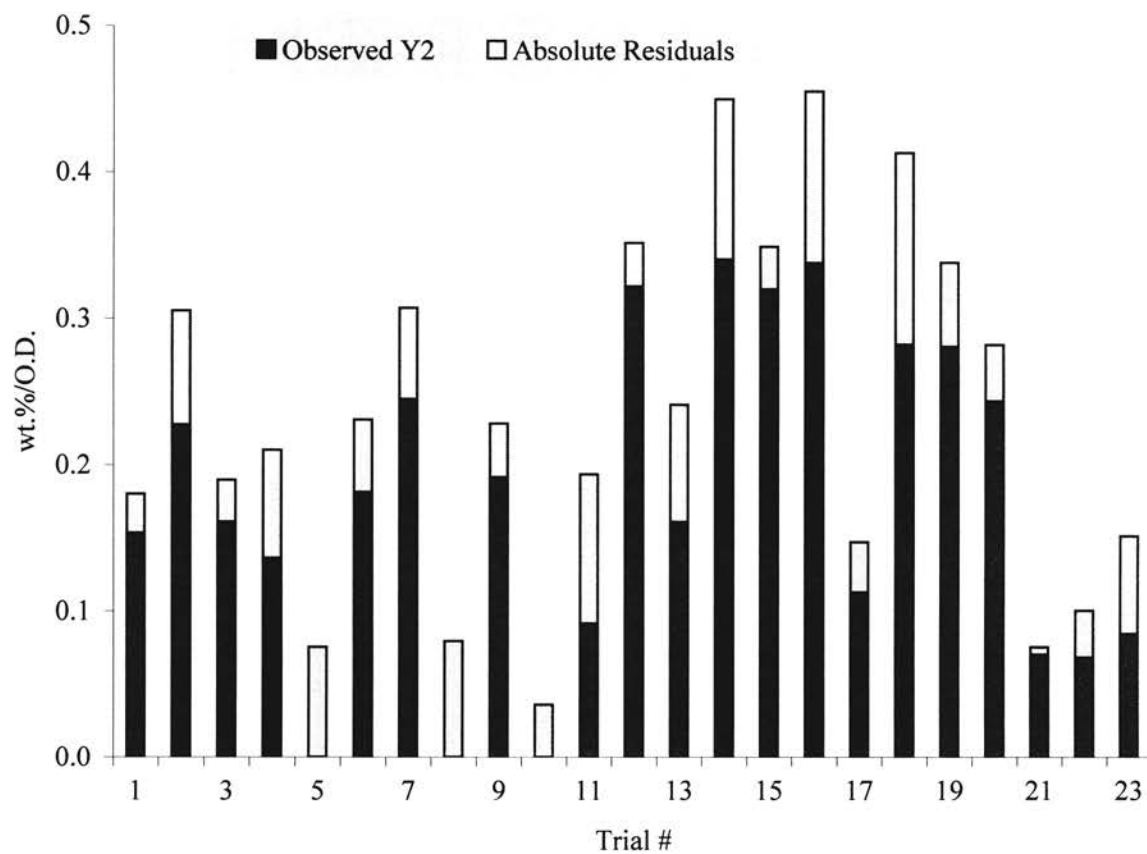


Figure 6.16. Experimental ethanol yield (Y2) and absolute residuals from the regression of Eq. 6.5.

buffer (X7) and methyl viologen (X8). Each nutrient has a different role in the metabolic pathway of the bacteria P7. Cobalt ions are the active components of the corrinoid enzyme responsible for the synthesis of the acetyl-CoA intermediate in the metabolic pathway (see Appendix I)). MES is a biological buffer used commonly in clostridial fermentations (Vega et al., 1987). The buffer maintains a stable pH at least during the initial growth phase. Methyl viologen is a reducing agent providing anoxic conditions for clostridial cell growth (Klasson et al., 1992). The fact that the cell concentration was higher with lower levels (-1) of the nutrients indicated the possibility of substrate inhibition on cell growth. The studies need to be expanded to consider potential interaction effects and estimations of optimal nutrient levels.

6.5. Conclusions

Process enhancement methods experimentally verified in this Chapter included incorporating H₂ in the feed gas, recycling cells to improve cell concentrations in the bioreactor, and screening nutrients that may affect cell growth and ethanol yield.

Hydrogen was utilized by the cells for growth only in the one-liter flask but not in the five liter bubble column bioreactor. Future experiments to facilitate H₂ uptake by P7 will include targeted enzymatic studies to estimate the activity levels of the enzymes involved in the process, metabolic engineering of P7, and changes in inoculum preparation for the bioreactor.

Cell recycle did not affect cell concentrations in the bubble column bioreactor. Filter fouling was one of the major problems encountered during the study. The fouling

characteristics of the recycle filter will be determined in future studies. Also, the optimal filter system for providing continuous and long operations will be required.

Screening and identifying factors significantly affecting cell growth and ethanol yield from a synthetic mixture of gases containing CO, CO₂ and N₂ were studied. A two-level, Plackett-Burman technique with ten factors and 20 trials was experimented on small semi-batch bioreactors. Results from the experiments showed that cell concentration was inversely affected by the amounts of cobalt chloride, MES buffer and methyl viologen in the fermentation media. Ethanol yield per unit cell mass was not significantly affected by the media composition. Only the main effects of the factors were studied during the screening experiments. In the future, full factorial experiments will be performed to determine two factor interactions between the selected variables, namely, cobalt chloride, MES buffer and methyl viologen. Response surfaces methodology will be used to identify the optimum concentrations of the nutrients.

CHAPTER 7

CONCLUSIONS

The conversion of renewable biomass to fuel ethanol is an important process being investigated as a possible alternative to the fast depleting resources of petroleum. Unlike fossil fuels, ethanol from renewable biomass is environmentally benign in maintaining global CO₂ balance and reducing toxic emissions. Despite the current low utilization of ethanol in the United States as an additive to gasoline, ethanol based fuels have been projected as a primary candidate to supplement and even replace gasoline in the future.

A major constraint for the use of fuel ethanol as an additive or possibly, as a future replacement to gasoline, is the high price of ethanol. Wholesale ethanol prices, prior to incentives from the federal and state governments, are approximately twice that of gasoline. Arguably, the ethanol as a fuel could not survive without the tax exemption, emphasizing a need for inexpensive routes for production.

Lignocellulosic materials, such as grasses, wood chips or paper wastes, are inexpensive carbohydrate sources available for the production of ethanol. Several processes are currently popular for the production of ethanol from lignocellulosic materials. One such process showing potential for commercial production of ethanol is the gasification and fermentation process. Gasification of agricultural crops and residues can convert almost all of the carbon contained in lignocellulosic materials to gaseous

products that can be fermented by bacteria. During the last decade, significant work has been in progress to develop cost-efficient processes and high-yielding strains to commercially produce bio-ethanol from syngas. A key step in the overall biomass energy strategy, currently investigated by Oklahoma State University and the University of Oklahoma, is the bioconversion of syngas to ethanol using a recently isolated anaerobic bacterium. Currently, a 5-liter bubble column bioreactor is in operation at Oklahoma State University.

In view of the limited knowledge available in syngas fermentations, the research was targeted on investigating some of the critical engineering issues involved with the bioreactor process. Characteristics of the process, such as cell stability, productivities, inhibitory effects of substrates/products, pH and temperature effects, and optimization of the media for maximum ethanol productivities were focused.

To successfully grow P7 and produce ethanol on a continuous mode for long operational periods, data on critical process conditions for stable cell concentration and ethanol production, such as the optimum pH and temperature ranges, gas and liquid flow rates, nutrient and feed gas compositions, and mass transfer and kinetic rate limitations were investigated in this research using synthetic blends CO, H₂, CO₂ and N₂.

Key Research findings

Cell instability in the bioreactor was initially experienced due to lack of sufficient sodium sulfide concentrations in the media. Without regular additions of sodium sulfide, experiments resulted in cell concentration instability. On the other hand, cell growth was stable when the sodium sulfide concentration was closely monitored and maintained in

the range of 0.1 ppm to 1 ppm. The role of reducing agents, such as sodium sulfide, in altering electron flow pathways was reportedly responsible for active cell growth rates and product distributions in several anaerobes similar to P7 (Rao and Mutharasan, 1988, Rao, 1987). The experiments conducted on the bubble column bioreactor established the mandatory requirement of sodium sulfide for stable cell growth conditions under both chemostat and total cell recycle modes of operation.

In previous research on syngas fermentations, the main resistance for gas transfer to the cells was observed to be the liquid film surrounding the bubbles (Worden et al., 1997, Vega et al., 1991). On the other hand, the bubble column bioreactor was found to be limited by the intrinsic kinetics of the bacterial cells (nutrient limitations) and not by the mass transfer rate of CO from the bulk gas phase to the cells. The fine size of the bubbles dispersed by the porous fritted disc provided sufficient mass transfer area for CO transfer.

The ability of the bacterium P7 to recover from process shocks due to changes in process conditions were investigated. Process variations, such as, changes in nutrient flows and composition, pH, temperature and changes in feed gas compositions were introduced in the bioreactor to assess the effects on the performance of P7.

Higher dilution rates favored the production rates of cells and ethanol. The bioreactor is limited by the intrinsic kinetics of the cells, influenced directly by the nutrient compositions in the media. Increasing trace metal content in the bioreactor increased cell and product concentrations and the CO uptake without affecting the yields of products. CO₂ is required for initiating and sustaining cell growth in the bioreactor. Interestingly, CO₂ is a by-product of the conversion of CO by P7 but appears not to be

utilized. Sudden spikes in pH and temperature temporarily affected cell growth and metabolic activities. However, the cells rapidly recovered from pH and temperature shocks and performed normal metabolism once normal operating conditions were restored. The results show that P7 is tolerant to certain process shocks likely to occur in any industrial scale bioreactor.

The productivity and yield of ethanol from the components of syngas was desired to be improved by incorporating H₂ in the feed gas, recycling cells to improve cell concentrations in the bioreactor, and screening nutrients that may affect cell growth and ethanol yield. Hydrogen was utilized by the cells for growth only in the one-liter flask but not in the 5 L bubble column bioreactor. Cell recycle did not affect cell concentrations in the bubble column bioreactor.

Screening and identifying factors significantly affecting cell growth and ethanol yield from synthetic blends CO, CO₂ and N₂ were studied. The cell concentration was inversely affected by the amounts of cobalt chloride, MES buffer and methyl viologen in the fermentation media. Ethanol yield per unit cell mass was not significantly affected by the media composition.

The following summarize the significant findings in this research work,

- Maintaining sodium sulfide concentration (0.1 – 1 ppm) is essential for cell stability in the bioreactor.
- Intrinsic kinetic parameters of P7 for cell growth, CO uptake and product formation were estimated. The performance of P7 was compared with other CO consuming bacteria. Key areas for improvement of P7 were identified as shown in Chapter 4.

- Higher dilution rates favored the production rates of cells and ethanol.
- The bioreactor is currently limited by the intrinsic kinetics of the cells (nutrient limitations).
- Increasing trace metal content in the bioreactor increased cell and product concentrations and the CO uptake without affecting the yields of products.
- CO₂ is required for initiating and sustaining cell growth in the bioreactor.
- P7 is tolerant to pH and temperature shocks over the ranges studied.
- Hydrogen was utilized by the cells for growth only in the small-scale bioreactor (one-liter flask) but not in the 5 L bubble column bioreactor.
- Cell recycle did not affect cell concentration in the bioreactor.
- Cell concentration was inversely affected by cobalt chloride, MES buffer and methyl viologen in the fermentation media. Ethanol yield per unit cell mass was not significantly affected by the media composition.

Future studies

Hydrogen uptake: Hydrogen uptake by acetogens, similar to P7, was found due to the enzyme hydrogenase (Menon et al., 1996, Adams et al., 1981). The active site of the enzyme has iron-sulfur centers known as the “H cluster” (Bennett et al., 2000). The enzyme reversibly catalyzes the uptake or the synthesis of hydrogen. In the future, specific studies will target,

- Hydrogenase activity in the bioreactor
- Metabolic engineering of P7 to promote hydrogenase production

Cell recycle: Filter fouling was one of the major problems encountered during the study. The fouling (clogging) characteristics of the recycle filter will be determined in future studies. Optimal filter configurations will be determined to provide long operational periods. Hollow fiber membrane filters, ceramic and stainless steel fritted tubes, and plate and frame filters are some of the likely candidates to be tested for increasing cell concentrations.

Media optimization: The next step in media optimization will be to perform full factorial experiments on the key nutrients identified by the initial screening design, namely, cobalt chloride, MES and methyl viologen . Response surfaces will be generated and the optimal nutrient compositions will be determined. Nutrient optimization with H₂ in the feed gas will also be performed in a similar way.

Aphrons for mass transfer enhancement: In the future, the bioreactor may be mass transfer limited due to the cell concentration enhancement with an efficient cell recycle system. Also, the bioreactor is expected to be scaled-up to a working volume of 50 L. The scaled-up version of the current fritted disc sparger may result in high pressure drops leading to high operational costs. Under these circumstances, the mass transfer rate of the syngas can be increased by the use of microbubble dispersions called “aphrons”. An aphron generator has been designed and the operational characteristics of the unit are currently being investigated. In the future, syngas will be incorporated as aphrons using suitable surfactants to enhance mass transfer. Improvements in aphron-generator design specific to the research will include recycling of unabsorbed gases exiting the tank.

Process scale-up : In the future, the bubble column bioreactor is expected to be scaled up to a 50 L volume. The existing fritted disc sparger could possibly result in high pressure drops at the 50L scale. Therefore, the gaseous reactants will be dispersed using the aphon generator. The process is expected to be scaled up based on mass transfer requirements of the bioreactor.

Economic analysis : The overall model for the gasification-fermentation process will be determined. Economic analysis on the integrated system will be performed to evaluate the final product ethanol costs. The ethanol cost for the integrated system will be compared with that of similar processes, such as the hydrolysis-fermentation process for lignocellulosic materials and the fermentation process for corn. Specific areas requiring process enhancement, such as process parameters for the gasifier and the bioreactor will be identified using the economic model of the overall process.

REFERENCES

- Abrini, H., H. Naveau, and E.J. Nyns. (1994). *Clostridium autoethanogenum*, sp. nov., an anaerobic bacterium that produces ethanol from carbon monoxide. Arch Microb, 161, 345-351.
- Adler, H.I., and W. Crow. (1987). A technique for predicting the solvent producing ability of *Clostridium acetobutylicum*. Applied and Environmental Microbiology, 53(10), 2496-2499.
- Afschar, A.S., K. Shaller, and K. Schugerl. (1986). Continuous production of acetone and butanol with shear activated *Clostridium acetobutylicum*. Appl Microbiol Biotechnol, 23, 315-321.
- Akita, K., and F. Yoshida. (1974). Bubble size interfacial area and liquid phase mass transfer coefficient in bubble columns. Ind Eng Chem Proces Des Develop, 13(1), 84-90.
- Andersch, W., H. Bahl, and G. Gottschalk. (1983). Level of enzymes involved in acetate butyrate acetone and butanol formation by *Clostridium acetobutylicum*. Eur J Appl Microb Biotechnol, 18, 327-332.
- Bahl, H, M.Gottwald, A. Kuhn, W.Andersch, and G.Gottschalk. (1986). Nutritional factors affecting the ratio of solvents produced by *Clostridium acetobutylicum*. Appl Env Microb, 52(1), 169-172.
- Baronofsky, J.J., Scheurs W.J.A., and E.R. Kashket. (1984). Uncoupling of acetic acid limits growth of and acetogenesis by *Clostridium thermoaceticum*. Appl Env Microb, 48(6), 1134-1139.
- Baskaran, S, H Ahn, and LR Lynd. (1995). Investigation of the ethanol tolerance of *Clostridium thermosaccharolyticum* in continuous culture. Biotechnology Progress, 11, 276-281.
- Bello, R. Ade, C. W. Robinson, and M. Moo-Young. (1984). Liquid circulation and mixing characteristics of airlift contactors. The Canadian Journal of Chem Eng, 62, 573-577.
- Bettagli, N., Desideri U., and Fiaschi D. (1995). A biomass combustion-gasification model validation and sensitivity analysis. Journal of Energy Resources Technology,

117, 329-336.

Blackburn, W.J., and Teague J.M. (1998). Coordinating California's efforts to promote waste to alcohol production. Appl Biochem Biotech, 70-72, 821-841.

Bowman, L., and E. Geiger. (1984). Optimization of fermentation conditions for alcohol production. Biotech Bioeng, 26, 1492-1497.

Bredwell M, Telgenhoff M, Worden R. (1995). Formation and Coalescence Properties of Microbubbles. Applied Biochem Biotech, 51-52, 501-508.

Bredwell M., Worden R. M. (1998). Mass-Transfer Properties of Microbubbles. 1. Experimental studies. Biotechnology Prog., 14(1), 31-38.

Chang, H.N., W.G. Lee, and B.S. Kim. (1992). Cell retention culture with an internal filter module continuous ethanol fermentation. Biotech & Bioeng, 41, 677-681.

Christoph, Grote, and Pawliszyn Janusz. (1997). Solid phase microextraction for the analysis of human breath. Analytic Chemistry, 69, 587-596.

Clausen, E., and J.L. Gaddy. (1993). Concentrated sulfuric acid process for converting lignocellulosic materials to sugars. United States Patent 5188673, 5.

Dale, M.C., Chen. C., and M.R. Okos. (1990). Cell growth and death rates as factors in the long-term performance, modeling, and design of immobilized cell reactors. Biotech. Bioeng, 36, 983-992.

Deckwer, W.D., and A. Schumpe. (1993). Improved tools for bubble column reactor design and scale up. Chem Eng Sci, 48(5), 889-911.

Espinosa-Solares, T., E. Brito-De La Fuente., A. Tecante., P.A. Tanguy. (1997). Power consumption of a dual turbine helical ribbon impeller mixer in ungasged conditions. Chemical Engineering Journal, 67, 215-219.

Fontecilla-Camps, J.C., M. Frey, E. Garcin, C. Hatchikian, Y. Monet, C. Piras, X. Vernede, and A. Volbeda. (1997). Hydrogenase a hydrogen metabolizing enzyme what do the crystal structures tell us about its mode of action. Biochimie, 79, 661-666.

Gaddy. (1982). Ethanol production with an immobilized cell reactor. United States Patent.

Gaddy, Vega, Holmberg, and Clausen. (1989). Fermentation parameters of *Peptostreptococcus productus* on gaseous substrates (CO₂/H₂/CO₂). Arch Microbiol, 151, 65-70.

Gaddy, Tyree, and Clausen. (1991). The production of propionic acid from sugars by fermentation through lactic acid as an intermediate. J Chem Tech Biotechnology, 50, 157-166.

Gaddy, J.L. (1997). Clostridium stain which produces acetic acid from waste gases. United States Patent 5593886, 4.

Gottschal, J.C., and J.G. Morris. (1981). The induction of acetone and butanol production in cultures of *Clostridium acetobutylicum* by elevated concentrations of acetate and butyrate. FEMS Microb Lett, 12, 385-389.

Grado, S.C., and M.J. Chandra. (1998). A Factorial Design Analysis of a Biomass to Ethanol Production System. Biomass and Bioenergy, 15(2), 115-124.

Grote, C., and J. Pawliszyn. (1997). Solid phase microextraction for the analysis of human breath. Anal. Chem, 69, 587-596.

Grupe, H., and G. Gottschalk. (1992). Physiological events in *Clostridium acetobutylicum* during the shift from acidogenesis to solventogenesis in continuous culture and presentation of a model for shift induction. Applied and Environmental Microbiology, 58(12), 3896-3902.

Guell, C., and J. Giralt. (1994). Determination of $k_L a$ values using CO₂ mass balance technique in a coal desulfurization bioreactor. Ind Eng Chem and Research, 33(4), 950-956.

Herrero, A.A., and R.F. Gomez. (1980). Development of ethanol tolerance in *Clostridium thermocellum* effect of growth temp. Applied and Environmental Microbiology, 40(3), 571-577.

Hill, Paul, T. Klapatch, and L. Lynd. (1993). Bioenergies and end product regulation of *Clostridium thermosaccharolyticum* in response to nutrient limitation. Biotech and Bioeng, 43, 873-883.

Himmel, M.E., Adney, S.A., Baker, J.O., Elander, R., McMillan, J.D., Nieves, R. A., Sheehan, J.J., Thomas, S.R., Vinzant, T.B., Zhang, M. (1997), Fuels and Chemicals from Biomass, American Chemical Society, 1-45.

Hinman, N.D., and M.A. Yancey. (1998). Use of net present value analysis to evaluate a publicly funded biomass to ethanol research. Appl Biochem Biotech, 70-72, 807-820.

Hohenstein, W.G. and Wright, L.L. (1994), Biomass energy production in the United States: an overview, Biomass and Bioenergy 6, 161-173.

Hwang, S., and C.L. Hansen. (1997). Modeling and optimization on anaerobic

- bioconversion of complex substrates to acetic and butyric acids. Biotech Bioeng, 54(5), 451-460.
- Ingram, L.O., Lai, X., Moniruzzaman, Wood, B.E., York, S.W. (1997), Fuels and chemicals from biomass, 1997 American Chemical Society, 57-73.
- Jarzebski, A., and J. Malinowski. (1989). Modeling of ethanol fermentation at high yeast concentrations. Biotechnology and Bioengineering, 34, 1225-1230.
- Jauregi, P., and J. Varley. (1998). Colloidal gas aphrons a novel approach to protein recovery. Biotechnology and Bioengineering, 59(4), 471-481.
- Kalil, S.J., F.Maugeri, and M.I. Rodrigues. (2000). Response surface analysis and simulation as a tool for bioprocess design and optimization. Process Biochemistry, 35, 539-550.
- Kang, W., R. Shukla, and K.K. Sirkar. (1990). Ethanol production in a microporous hollow fiber based extractive fermentor with immobilized yeast. Biotechnology and Bioengineering, 36 , 826-833.
- Kanno, M., and K. Toriyama. (1986). Production of ethanol by a thermophilic anaerobic bacterium and its ethanol tolerant mutant. Agric Biol Chem, 50(1), 217-218.
- Kashket, E.R., Cao, Z. (1995). Clostridial strain degeneration. FEMS Microbiology Reviews, 17, 307-315.
- Kataoka, H., H. Takeuchi, K. Nakao, H. Yagi, T.Tadaki, T. Otake, T. Miyauchi, K. Washmi, K. Watanabe, and F. Yoshida. (1979). Mass transfer in a large bubble column. J Chem Eng Jap, 12(2), 105-110.
- Kawase, Y., B. Halard, and M. Moo-Young. (1992). Liquid phase mass transfer coefficients in bioreactors. Biotech and Bioeng, 39, 1133-1140.
- Kim, B.H., P.Bellows, R.Datta, and J.G. Zeikus (1984). Control of carbon and electron flow in *Clostridium acetobutylicum* fermentations utilization of carbon monoxide to inhibit hydrogen production and to enhance butanol yields. Appl Env Microb, 48(4), 764-770.
- Kim, S., Kang S.W., and Lee J. S. (1997). Cellulase and xylanase production by *Aspergillus niger* in various bioreactors. Bioresource Technology, 59, 63-67.
- Kim, J. H., K.H. Lee, and S.Y. Kim. (2000). Pervaporation separation of water from ethanol through polyimide composite membranes. J Mem Sci, 169, 81-93.
- Klasson, K, T., M. D. Ackerson, E.C. Clausen, and J.L. Gaddy (1991). Bioreactor

design for synthesis gas fermentations. Fuel, 70, 605-614.

Kumar, M., W.P. Lu, and S.W. Ragsdale. (1994). Binding of carbon disulfide to the site of acetyl CoA synthesis by the nickel iron sulfur protein carbon monoxide dehydrogenase from *Clostridium thermoaceticum*. 33, 9769-9777.

Lamed, L.J., Lobos J.H., and T.M. Su. (1988). Effects of stirring and hydrogen on fermentation products of *Clostridium thermocellum*. Appl Env Microb, 54(5), 1216-1221.

Lee, X.P., Kumazawa T., Sato K., Seno H., Ishii A., and Suzuki O. (1998). Improved extraction of ethanol from human body fluids by headspace solid phase microextraction with a Carboxen Polydimethylsiloxane coated fiber. Chromatographia, 47(9-10), 593-595.

Ljungdahl, L.G. (1986), in Annual Review of Microbiology, vol. 40, Annual Rev. Inc., Palo Alto, CA, pp 415-450.

Margaritis, A., and R.W. Wilke. (1978). The Rotorfermentor: 1. Description of the Apparatus, Power Requirements, and Mass Transfer Characteristics. Biotech. Bioeng., 20, 709-726.

Mitchell, J.W., K.A. Albasheri, and M. Yazdian (1995). Factors affecting utilization of carbohydrates by Clostridia. FEMS Microbiology Reviews, 17, 317-329.

Monbouquette, H.G. (1992). Modeling High-Biomass-Density Cell Recycle Fermenters. Biotech. Bioeng., 39, 498-503.

National Council for Science and the Environment, (2000) CRS Issue Brief for Congress, RL30369.

Nishiwaki, A., and I.J. Dunn. (1999). Analysis of the Performance of a Two-stage Fermenter with Cell Recycle for Continuous Ethanol Production using Different Kinetic Models. Biochem. Eng. J., 4, 37-44.

Oliveira, S.C., .C.B. Paiva, A.E.S. Visconti, and R. Guidici. (1998). Discrimination between ethanol inhibition models in a continuous alcoholic fermentation using flocculating yeast. App Biochem Biotech, 74, 161-172.

Oliviera, A.C., M.F. Rosa, J.M.S. Cabral, and M.R. Aires-Barros. (1998). Improvement of alcoholic fermentations by simultaneous extraction and enzymatic esterification of ethanol. J Mole Cata B Enzymatic, 5, 29-33.

Pironti, F.F., Medina V.R., Calvo R., and Saez A.E. (1995). Effect of draft tube position on the hydrodynamics of a draft tube slurry bubble column. The Chemical Engineering Journal, 60, 155-160.

- Pitts, W., Johnson E., and Nelson B. (1994). Carbon monoxide formation in fires by high temperature anaerobic wood pyrolysis. The Combustion Institute, 1455-1462.
- Poulsen, B.R., and J.J.L. Iversen. (1998). Characterization of gas transfer and mixing in a bubble column equipped with a rubber membrane diffuser. Biotechnology and Bioengineering, 58(6), 633-641.
- Rao, G., and R. Mutharasan. (1987). Altered electron flow in continuous cultures of *Clostridium acetobutylicum* induced by viologen dyes. Applied and Environmental Microbiology, 53(6), 1232-1235.
- Rao, G., and R. Mutharasan. (1988). Altered electron flow in a reducing environment in *Clostridium acetobutylicum*. Biotechnology Letters, 10(2), 129-132.
- Riet, Klass Van't. (1979). Review of Measuring Methods and results in Non Viscous Gas-Liquid Mass Transfer in Stirred Vessels. Ind. Eng. Chem. Process. Des. Dev., 18(3), 357-364.
- Roy, D., K.T. Valsaraj, and S.A. Kottai. (1992). Separation of organic dyes from wastewater by using colloidal gas aphanes. Sep Sci Tech, 27(5), 573-588.
- Sato, K., S. Goto, S. Yonemura, K. Sekine, E. Okuma, Y. Takagi, K. Hon-Nami, and T. Saiki. (1992). Effect of yeast extract and vitamin B12 on ethanol production from cellulose by *Clostridium thermocellum* I1B. Applied and Environmental Microbiology, 58(2), 734-736.
- Sato, Kanji, S. Goto, S. Yonemura, K. Sekine, E. Omuka, Y. Takagi, K. Hon Nami, and T. Saiki. (1992). Effect of yeast extract and vitamin B12 on the ethanol production from cellulose by *C. thermocellum* I1B. Appl Env Microb 58(2), 734-736.
- Schmidt, J.N, R. Nassar, and A. Lubbert. (1992). Local dispersion in the liquid phase of gas liquid reactors. Chemical Engineering Science, 47(13-14), 3363-3370.
- Schroen, C.G.P.H., and Woodley J.M. (1997). Membrane separation for downstream processing of aqueous organic bioconversions. Biotechnology Prog, 13(3), 276-283.
- Sebba, F. (1985). An improved generator for micron sized bubbles. Chem. Ind., 91-92.
- Seong-Woo, Kang, Kim Seung-Wook, and Lee Jin-Suk. (1995). Production of cellulase and xylanase in a bubble column using immobilized *Aspergillus niger*-kks. Applied Biochemistry and Biotechnology, 53.
- Serabryakova, L.T., M. Medina, N.A. Zorin, I.N. Gogotov, and R. Gammack. (1996). Reversible Hydrogenase of *Anabena variabilis* ATCC 29413 : catalytic properties

- and characterization of redox centres. FEBS Letters, 383, 79-82.
- Slaff, G.F. (1984), Ph.D. thesis, University of Pennsylvania, University Microfilms International, Ann Arbor, MI.
- Sotelo, J.L., F.J. Benitez, J.B. Heredia, and C. Rodriguez. (1994). Gas hold up and mass transfer coefficients in bubble columns 1. porous plate diffusers. Int Chem Eng, 34(1), 82-90.
- Sublette, K. , Hesketh R., and Hasan S. (1994). Microbial oxidation of hydrogen sulfide in a pilot scale bubble column. Biotechnology Prog, 10, 611-614.
- Sudha, Rani K., Swamy M.V., and Seenayya G. (1994). High ethanol production by new isolates of *C. thermocellum*. Biotech Letters, 18(8), 957-962.
- Sudha, Rani K., M.V. Swamy, and G. Seenayya. (1997). Increased ethanol production by metabolic modulation of cellulose fermentation in *C. thermocellum*. Biotech Letters, 19(8), 819-823.
- Sudha Rani, K., M.V. Swamy, and G. Seenayya. (1997). Increased ethanol production by metabolic modulation of cellulose fermentation in *Clostridium thermocellum*. Biotechnology Letters, 19(8), 819-823.
- Sulfito, J.M , and M.R. Mormile. (1993). Anaerobic biodegradation of known and potential gasoline oxygenates in the terrestrial subsurface. Environmental Science Technology, 27, 976-978.
- Tanner, R.S., Miller, L.M., Yang, D., (1993), *Int. J. Sys. Bact.* 43, no. 2, 232-236.
- Tanner, R.S., (1998), Personal Communication, Oklahoma Agricultural Experiment Station, Stillwater, OK.
- Taherzadeh, M., C. Niklasson, and G. Liden. (1997). Acetic acid friend or foe in anaerobic batch conversion of glucose to ethanol by *Saccharomyces cerevisiae*. Chemical engineering science, 52(15), 2653-2659.
- US Department of Energy, (1997), Alternatives to Traditional Fuels: 1997-Advanced Data.
- Vega, J.L., Clausen, E.C., and Gaddy J.L. (1990). Design of bioreactors for coal synthesis gas fermentations. Resources, Conservation and Recycling, 3, 149-160.
- Wongsamuth, R., and Doran P. (1994). Foaming and cell flotation in suspended plant cell cultures and the effect of chemical antifoams. Biotechnology and Bioengineering, 44, 481-488.
- Wood, H.G., S.W. Ragsdale, and Pezacka E. (1986). The Acetyl CoA pathway for

autotrophic growth. FEMS Microb Rev, 39, 345-362.

Worden, R.M., and Bredwell M. (1998). Mass transfer properties of microbubbles 2 analysis using a dynamic model. Biotechnology Prog, 14(1), 39-46.

Yang, J., and N. Wang. (1992). Oxygen mass transfer enhancement via fermentor headspace pressurization. Biotechnology Prog, 8, 244-251.

APPENDIX I

THE “Acetyl-CoA” PATHWAY OF AUTOTROPHIC GROWTH

The production of ethanol and by-products from components of syngas namely, CO, CO₂ and H₂ by autotrophic bacteria such as *C. ljungdahlii* and P7 is expected to follow the acetyl-CoA metabolic pathway (Wood et al., 1984, Ljungdahl, 1986). The pathway was developed using experimental studies on *C. thermoaceticum* and *C. thermoautotrophicum* (Phillips et al., 1991). As shown in Figure A1, the metabolism of components of syngas is a complex process involving several individual reactions. The important characteristics of the metabolic pathway are:

- The formation of a methyl group from CO₂ (Step A)
- The condensation of the CH₃ group to a CO or CO₂ derived carboxyl group to form an acetyl- CoA (CH₃COSCoA) intermediate in the presence of a coenzyme, CoA (Steps B, C and D)
- The conversion of the acetyl-CoA to acetate and ethanol (Step E)

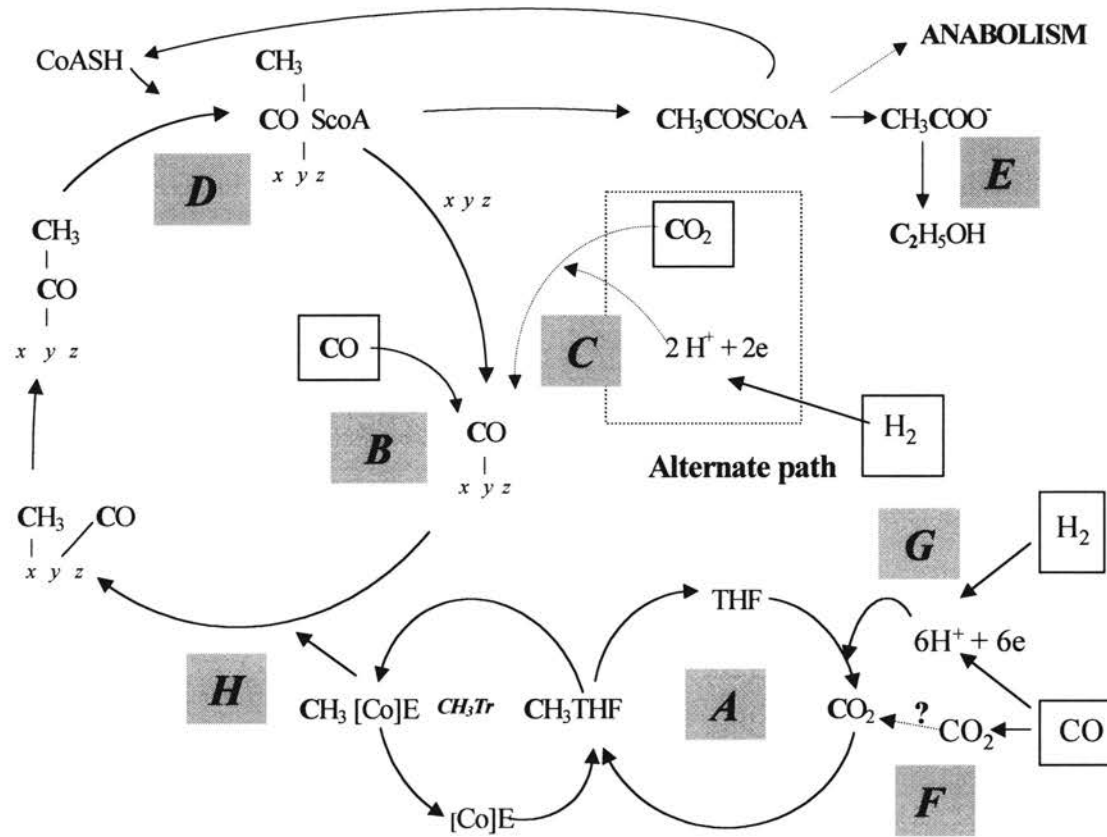


Figure A1. Acetyl-CoA pathway. “*x y z*” are the active sites on CO dehydrogenase, [Co]E is the coenzyme of methyl transferase (CH₃Tr), CoASH is coenzyme-A, and THF is tetrahydrofolate (Ljungdahl, 1986, Wood et al., 1984). A, B....H represent key steps in the pathway.

First, electrons and protons required for the process are generated either from CO or H₂. CO dehydrogenase (CODH) generates electrons and protons from CO and H₂O as (Step F)



Alternatively, electrons and protons can also be generated from H₂ via hydrogenase as (Step G)



CO₂ reacts with H⁺ and e to form methyl tetrahydrofolate, CH₃THF in the presence of the formate dehydrogenase (Step A). The methyl group of CH₃THF is transferred via a corrinoid protein to CODH (Step H). The carboxyl group of acetyl-CoA is derived from CO₂ (Step C) or CO (Step B) via CODH. The exact mechanism of the production of the carboxyl group from CO/CO₂ is yet to be totally resolved. However, a mechanism involving a CO channel within CODH has been recently proposed (Ragsdale et al., 2000). In this mechanism, CO₂ is reduced to CO on a C-cluster within CODH and the CO is channeled within the enzyme to an A-cluster where the condensation of CO and CH₃ intermediate takes place.

At the active sites of CODH shown as “x y z” in Figure A1 condensation of methyl and carboxyl groups takes place in the presence of coenzyme A, CoA (Step D). The acetyl-CoA intermediate is used both for building up of cell materials (anabolism) and synthesizing products (Step E).

For the production of butanol, the acetyl-CoA pathway is extended as follows (Wood et al., 1986).

- The acetyl-CoA intermediate is converted to acetoacetyl-CoA via thiolase
- The acetoacetyl-CoA is converted to 3-hydroxybutyryl CoA via 3-hydroxybutyryl CoA dehydrogenase
- 3-hydroxybutyryl CoA is converted to crotonyl CoA via crotonase
- Crotonyl CoA is converted to butyryl CoA via butyryl CoA dehydrogenase
- Butyryl CoA is converted to butyraldehyde via butyraldehyde dehydrogenase
- Butyraldehyde is converted to butanol via butanol dehydrogenase.

Important enzymes in the acetyl-CoA pathway

The enzymes responsible for H₂, CO and CO₂ uptake are discussed in this section. Enzyme hydrogenase (H₂ase) is responsible for H₂ uptake while carbon monoxide dehydrogenase (CODH) aids CO/CO₂ uptake.

Hydrogenase in anaerobic bacteria reportedly contains iron, sulfur and nickel sites (Adams, 1987). The enzyme catalyzes the reversible reaction shown by Eq. A2. Hydrogen is utilized by autotrophs such as *C. thermoaceticum* growing on CO₂/ H₂ (Ljungdahl, 1986). An H₂-cycling system has been postulated for the H₂ uptake or production for the bacterium, *C. thermoaceticum*, as shown in Figure A3. When growing on H₂/CO₂, the external H₂ is oxidized by the periplasmic H₂ase. The electrons generated from the reaction are captured by the electron transport system of the cells, while the

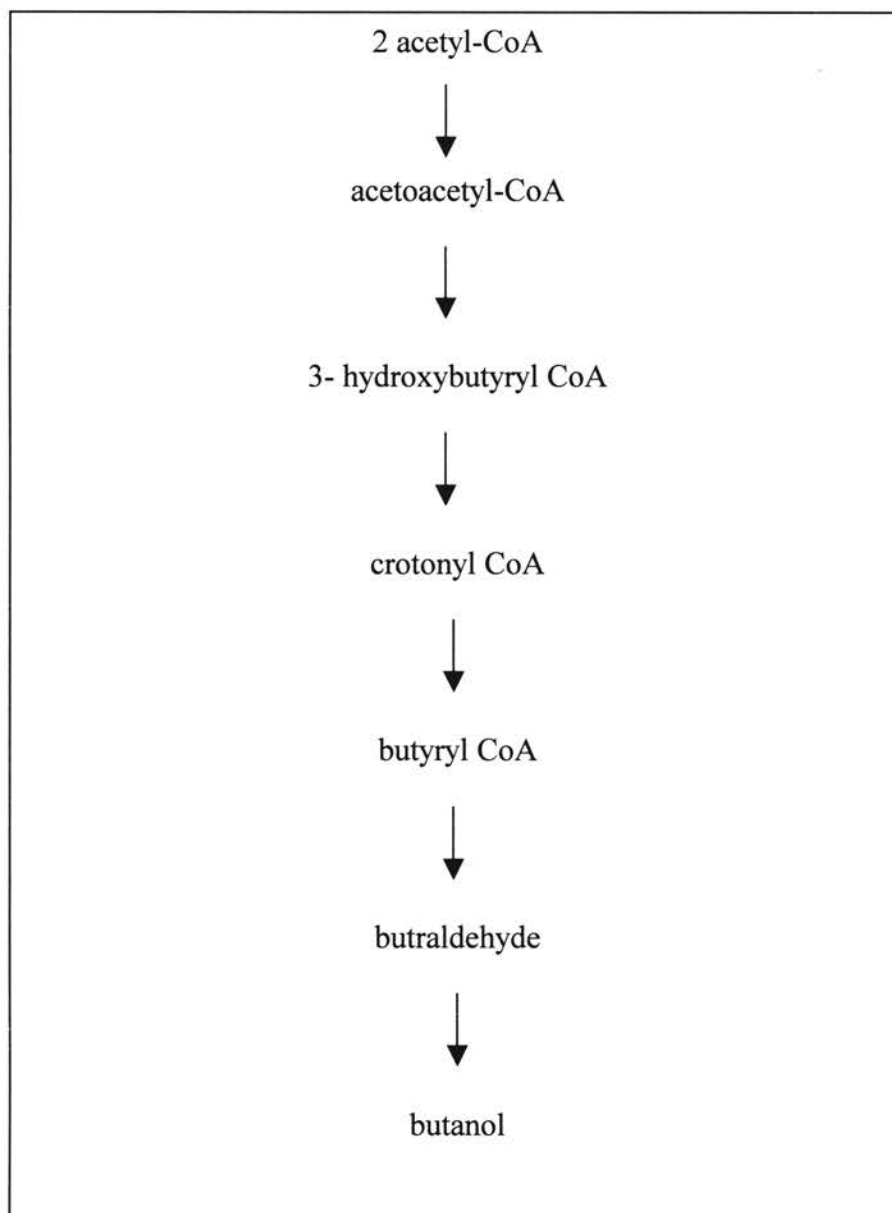


Figure A2. Proposed metabolic steps for butanol production by P7. The pathway was proposed by Wood et al. (1986) for *C.acetobutylicum*.

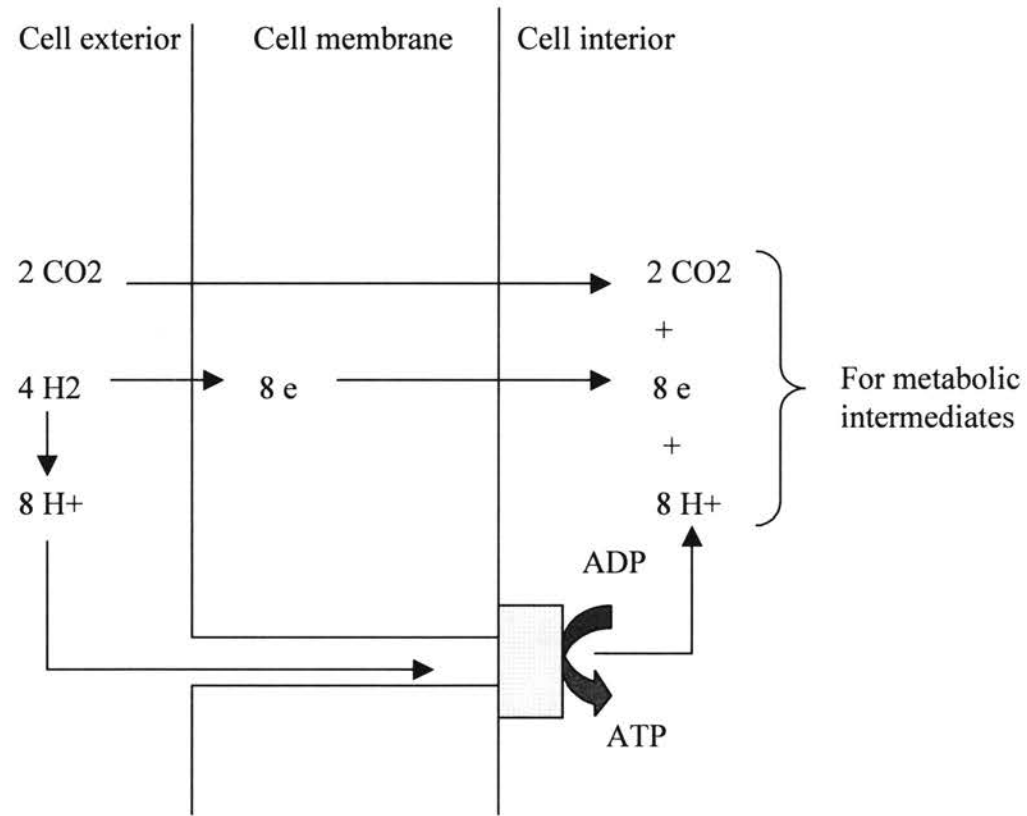


Figure A2. Hydrogen cycling system in *C. thermoaceticum* (Ljungdahl, 1986).

protons are transferred into the cells through a H^+ -translocating ATPase to generate ATP. Within the cells, CODH catalyzes the reaction of CO_2 with the electrons and protons to form acetyl-CoA intermediate (Ljungdahl, 1986).

The enzyme CODH is bifunctional. CODH reversibly oxidizes CO to form CO_2 and also catalyzes the condensation of CH_3 , CO and coenzyme A to form acetyl-CoA (Ljungdahl, 1986). The enzyme reportedly contains a C cluster with iron and sulfur sites and an A cluster with iron, sulfur and nickel sites (Seravalli and Ragsdale, 2000). CO is oxidized to CO_2 at the C cluster as shown by Eq. A1. The carboxyl group is then channeled within the enzyme to the A cluster where the condensation of CO, CH_3 and coenzyme A occurs, as shown in Figure A1. The acetyl-CoA intermediate generated via CODH is used for the formation of ethanol, acetate, and butanol and cell material. Both CODH and H²ase are reportedly very sensitive to the presence of oxygen in the system (Wood, 1984).

Altered electron flow in the metabolic pathway due to sodium sulfide

The role of sodium sulfide in stabilizing P7 cell concentration in the 5 L bioreactor is postulated as follows. In a similar study, reducing agents such as sodium sulfide and sodium thioglycolate were found to alter cell growth rate and electron flow pathways (Rao and Mutharasan, 1988). However, the mode of action of sulfide was not fully understood. Reducing agents are electron donors and can potentially reduce a metabolic intermediate formed during the acetyl-CoA pathway. End product distribution in *C. thermoaceticum* was reportedly altered by reducing agents such as sodium sulfide and cysteine (Rao and Mutharasan, 1988).

The stability of cell concentration of P7 is expectedly due to the effect of sodium sulfide on the electron flow in the metabolic pathway. Individual steps, such as, the synthesis of CH₃THF from CO₂ and H⁺ in the acetyl-CoA pathway require electrons as shown in Figure A1. When sufficient sodium sulfide concentration was maintained in the bioreactor the individual steps were expected to be enhanced by the sulfide.

APPENDIX II

ERROR ANALYSIS FOR THE ESTIMATION OF THE SPECIFIC CELL

GROWTH RATE

The rate of increase of cell concentration (X) in the bioreactor is proportional to the concentration of the cells. The constant of proportionality is the specific cell growth rate, μ , in units of reciprocal time.

$$\mu = \frac{1}{X} \frac{dX}{dt} \quad \text{B1}$$

μ can be experimentally calculated for different operating conditions of the bioreactor as follows:

In the batch mode, cell concentrations are measured over time during the exponential growth phase. The specific cell growth rate at the initial phase of exponential growth is the parameter of interest. To estimate μ , equation B.1 is integrated to give,

$$\ln(X/X_0) = \mu (t - t_0) \quad \text{B2}$$

where,

X is the cell concentration in O.D. units at time, t

X_0 is the initial cell concentration at the onset of the exponential growth phase at time, t_0

The values of $\ln(X/X_0)$ are plotted against $(t - t_0)$ to yield a straight line with slope equal to μ , the specific cell growth rate. The error in the measurement of X and X_0 affecting the estimation of μ is determined as follows:

The error in the term $j = \ln(X/X_0)$ is given by,

$$\sigma_j^2 = \left(\frac{dj}{dX}\right)^2 \sigma^2_x + \left(\frac{dj}{dX_0}\right)^2 \sigma^2_{x_0} \quad \text{B3}$$

$$\sigma_j^2 = \left(\frac{1}{X}\right)^2 \sigma^2_x + \left(-\frac{1}{X_0}\right)^2 \sigma^2_{x_0} \quad \text{B4}$$

Assuming, the error in the measurement of X equals that in X_0 ,

$$\sigma^2_x = \sigma^2_{x_0} \quad \text{B5}$$

Therefore,

$$\sigma_j^2 = \left(\frac{1}{X} + \frac{1}{X_0}\right)^2 \sigma^2_x \quad \text{B6}$$

For the estimation of σ_x , five measurement points from the same cell sample were collected (Table B1). The mean of the sample data is 0.1948 O.D. and the standard deviation σ_x is 0.0099 O.D. The value of σ_x is used to estimate σ_j using the data points shown in Table B2. The errors in σ_j are incorporated in the plot of $\ln(X/X_0)$ versus $t-t_0$ as shown in Figure B1. The initial estimate for the plot of $\ln(X/X_0)$ versus $t-t_0$ is a straight

line ($y = mx + c$) with a slope (m) of 0.0018 and an intercept (c) of 0.1044 using linear regression. The next step is to minimize the objective function, J ,

$$\min J = \sum_i \left(\frac{j_{\text{cal}} - j_{\text{exp}}}{\sigma_j} \right)^2 \quad \text{B7}$$

where, j_{cal} is the calculated value of $\ln(X/X_0)$ from the linear model, $y = mx + c$, j_{exp} is the experimental value of $\ln(X/X_0)$ and x is $(t-t_0)$. The minimal value for J was calculated with m and c as the independent variables. The minimum value of the function J calculated on a spreadsheet was 86.6 and the optimal values of $m = 0.00186$ and $c = 0.096$, as shown in Table B3.

To conclude, the errors in the experimentally calculated values of the specific cell growth rate are estimated. Error plots for $\ln(X/X_0)$ are determined. Using the error minimization criteria (shown in Eq. B7), the optimal values for the slope and intercept for the plot of $\ln(X/X_0)$ versus time, t are determined. The optimized values are approximately equal to the previously determined values using linear regression of the experimental values of $\ln(X/X_0)$ and time.

Trial #	X	X-Xav	(X-Xav)^2
1	0.194	-8.00E-04	6.40E-07
2	0.211	1.62E-02	2.62E-04
3	0.196	1.20E-03	1.44E-06
4	0.193	-1.80E-03	3.24E-06
5	0.180	-1.48E-02	2.19E-04

Number of samples, $n = 5$

Average, $X_{av} = 0.1948$

Standard error, $\sigma_x = 0.0099$

Table B1. Sample points for the estimation of error, σ_x , in the measurement of cell concentration, X in O.D. units. Five measurements of the same sample were performed to determine the average (X_{av}) and standard deviation (σ_x) in X.

$t-t_0$ (min)	X (O.D.)	$j = \ln X/X_0$	σ_j^2	σ_j	$3 \sigma_j$
0	0.178	0.000	0.0004	0.020	0.059
60	0.235	0.278	0.0003	0.018	0.055
120	0.245	0.319	0.0003	0.018	0.055
180	0.280	0.453	0.0003	0.018	0.053
265	0.304	0.535	0.0003	0.017	0.052
300	0.325	0.602	0.0003	0.017	0.052
360	0.355	0.690	0.0003	0.017	0.051
405	0.450	0.927	0.0003	0.016	0.049
495	0.500	1.033	0.0003	0.016	0.048
565	0.538	1.106	0.0003	0.016	0.048
635	0.640	1.280	0.0002	0.016	0.047
715	0.756	1.446	0.0002	0.015	0.046

Table B2. Calculation of errors (σ_j) in the estimation of the term $j = \ln(X/X_0)$. X is the cell concentration in O.D. at time t and X_0 is the initial cell concentration at time t_0 .

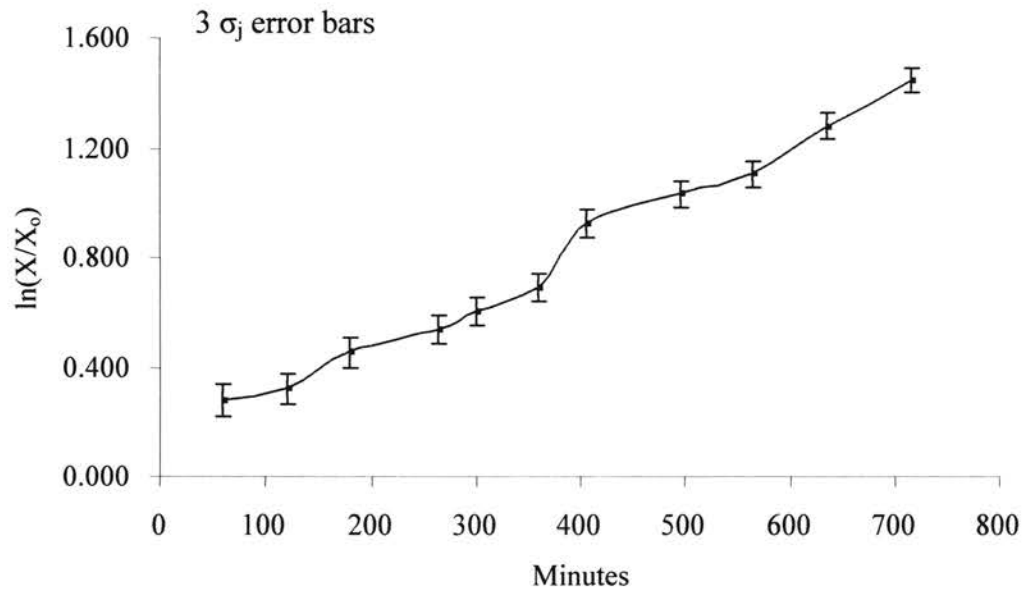


Figure B1. Errors (σ_j) in the estimation of $\ln(X/X_0)$. The error bars are plotted for $3 \sigma_j$ values. Theoretically, 67% of the errors in the estimates of $\ln(X/X_0)$ should lie within $\pm 3 \sigma_j$ values. The slope of the curve is the specific cell growth rate.

$t-t_0$ (min)	σ_j	j_{cal}	j_{cal}/σ_j	j_{exp}	j_{exp}/σ_j	Y	Y^2
60	0.018	0.207	11.292	0.278	15.134	3.843	14.765
120	0.018	0.319	17.528	0.319	17.569	0.041	0.002
180	0.018	0.430	24.333	0.453	25.625	1.291	1.667
265	0.017	0.588	33.799	0.535	30.762	-3.036	9.220
300	0.017	0.653	37.995	0.602	35.025	-2.970	8.821
360	0.017	0.765	45.155	0.690	40.772	-4.383	19.213
405	0.016	0.848	51.897	0.927	56.750	4.854	23.558
495	0.016	1.015	62.974	1.033	64.060	1.085	1.178
565	0.016	1.145	71.661	1.106	69.203	-2.458	6.041
635	0.016	1.275	81.288	1.280	81.562	0.274	0.075
715	0.015	1.424	92.154	1.446	93.594	1.441	2.075

σ_j is the error in $j = \ln(X/X_0)$

j_{cal} and j_{exp} are the estimated and experimental values of $\ln(X/X_0)$, respectively

$$Y = (j_{cal} - j_{exp}) / \sigma_j$$

$$\min J = \sum_i \left(\frac{j_{cal} - j_{exp}}{\sigma_j} \right)^2 = 86.6$$

The optimal values of slope = 0.00186 and intercept = 0.096.

Table B3. Optimization of the estimate of specific cell growth rate.

**OKLAHOMA STATE UNIVERSITY
INSTITUTIONAL REVIEW BOARD
FOR HUMAN SUBJECTS RESEARCH**

Date:

IRB#:

Proposal Title: MICROBIAL CONVERSION OF SYNGAS TO ETHANOL

Principal Investigator(s): Randy Lewis Professor, Sriniraj Student

Reviewed and Processed as: Exempt

Approval Status Recommended by Reviewer(s): Approved with Provisions

APPROVAL STATUS SUBJECT TO REVIEW BY FULL INSTITUTIONAL REVIEW BOARD AT NEXT MEETING.

APPROVAL STATUS PERIOD VALID FOR ONE CALENDAR AFTER WHICH A CONTINUATION OR RENEWAL REQUEST IS REQUIRED TO BE SUBMITTED FOR BOARD APPROVAL. ANY MODIFICATIONS TO APPROVED PROJECT MUST ALSO BE SUBMITTED FOR APPROVAL.

Comments, Modifications/Conditions for Approval or Reasons for Deferral or Disapproval are as follows:

Signature: _____

Chair of Institutional Review Board

Date:

VITA

2

Srinivasan Rajagopalan

Candidate for the Degree of

Doctor of Philosophy

Thesis: MICROBIAL CONVERSION OF SYNGAS TO ETHANOL

Major Field: Chemical Engineering

Biographical:

Personal Data: Born in Madras, India, On February 12, 1972, the son of V. Rajagopalan and Kamalaveni Rajagopalan.

Education: Graduated from AVM High School, Madras, India in May 1990; received Bachelor of Technology degree in Chemical Engineering from Anna University, Madras, India in May 1994; received Master of Technology degree in Chemical Engineering from Indian Institute of Technology, Madras, India in January 1997. Completed the requirements for the Doctor of Philosophy degree with a major in Chemical Engineering at Oklahoma State University in May 2001.

Experience: Research Assistant, Chemical Engineering, Oklahoma State University from August 1997 to May 2001; Research Assistant, Oklahoma Industrial Assessment Center, Stillwater from May 1998 to May 2000; Teaching Assistant, Fluid Mechanics, Oklahoma State University from August 1997 to Dec 1997; Senior Executive, EID Parry Fertilizers, Madras, India from June 1994 to July 1995.

Professional Memberships: AIChE.